

Synthesis and Characterization of Oxatriquinanes

By

NEMA HAFEZI

B.A.S (University of California, Davis) 2005

DISSERTATION

Submitted in partial satisfaction of the requirement for the degree of

DOCTOR OF PHILOSOPHY

in

Chemistry

in the

OFFICE OF GRADUATE STUDIES

of the

UNIVERSITY OF CALIFORNIA

DAVIS

Approved:

Dr. Mark Mascal

Dr. Mark J. Kurth

Dr. Neil E. Schore

Committee in Charge
2010

UMI Number: 3444022

All rights reserved

INFORMATION TO ALL USERS

The quality of this reproduction is dependent upon the quality of the copy submitted.

In the unlikely event that the author did not send a complete manuscript and there are missing pages, these will be noted. Also, if material had to be removed, a note will indicate the deletion.



UMI 3444022

Copyright 2011 by ProQuest LLC.

All rights reserved. This edition of the work is protected against unauthorized copying under Title 17, United States Code.



ProQuest LLC
789 East Eisenhower Parkway
P.O. Box 1346
Ann Arbor, MI 48106-1346

Synthesis and Characterization of Oxatriquinanes

Abstract

The term “oxonium ion” is freighted with significance and evokes images of fleeting intermediates or highly reactive chemical reagents. Indeed, only trialkyloxonium salts with inert counterions (such as BF_4^- or PF_6^-) can normally be isolated, and they are among the most powerful alkylating agents known. This work describes the synthesis of oxatriquinanes; rigid, fused, tricyclic oxonium salts, the framework of which impart to them properties unheard of in alkyl oxonium ion chemistry.

Oxatriquinane, a fused, time-averaged C_3 symmetric, tricyclic alkyl oxonium ion of unprecedented stability, was synthesized in five steps from 1,4,7-cyclononatriene. It survives reflux in H_2O , and is not attacked by alcohols, alkyl thiols, halide ions, or hindered amine bases. The X-ray crystal structure shows longer C–O bond distances and more acute C–O–C bond angles than any reported alkyl oxonium salt.

The corresponding oxatriquinene and oxatriquinacene were also synthesized and represent the first examples of stable allyl oxonium species. Although more reactive than their saturated counterparts, an NMR spectrum of these compounds can be recorded in acetonitrile, which is known to attack simple alkyl oxonium salts.

The synthesis of 1,4,7-trimethyloxatriquinane, a 3-fold tertiary alkyl oxonium salt, is described. It is inert to solvolysis with alcohols, even at elevated temperatures, but undergoes facile substitution with the strongly nucleophilic azide anion via the S_N2 pathway, despite the fact that substitution is occurring at a tertiary carbon center. This finding is supported by computational modeling and a study of the reaction kinetics, and is also consistent with observed solvent and salt effects.

Abbreviations

Å	Angstrom
Ac	acetyl
AIBN	azobisisobutyronitrile
aq	aqueous
B3LYP	Becke, (3), Lee, Yang, Par
Bu	butyl
°C	celsius
ca.	approximately
calcd	calculated
conc.	concentrated
Cp*	1,2,3,4,5-pentamethylcyclopentadiene
d	doublet
DBU	1,8-Diazabicyclo[5.4.0]undec-7-ene
ddd	doublet of doublet of doublets
ddq	doublet of doublet of quartets
dec	decomposes
DFT	Density Functional Theory
DIBAL	diisobutylaluminum hydride
DMF	<i>N,N</i> -dimethylformamide
DMSO	dimethylsulfoxide
dt	doublet of triplets
EI	Electron Impact

eq	equivalent
ESI	Electrospray Ionization
Et	ethyl
g	gram
h	hour
HRMS	High Resolution Mass Spectrometry
Hz	Hertz
IBX	2-Iodoxybenzoic acid
iPrOH	isopropanol
IR	infrared
K	Kelvin
kbar	kilobar
L	liter
LDA	lithium diisopropylamide
LiHMDS	lithium hexamethyldisilazide
ln	natural log
m	multiplet
M	molar
m-CPBA	<i>meta</i> -chloroperbenzoic acid
Me	methyl
MeOH	methanol
mg	milligram
MHz	megahertz

μL	microliter
min	minute
mL	milliliter
mM	millimolar
mmol	millimole
N	normal
NBS	N-bromosuccinimide
NMO	N-methylmorpholine N-oxide
NMR	nuclear magnetic resonance
N-PSP	N-phenylselenophthalimide
Nu	nucleophile
$\nu\text{-max}$	maximum frequency
obs	observed
PCC	pyridinium chlorochromate
Ph	phenyl
pH	potential of hydrogen
ppm	parts per million
PTSA	<i>para</i> -toluenesulfonic acid
Ra-Ni	Raney Nickel
rt	room temperature
s	singlet (NMR), second (time)
sat.	saturated
$\text{S}_{\text{N}}2$	bimolecular nucleophilic substitution

S_N1	unimolecular nucleophilic substitution
S_NAr	aromatic nucleophilic substitution
t	triplet
tBuOK	potassium tertiary-butoxide
tBuOH	tertiary-butanol
TFA	trifluoroacetic acid
TfOH	triflic acid
TfO ⁻	triflate
THF	tetrahydrofuran
THP	tetrahydropyranyl
TLC	thin layer chromatography
TMS	trimethylsilyl
Ts	tosyl

Table of Contents

Abstract.....	ii
Abbreviations.....	iv
Table of Contents.....	viii
List of Schemes.....	xii
Figures and Tables.....	xv
Acknowledgments.....	xvi
Dedication.....	xviii
Chapter 1 – Introduction	1
1.1 – Hydronium: The Simplest Oxonium Ion.....	2
1.2 – Oxygen Bonded to Three Inorganic Atoms.....	2
1.2.1– Mercury.....	2
1.2.2–Tin.....	3
1.2.3 –Antimony.....	4
1.3 – Organic Oxonium Ions: Meerwein’s Salt.....	5
1.4 – Different Synthetic Approaches to Oxonium Ions.....	6
1.5 – Complex Oxonium Ions.....	7
1.6 – Reactions of Oxonium Ions.....	9
1.7 – Stable Oxonium Ions.....	10
1.8 – Oxonium Ions as Unstable Intermediates.....	12
1.9 – Heterotriquinanes: Synthesis of Azatriquinanes, Azatriquinacene, and the Azaaceptalenenide Anion.....	14
1.10 – Aims and Objectives.....	18

References	19
Chapter 2 – Oxatriquinane	22
2.1 – Introduction.....	23
2.2 – Retrosynthetic Analysis.....	23
2.3 – Preparation of Cyclonona-3,6-dien-1-ol	23
2.4 – Transannulation of Cyclonona-3,6-dien-1-ol	26
2.5 – Haloetherification.....	28
2.6 – Hydrodehalogenation of 6-Iodo-10-oxa-bicyclo[5.2.1]dec-3-ene (56).....	30
2.6.1 – Sodium and Zinc Metals in Protic Solvent.....	30
2.6.2 – Hydrogen Iodide.....	30
2.6.3 – Tributyltin Hydride.....	31
2.6.4 – Lithium Aluminum Hydride.....	31
2.6.5 – Raney Nickel.....	31
2.6.5.1 – Tuning the Reactivity of Raney Nickel with Poisons.....	32
2.7 – Endgame: Synthesis of Oxatriquinane.....	34
2.7.1 – The Bromide Salt of Oxatriquinane.....	35
2.8 – Reactivity of Oxatriquinane.....	37
2.8.1 – Explanation of the Unusual Stability of Oxatriquinane.....	38
2.8.2 – Anion Exchange and X-Ray Crystal Structure Determination.....	39
2.9 – Conclusion.....	41
Experimental Procedures.....	42
References.....	46

Chapter 3 – Oxatriquinacene	48
3.1 – Introduction.....	49
3.2 – Proposed Synthesis from Fructose.....	50
3.2.1 – Retrosynthetic Analysis.....	50
3.2.2 – Attempted Synthesis of Oxatriquinacene from Fructose.....	51
3.3 – Reassessment and New Approach Towards Oxatriquinacene.....	52
3.3.1 – Introduction of Unsaturation in 10-Oxa-bicyclo[5.2.1]dec-8-en-4-one.....	55
3.3.1.1 – Bromination with NBS.....	55
3.3.1.2 – Nicolaou’s Oxidation Using IBX/NMO in DMSO.....	55
3.3.1.3 – Exhaustive Bromination with Bromine.....	56
3.3.1.4 – Selective Bromination of 10-Oxa-bicyclo[5.2.1]dec-8-en-4-one.....	57
3.3.2 – Elimination, Reduction, and Endgame.....	57
3.4 – Reactivity of Oxatriquinacene.....	58
3.5 – Conclusion.....	58
Experimental Procedures.....	60
References.....	63
Chapter 4 – 1,4,7-Trimethyloxatriquinane	64
4.1 – Introduction.....	65
4.2 – Retrosynthetic Analysis.....	65
4.3 – Preparation of 1,4,7-Trimethyloxatriquinane.....	66
4.4 – Reactivity of 1,4,7-Trimethyloxatriquinane.....	68

4.4.1 – S _N 2 Bimolecular Displacement at a Tertiary Carbon: A Brief Review.....	70
4.4.2 – The Case for the S _N 2 Mechanism.....	71
4.4.3 – Existence of a Possible Equilibrium.....	72
4.5 – Conclusion.....	73
Experimental Procedures.....	74
References.....	81

Chapter 5 – Future Work

5.1 – Introduction.....	84
5.2 – The Diels-Alder Reaction.....	84
5.3 – Preparation of Diels-Alder Adducts of Trienone 75	85
5.4 - Formation of Beta-substituted Oxatriquinanes Through 1,4,7-Cyclononatriene Trioxide.....	86
5.5 – Conclusion.....	87
References.....	88

Appendix	89
¹ H- and ¹³ C-NMR Spectra for Chapter 2.....	90
¹ H - and ¹³ C-NMR Spectra for Chapter 3.....	98
¹ H - and ¹³ C-NMR Spectra for Chapter 4.....	106
Crystal Structure Determination and Refinement for Oxatriquinanium SbF ₆ ⁻ (41).....	122
Crystal Structure Determination and Refinement for Trimethyloxatriquinanium PF ₆ ⁻ (42).....	134

List of Schemes

Scheme 1.1 - Synthesis of triethyloxonium tetrafluoroborate.....	5
Scheme 1.2 - Synthesis of trimethyloxonium hexafluorophosphate.....	6
Scheme 1.3 - Mechanism of the formation of trimethyloxonium hexafluorophosphate according to Olah <i>et al.</i>	6
Scheme 1.4 - Synthesis of O-methyltetrahydrofuranium perchlorate.....	7
Scheme 1.5 - Synthesis of oxaquinuclidine.....	8
Scheme 1.6 - Synthesis of oxaadamantane.....	8
Scheme 1.7 - Synthesis of a fluorinated oxonium salt.....	9
Scheme 1.8 - Reactions of trialkyloxonium and various nucleophiles.....	9
Scheme 1.9 - Proposed mechanism for Friedel-Crafts alkylation using Meerwein's salt.....	10
Scheme 1.10 - Synthesis of triphenyloxonium halide.....	11
Scheme 1.11 - Synthesis of parent pyrylium.....	12
Scheme 1.12 - Reactions of oxocarbenium ions.....	13
Scheme 1.13 - Synthesis of fumagillin via an oxonium intermediate.....	13
Scheme 1.14 - Synthesis of (-)laurefucin via an oxonium intermediate.....	14
Scheme 1.15 - Synthesis of azatriquinane.....	15
Scheme 1.16 - Mascial and co-workers found no evidence of the formation of keto-amine 33 based on ¹ H- and ¹³ C- NMR.....	16
Scheme 1.17 - Synthesis of azatriquinacene, hexachloroazaacepentalene, and azaacepentalene.....	17
Scheme 2.1 - Retrosynthetic analysis for oxatriquinane.....	23
Scheme 2.2 - Synthesis of 1,4,7-cyclononatriene.....	24
Scheme 2.3 - Synthesis of cyclonona-3,6-dien-1-ol.....	25

Scheme 2.4 - Suggested mechanism for the direct transformation of cyclonona-3,6-dien-1-ol to oxatriquinane.....	26
Scheme 2.5 - Synthesis of 10-Oxa-bicyclo[5.2.1]dec-3-ene from cyclonona-3,6-dien-1-ol.....	27
Scheme 2.6 - Widenhoefer's platinum-catalyzed hydroalkoxylation of olefins.....	28
Scheme 2.7 - Synthesis of 6-iodo-10-Oxa-bicyclo[5.2.1]dec-3-ene.....	29
Scheme 2.8 - Hydrodehalogenation of 6-iodo-10-Oxa-bicyclo[5.2.1]dec-3-ene.....	30
Scheme 2.9 - Effects of poisons on the hydrodehalogenation reaction using Raney Nickel.....	33
Scheme 2.10 - Synthesis of oxatriquinane.....	34
Scheme 2.11 - Possible outcomes from the treatment of 10-Oxa-bicyclo[5.2.1]dec-3-ene with $\text{HBr}_{(g)}$	36
Scheme 3.1 - Attempted synthesis of 1,4-dihydroxy oxatriquinacene.....	49
Scheme 3.2 - Retrosynthetic analysis of oxatriquinacene from fructose.....	50
Scheme 3.3 - Attempted synthesis of oxatriquinacene from fructose.....	51
Scheme 3.4 - Mechanism for the formation of hydroxymethylfurfural from 2,5 diformylfuran.....	52
Scheme 3.5 - Synthesis of oxatriquinacene.....	53
Scheme 3.6 - Mechanistic explanation for the failed Swern oxidation.....	54
Scheme 3.7 - Mechanistic explanation for the failed dehydrohalogenation.....	57
Scheme 3.8 - Synthesis of oxatriquinacene from 3,5-dibromo-10-Oxa-bicyclo[5.2.1]dec-8-en-4-one	58
Scheme 4.1 - Retrosynthetic analysis of 1,4,7-trimethyloxatriquinane.....	66
Scheme 4.2 - Synthesis of 1,4,7-trimethyloxatriquinane.....	67
Scheme 4.3 - DFT calculations were unable to detect a transition state or a local energy minimum for the following equilibrium.....	73

Scheme 5.1 - Diels-Alder reaction performed by Prinzbach and co-workers.....	85
Scheme 5.2 - Proposed synthesis of the Cp* adduct of oxatriquinane.....	86
Scheme 5.3 – Beta-substituted oxatriquinanes via triepoxide 98	87

Figures and Tables

Figure 1.1 - Examples of oxonium salts which possess an oxygen atom bonded to three inorganic atoms.....	3
Figure 1.2 - Illustration depicting the solid state structure of tris(trimethyltin)oxonium chloride forming two dimensional sheets similar to graphite.....	3
Figure 1.3 - Orbital explanation of the planarization of tris-(trimethyltin)- and tris-(dimethylantimony) oxonium.....	4
Figure 1.4 - Example of pyrylium oxonium ions.....	12
Figure 1.5 - Oxatriquinane and various derivatives.....	18
Figure 2.1 - The crown conformation of 51 prevents the tetrahydroaluminate ion from reacting in a S_N2 -type manner.....	25
Figure 2.2 - The lone pair of the THF oxygen in 53 is thought to be poised directly over the π^* orbital of the double bond.....	37
Figure 2.3 - X-ray crystal structure of oxatriquinane SbF_6^-	40
Figure 3.1 - Steric congestion presented by the bromines could explain the inability of 77 to undergo dehydrohalogenation.....	56
Figure 3.2 - Neutral trivalent oxygen compounds 78 and 79	59
Figure 4.1 - X-ray crystal structure of cation of 42 PF_6^-	68
Table 4.1 - Details regarding the reactivity of 1,4,7-trimethyloxatriquinane towards various nucleophiles.....	69
Figure 4.2 - Plot of $[90]$ versus time for the reaction of 0.003 M 42 and NaN_3 at three different concentrations with observed pseudo-first order rate constants and plot of k_{obs} versus NaN_3 concentration.....	72

Acknowledgements

I would like to thank my advisor, Dr. Mark Mascal, for supporting me in accomplishing this work, for his tough love, continuing inspiration, mentorship, and for putting up with my antics. I consider myself beyond fortunate to have worked with someone who possesses an indelible resolve to his field of work and serves as the paradigm of discipline for life in general. You sir, have changed my life for the better.

I would also like to thank the members of my thesis committee, Dr. Mark Kurth and Dr. Neil Schore for their guidance and consultation in writing this dissertation. I must also thank Dr. Michael Toney for helping me with the kinetic measurements and his valuable advice on my work. I want to thank Dr. James C. Fettinger and Dr. Håkon Hope for their help in determining the x-ray crystal structures of my compounds. Thanks are also given to the National Science Foundation and the R. Bryan Miller Fellowship for their funding of these projects.

I would like to express thanks to all the members, past and present, of the Mascal group for their support. Big thanks must be given to Gorkem Gunbas for his friendship and for our lively exchange of ideas on both of our projects. I also feel obligated to thank Dr. Mark Kurth again for introducing me to organic chemistry and helping me discover that I am actually good at something as well as helping me earn my first 'A' grade in my undergraduate career. Thanks are also given Dr. Seth Dixon and Dr. Jordi Ceron-Bertran for their mentorship and helping me get a handling of the basics in the laboratory.

I would like to thank my girlfriend Tao for her love and support and maintaining my sanity throughout this endeavor.

Most importantly, I must thank my mother Bibi and my brother Sena for their never-ending love and support for me while accomplishing this work.

For Mom

Chapter 1
Introduction

1.1 - Hydronium: The Simplest Oxonium Ion

Oxonium ions are cationic molecules consisting of a trivalent oxygen atom. Hydronium, H_3O^+ , is the simplest and most thoroughly studied oxonium ion. It was first observed by Danneel who noted the unusually fast rate of hydrogen ion migration in water based on observations from potentiometric measurements.¹ Danneel's work was later expanded by Hantzsch² and co-workers who ultimately postulated the existence of the hydronium ion. This work eventually laid the foundation to the modern acid-base theory of Bronsted and Lowry.³ Decades later, Hantzsch's postulate was confirmed by ab initio,⁴ IR,⁵ Raman,⁶ ^1H -NMR and ^{17}O -NMR spectroscopies,^{4,7} neutron-diffraction,⁸ and x-ray crystallography.⁹

1.2 - Oxygen Bonded to Three Inorganic Atoms

1.2.1 - Mercury

There are numerous examples of oxygen atoms possessing a three coordinate relationship with metals through ionic bonds, such as those found in metal oxides in rutile structures. They are also observed in more complex structures such as antimony(V) oxide rings and cages.^{10,11} However, oxonium ions possessing three *covalent* bonds between oxygen and inorganic ions are far less common (Figure 1.1). In 1926, Carozzi prepared tris(chloromercuric)oxonium chloride by leaving pieces of calcite in an aqueous solution of mercuric chloride for several days.¹² Thirty years later, the x-ray diffraction study of the product confirmed the structure to possess a cubic arrangement. The molecule itself was found to be slightly pyramidal with Hg-O-Hg bond angles of 118° and Cl-Hg-O angles of 180° .¹³

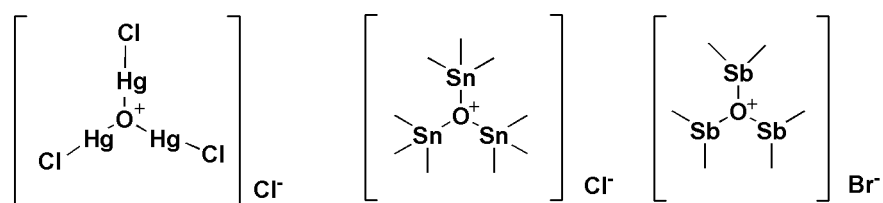


Figure 1.1 – Examples of oxonium salts which possess an oxygen atom bonded to three inorganic atoms.

1.2.2 - Tin

In addition to metal ions, oxygen is also capable of bonding to three metalloid atoms to form oxonium salts. In 1940, Harada reported the synthesis of tris(trimethyltin)oxonium iodide.¹⁴ Hippel *et.al.* was able to prepare the chloride salt by refluxing hexamethyldistannoxane with trimethyltin chloride in THF. An alternative preparation was accomplished by refluxing a mixture of trimethyltin bromide and lithium oxide. Cooling the solution of the chloride salt to gave crystals of tris(trimethyltin)oxonium chloride and the x-ray crystal structure revealed that it adopts a trigonal planar geometry with Sn-O-Sn bond angle of 120°. Furthermore, the extended structure of the tin compound formed thin planar sheets that stack upon each other similar to that of graphite (Figure 1.2).¹⁵

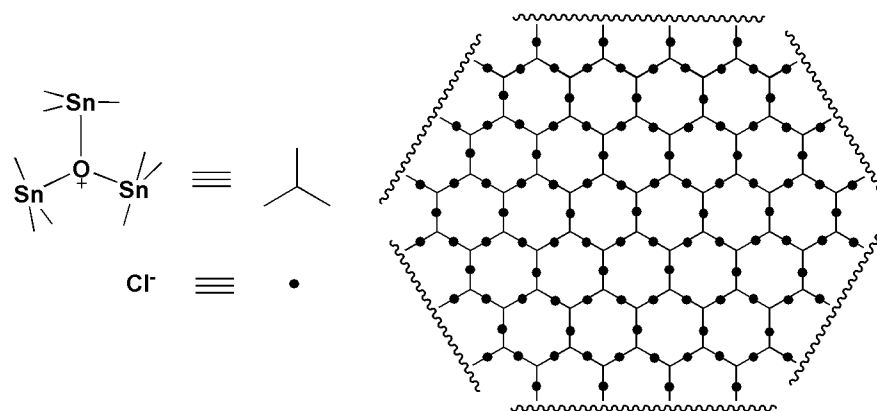


Figure 1.2 – Illustration depicting the solid state structure of tris(trimethyltin)oxonium chloride forming two dimensional sheets similar to graphite.

The chloride ions are situated behind the tin atoms, causing the C-Sn-O bonds of trimethyltin to form 96.2° angles.

1.2.3 - Antimony

Not all oxonium salts are formed from an oxide source. For example, an oxonium salt composed of oxygen bonded to three antimony(III) atoms was prepared by Breunig *et al* by stirring 1,1,2,2-tetramethyldistibine with dimethylantimony bromide in the presence of air at room temperature.¹⁶ The air-sensitive distibine reacts with oxygen to give tetramethyldistiboxane which subsequently reacts with dimethylantimony bromide to give the product as colorless crystals. Remarkably, an $^1\text{H-NMR}$ spectrum of the antimony compound could be recorded in D_2O .

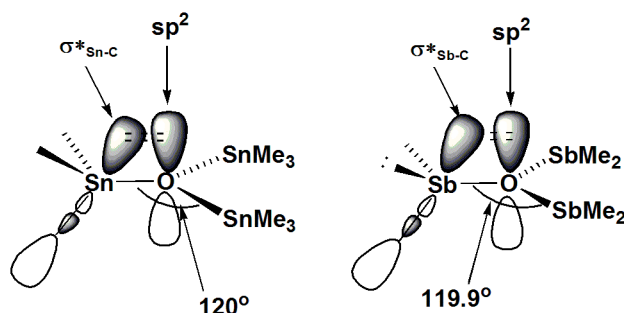
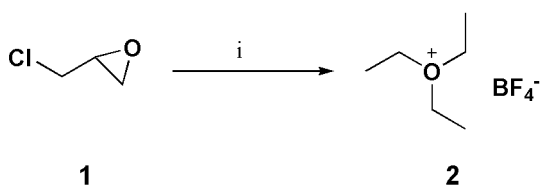


Figure 1.3- Orbital explanation of the planarization of tris-(trimethyltin)- and tris-(dimethylantimony) oxonium. The oxygen is capable of donating its lone pair into the Sn-C or Sb-C antibonding orbital.

A structural characteristic shared by the tin and antimony compounds is the trigonal planar geometry of the oxygen, a characteristic not seen in hydronium. The oxygens in the tin and antimony compounds are able to back-bond to the σ^* orbital of the C-Sn and C-Sb bond, respectively, causing planarization (Figure 1.3).

1.3 - Organic Oxonium Ions: Meerwein's Salt

Trialkyl oxonium ions are often depicted as fleeting intermediates in reaction mechanisms or highly reactive alkylating agents. The trivalent oxygen assumes a pyramidal geometry and is capable of inversion like that of its nitrogen analogue. Indeed, mechanisms such as those for the cleavage of dialkyl ethers and substitution at the anomeric carbon of sugars involve highly reactive oxonium intermediates. Commonly referred to as Meerwein's salts, trialkyloxonium salts are among the most powerful alkylating agents at a chemist's disposal and are reactive towards even the weakest of nucleophiles such as water. Meerwein salts are stable in the solid state only as long as the counterion is inert (i.e. BF_4^- , PF_6^- , etc.). The synthesis of triethyloxonium tetrafluoroborate (**2**) involved the reaction of epichlorohydrin (**1**), diethyl ether and boron trifluoride etherate (Scheme 1.1).¹⁷

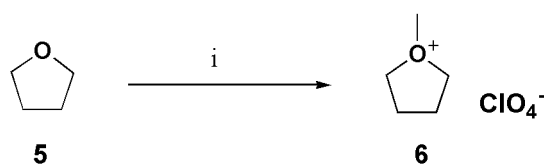


Scheme 1.1 - Reagents and conditions: i) $\text{BF}_3\text{-OEt}_2$, Et_2O , $0\text{ }^\circ\text{C}$

The reaction mechanism is shown in Scheme 1.3. Thus, one orthoformate molecule reacts with two molecules of PF_5 to give an oxocarbenium salt and MeOPF_4 . The latter decomposes to phosphoryl fluoride and methyl fluoride, which then reacts with $\text{PF}_5\text{-OMe}_2$ to give **4**. The oxocarbenium intermediate is able to combine with dimethyl ether to give methylated orthoformate oxonium **3**, which undergoes equilibrium to form **4** and methyl formate.

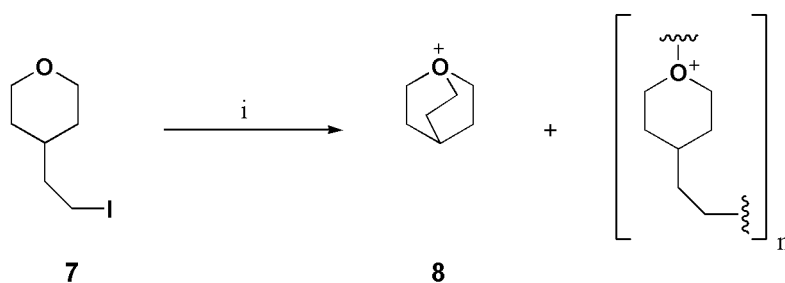
1.5 - Complex Oxonium Ions

The aforementioned methods of Meerwein, Goodrich, and Treichel are useful ways of preparing simple oxonium salts. However, their utility in preparing more complex oxonium salts is limited. Helmkamp and Pettit showed that oxonium salts could be prepared by treating dialkyl ethers with a diazoalkane in the presence of acid (Scheme 1.4).¹⁹ In acidic media, diazomethane is protonated to give the highly reactive methyl diazonium cation. This ion is immediately attacked by **5** to give **6**.



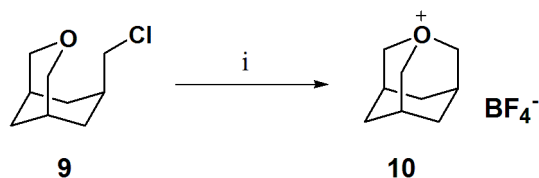
Scheme 1.4 Reagents and conditions: i) CH_2N_2 , HClO_4

Alkyl halide activation using silver(I) salts is a powerful way of synthesizing complex oxonium ions. Klages *et al.*²⁰ utilized silver(I) salts in preparing **8**, the oxo-analogue of quinuclidine. The reaction proceeds via intramolecular $\text{S}_{\text{N}}2$ displacement of a terminal iodide by oxygen, albeit in low yield due to competing polymerization (Scheme 1.5).



Scheme 1.5 Reagents and conditions: i) AgSbF₆, 1,2-dichloroethane, 6.5% yield

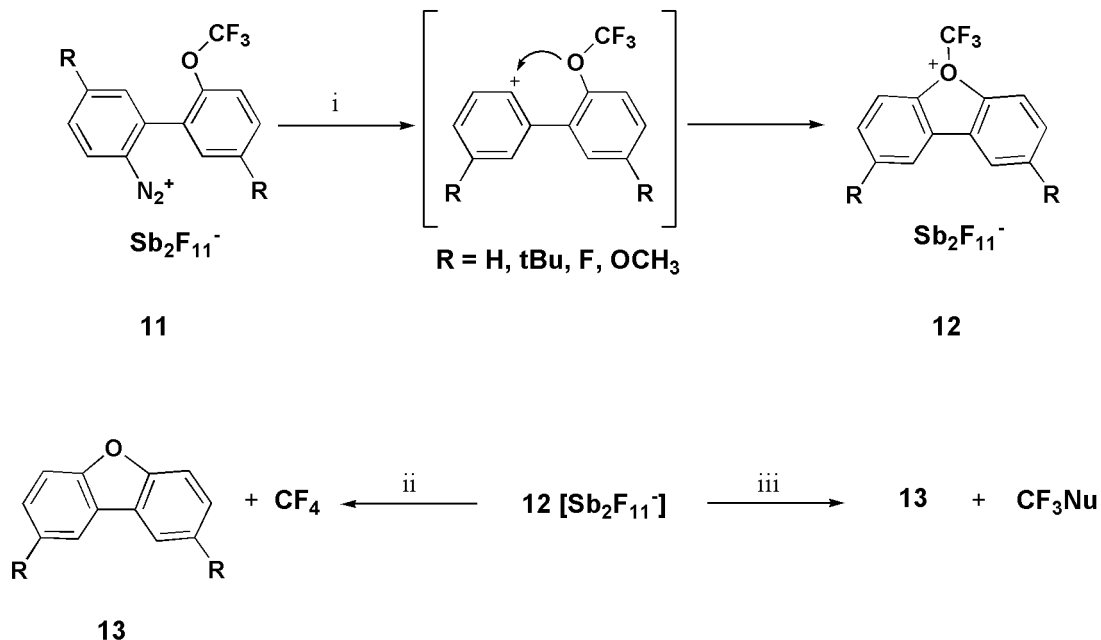
Recently, Olah and co-workers were able to synthesize oxadamantium tetrafluoroborate (**10**) by treating **9** with silver tetrafluoroborate in liquid sulfur dioxide (Scheme 1.6).²¹



Scheme 1.6 Reagents and conditions: i) AgBF₄, SO₂(liq)

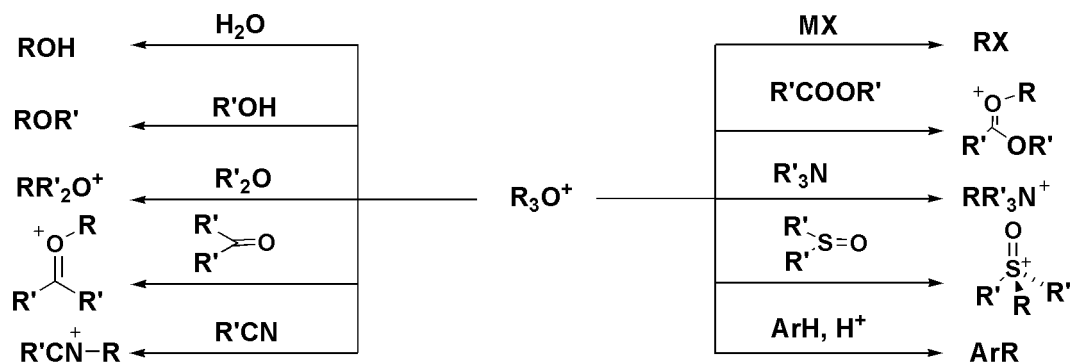
Another recent advance in oxonium chemistry was made by Umemoto *et al.* in their synthesis of *O*-trifluoromethyl-dibenzofuran oxonium ions.²² This is a rare example of an oxonium ion bearing an electron withdrawing substituent. The biphenyl diazonium salt (**11**) was irradiated at -106 °C producing a phenyl cation intermediate, which is attacked by the oxygen to give **12** which is only stable at temperatures below -70°C. When warmed above that temperature, the authors claim that **12** disassociates in an S_N1 manner to **13** and CF₃⁺ and abstracts fluoride from Sb₂F₁₁⁻ to give carbon tetrafluoride. On the other hand, nucleophilic substrates such as alcohols and amines are immediately alkylated by **12** to give their trifluoromethyl

derivatives by an S_N2 mechanism. Furthermore, it was also found that **12** was unreactive towards simple aromatic compounds such as toluene and naphthalene (Scheme 1.7).



Scheme 1.7 - Reagents and conditions: i) $h\nu$, CH_2Cl_2 , $-106\text{ }^\circ\text{C}$; ii) $>-70\text{ }^\circ\text{C}$, iii) HNu (alcohols, phenols, amines, pyridines, sulfonates)

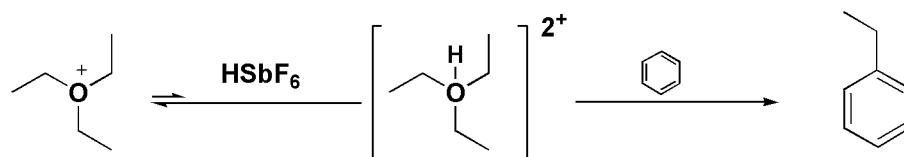
1.6 - Reactions of Oxonium Ions



Scheme 1.8 Reactions of trialkyloxonium and various nucleophiles.

Trialkyloxonium salts are generally the most powerful alkylating agents available. The high reactivity of these salts allows for chemical conversions that are otherwise difficult to accomplish using traditional alkylating agents such as alkyl halides (Scheme 1.8). Asymmetric ketals can be obtained by treating a ketone with a trialkyl oxonium salt to give an oxocarbenium ion,²³ which is subsequently treated with alcohols. Ortho esters can also be obtained in an analogous fashion starting from an ester.²⁴

A remarkable use of oxonium salts was demonstrated by Olah and co-workers.⁷ It was found that when arenes were treated with triethyloxonium tetrafluoroborate in an effort to perform Friedel-Crafts alkylation, no alkylated products were formed. However, when the mixture was treated with a catalytic amount of the superacid HSbF_6 ($\text{pK}_a \approx -31$), the arenes would undergo Friedel-Crafts alkylation to give ethyl arenes. Olah postulates that the oxonium ion becomes protonated to give a fleeting oxadication intermediate, a superelectrophile which is immediately attacked by the arene (Scheme 1.9).

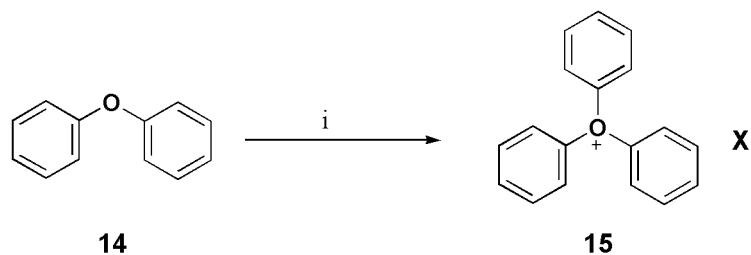


Scheme 1.9 – Proposed mechanism of Friedel-Crafts alkylation using Meerwein's salt activated with the superacid, HSbF_6 .

1.7 - Stable Oxonium Ions

Alkyl oxonium salts require an inert anion to remain stable in solution or in the solid phase. An exception to this were the triphenyloxonium halides synthesized by Nesmeyanov and Tolstaya.²⁵ The stability of **15** is mainly attributed to its aromaticity. Thus, diphenyl ether (**14**) was treated with phenyldiazonium halide to give **15** with

yields ranging between 60-72% (Scheme 1.10). These salts can undergo S_NAr reactions with a wide range of nucleophiles. It was found that refluxing **15** in water for 25 h resulted in decomposition of 50% of the starting material back to phenol and diphenyl ether.



Scheme 1.10 Reagents and conditions: i) PhN_2^+X^- ($\text{X}^- = \text{Cl}^-, \text{Br}^-, \text{I}^-$)

Another well-known example of a stable oxonium ion is the pyrylium ion (**16**), the oxa-analogue of benzene. Unlike typical oxonium salts like **2** and **4**, the oxygen atom is sp^2 hybridized. This particular class of oxonium salts has been well-documented in the literature as versatile synthons in Diels-Alder reactions,²⁶ and for the preparation of substituted pyridines,²⁷ acid/base indicators²⁸ and a wide variety of fluorescent dyes.²⁹ Pyrylium salts are also ubiquitous in nature, being responsible for the vibrant pigments of some flowers³⁰ as well as serving as antioxidants.³¹ A few examples of pyrylium salts are shown below (Figure 1.4). Delphinidin (**17**) is a pyrylium ion which is responsible for the blue-violet color of Cabernet Sauvignon grapes, cranberries and pomegranates.³² Compounds such as Alexa 532 (**18**) are a class of pH insensitive dyes widely used as fluorescent tags in protein assays.³³

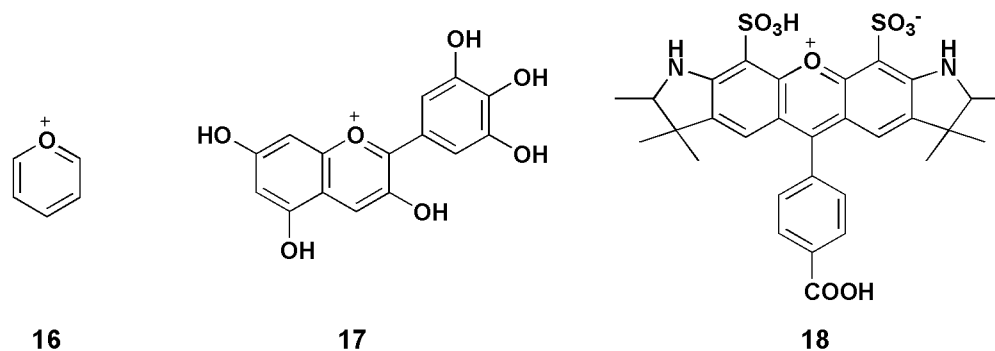
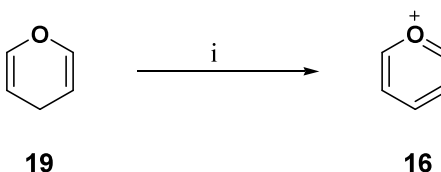


Figure 1.4 – Example of pyrylium oxonium ions.

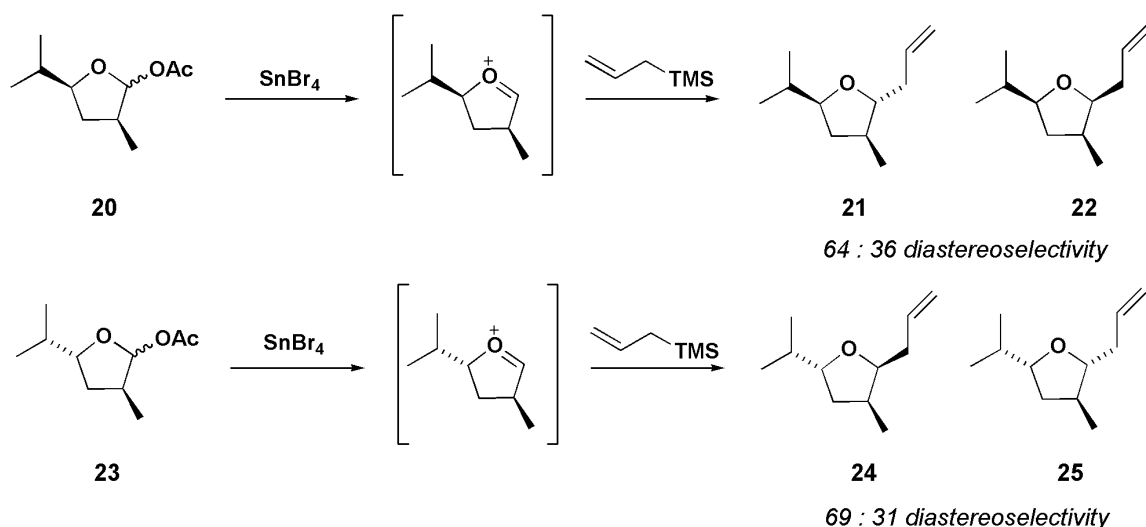
Preparation of **16** is accomplished by treating **19** with triphenylcarbenium tetrafluoroborate, which induces hydride abstraction with the aid of oxygen donating its lone pair electrons in a vinylogous fashion to the σ^* orbital of the C-H bond (Scheme 1.11).³⁴



Scheme 1.11 – Reagents and conditions: i) Ph₃C⁺BF₄⁻.

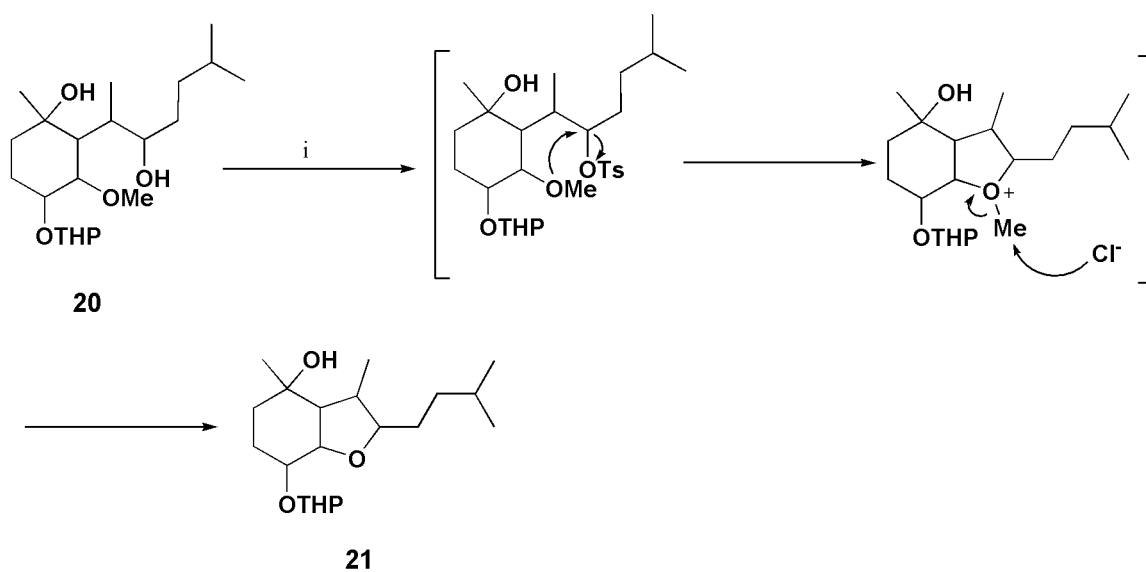
1.8 - Oxonium Ions as Unstable Intermediates

A remarkable volume of literature describes the formation of oxonium ions as unstable intermediates in organic synthesis, the most common of which is the oxo-carbenium ion. The work of Shaw and Woerpel is representative among the myriad of papers in the literature describing oxo-carbenium ions.³⁵ Treatment of a lactol acetate with tin tetrabromide results in the formation of an oxo-carbenium ion, which is subsequently attacked by allyltrimethylsilane in a diastereoselective fashion to give substituted tetrahydrofurans (Scheme 1.12).



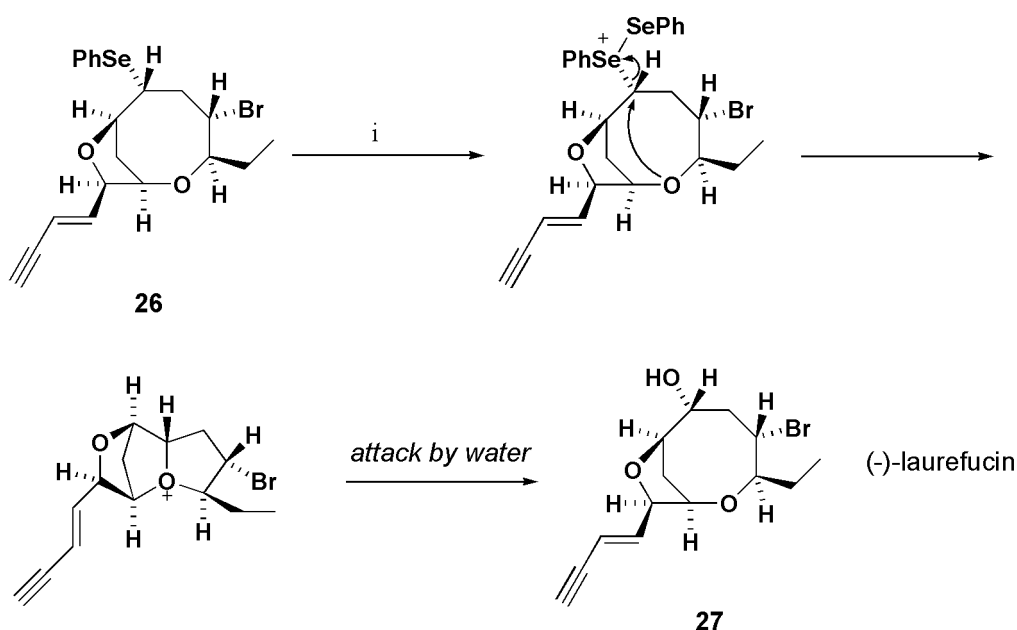
Scheme 1.12 – Lewis acid catalyzed diastereoselective allylation of THF acetals using allyltrimethylsilane described by Shaw and Woerpel.³⁵

Tarbell *et al.* encountered a trivalent oxonium intermediate in their investigations into the chemistry of fumagillin series (Scheme 1.13). Upon treatment of **20** with tosyl chloride in pyridine, the tosylate was displaced by the proximate methoxy group to give an *O*-methyltetrahydrofuranium intermediate. This intermediate was immediately attacked by a halide ion to displace the methyl group to give **21**.³⁶



Scheme 1.13 - Reagents and conditions: i) TsCl, pyridine

Recent work by Kim *et al.* in the biomimetic asymmetric total synthesis of (-)-laurefucin includes a proposed oxonium intermediate (Scheme 1.14).³⁷ When **26** is treated with the selenating reagent N-phenylselenenyl phthalimide (N-PSP), the selenyl ether is activated forming an onium intermediate. This results in transannular attack by the eight-membered ring oxygen to give an oxonium intermediate, which finally undergoes regioselective attack by water to give (-)-laurefucin (**27**). The authors postulate that the oxonium intermediate is also present in the biochemical synthetic pathway for **27**.

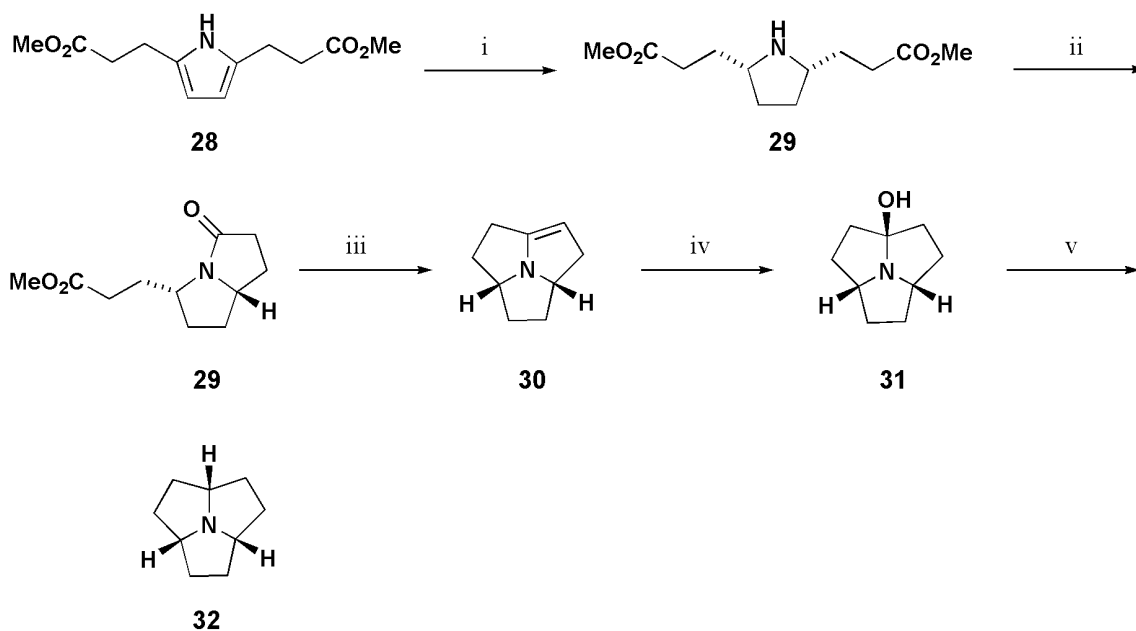


Scheme 1.14 - Reagents and conditions: i) N-PSP (3 eq), PTSA (0.2 eq), CH₃CN/H₂O (9:1), 5mM dilution, rt, 2.5 h, 100%

1.9 - Heterotriquinanes: Synthesis of Azatriquinane, Azatriquinacene and Azaacapentalenide Anion.

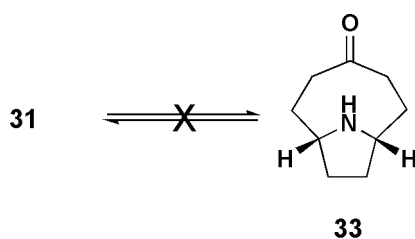
All of the aforementioned oxonium ions can alkylate water or weak nucleophiles due to their kinetic instability. This renders them difficult to examine thoroughly. However, the literature also establishes that molecular architecture can impart unusual reactivity or stability to species that are otherwise highly stable or reactive,

respectively. An interesting case of this is observed in azatriquinane, a bowl-shaped heterocycle with three fused five-membered rings synthesized by Mascali and co-workers as shown in Scheme 1.15.³⁸



Scheme 1.15 - Reagents and conditions: i) H_2 , $\text{Rh}/\text{Al}_2\text{O}_3$, 88%; ii) heat, 94%; iii) sodalime, heat, then iv) water, 70%; v) LiAlH_4 , heat, 97%

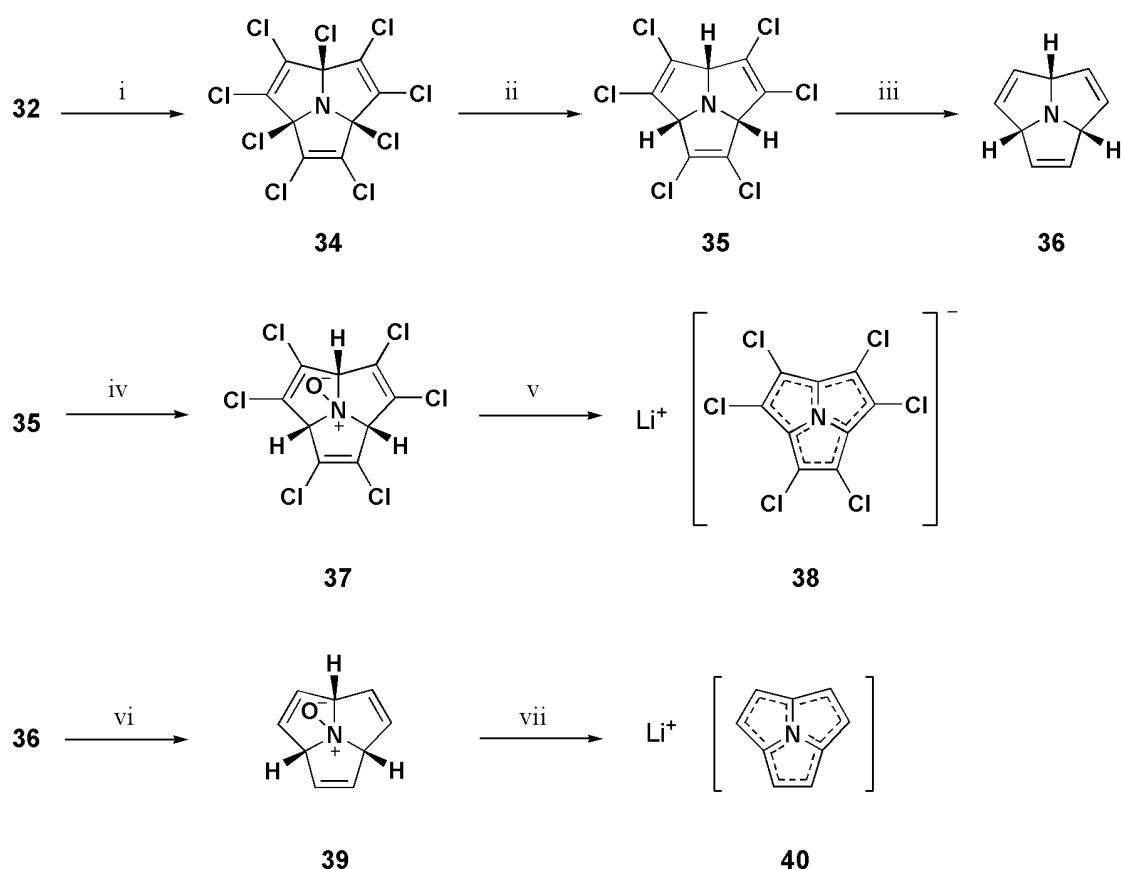
This synthesis underscores the important role that molecular topology plays in two strikingly different ways. The first is the formation of the stable hemiaminal **31**. Hemiaminals are often seen as intermediate structures which rapidly dehydrate to give the more stable imines and enamines. However in the case of enamine **30**, the double bond is strained due to one of the sp^2 carbons being located at a bridgehead position. Furthermore, the ^1H and ^{13}C -NMR indicate that **31** does not undergo equilibrium to amino ketone **33** (Scheme 1.16). This can be attributed to the lesser kinetic stability in forming an eight-membered ring in **33** as opposed to the greater kinetic stability in forming two fused five-membered rings in **31**.



Scheme 1.16 – Mascial and co-workers found no evidence of the formation of keto-amine **33** based on ^1H - and ^{13}C - NMR.

The other important role that molecular topology plays in is the increased basicity observed in **32**. The majority of amines possess structures which permit them to invert the lone pair of the nitrogen ($\Delta H_{\text{inversion}} = 5\text{-}6$ kcal/mol). This results in a decrease in basicity. However, the rigid molecular framework imposed by the fused trefoil structure of **32** prevents the central nitrogen from inverting, thus amplifying its basicity. The same observation is also seen in quinuclidine, which also possesses a nitrogen that is unable to invert. Mascial estimated the pKa of the conjugate acid of **32** to be approximately 10.3 in DMSO, which is 0.5 pKa units greater than quinuclidine and makes it the most basic trialkylamine known in the literature.³⁹

Following the synthesis of **32**, Mascial and co-workers successfully produced azatriquinacene and the azaaceptalenide anion, the dehydro-analogues of **32**.^{40,41} The synthesis of **36** and **40** are shown below in Scheme 1.17. Thus **32** is dissolved in SO_2Cl_2 and irradiated with light, which induces photochlorination and photoelimination to give **34**, an unusually stable chlorinated amine, which can be chromatographed with hexane on silica. The electron-withdrawing chlorines are responsible for the low reactivity of the nitrogen, which is unable to displace the neighboring bridgehead chlorine without the assistance of a strong Lewis acid.



Scheme 1.17 - Reagents and conditions: i) SO_2Cl_2 , hv; ii) Bu_3SnH , benzene; iii) Li, *t*BuOH; iv) *m*-CPBA CHCl_3 ; v) LiHMDS , THF; vi) *m*-cpba, CHCl_3 ; vii) LDA, THF

Compound **34** was found to decompose when exposed to hydrodehalogenation conditions in an attempt to directly prepare **36**. Thus, it was necessary to sequentially hydrodehalogenate by first treating **34** with tributyltin hydride in benzene, followed by a metal reduction with lithium in *tert*-butanol to obtain azatriquinacene (**36**). Despite the bowl-shaped architecture of azatriquinacene, it was conceived that **36** could be oxidized to azaacepentalenide (**40**), a non-planar, fused aromatic anion with a 10π periphery. The formation of **40** and its perchloro analogue **38** were realized when their respective N-oxides, **39** and **37** were treated with strong base to induce

elimination of the LiO^- anion. Although **40** was only found to be stable in solution, **38** was stable enough to be purified by chromatography.

1.10 - Aims and Objectives

Considering the impact molecular topology can make on the stability of **31**, **32**, **38**, and **40** as well as the enhanced basicity of **32**, we decided to utilize the triquinane scaffold for the preparation of novel oxonium ions, **41-44** (Figure 1.4).

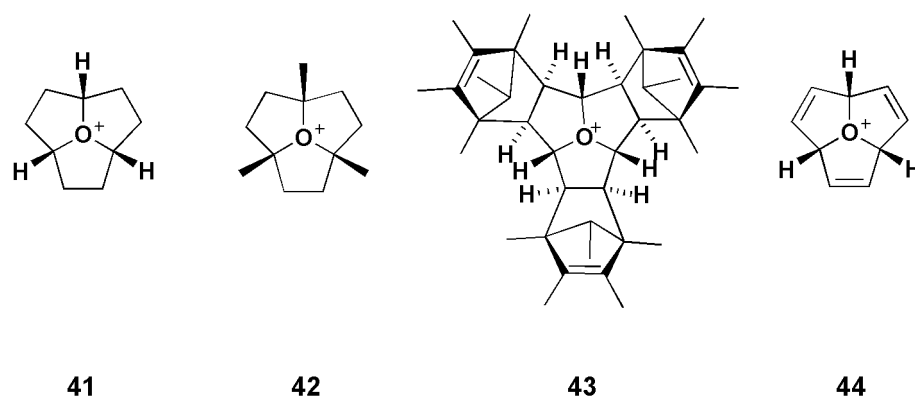


Figure 1.5 – Oxatriquinane and various derivatives.

The work described herein pertains to the synthesis, characterization and properties of *oxatriquinanes* **41** and **42**, *oxatriquinacene* (**44**) and the proposed synthesis of **43**. With these oxoniums in hand, we would be able to probe the reactivity with various nucleophiles.

References

- 1) Danneel, H. *Z. Elektrochem.* **1905**, *11*, 249-252.
- 2) a) Hantzsch, A.; Caldwell, K. C. *Z. physik. Chem.* **1907**, *58*, 575-84. b) Hantzsch, A. *Z. physik. Chem.* **1908**, *61*, 257-312
- 3) a) Bronsted, J. N. *Recl. Trav. Chim. Pays-Bas Belg.* **1923**, *42*, 718-28.
b) Bronsted, J. N. *J. Phys. Chem.* **1926**, *30*, 777-90. c) Lowry, T. M. *Trans. Faraday Soc.* **1930**, *26*, 45-6.
- 4) Farcasiu, D.; Hancu, D. *J. Phys. Chem. A* **1999**, *103*, 754-761.
- 5) a) Bethell, D. E.; Sheppard, N. *J. Chem. Phys.* **1953**, *21*, 1421. b) Ferriso, C. C.; Hornig, D. F. *J. Chem. Phys.* **1955**, *23*, 1464-8
- 6) Taylor, R. C.; Vidale, G. L. *J. Am. Chem. Soc.* **1956**, *78*, 5999-6002.
- 7) Olah, G. A.; Prakash, G. K.; Barzaghi, M.; Lammertsma, K.; Schleyer, P. V. R.; Pople, J. A. *J. Am. Chem. Soc.* **1986**, *108*, 1032-5.
- 8) a) Lundgren, J. O.; Williams, J. M. *J. Chem. Phys.* **1973**, *58*, 788-96. b) Lundgren, J. O.; Tellgren, R.; Olovsson, I. *Acta Crystallogr., Sect. B* **1978**, *B34*, 2945-7.
- 9) Christe, K. O.; Schack, C. J.; Wilson, R. D. *Inorg. Chem.* **1975**, *14*, 2224-30
- 10) Sowerby, D.B. *The Chemistry of Inorganic Homo and Heterocycles* (Edited by I. Haiduc and D. B.Sowerby), Vol. 2. Academic Press, London **1987**.
- 11) Breunig, H. J., *Main Group Metal Chemistry* **1993**, *16*, 143.
- 12) Carozzi, E. *Gazz. Chim. Ital.* **1926**, *56*, 175-9.
- 13) Šćavnićar, S.; Grdenić, D. *Acta Crystallogr.* **1955**, *8*, 275-9.
- 14) Harada, T. *Bull. Chem. Soc. Jpn.* **1940**, *15*, 455-8.
- 15) Räke, B.; Müller, P.; Roesky, H. W.; Usón, I. *Angew. Chem., Int. Ed.* **1999**, *38*, 2050-2052.

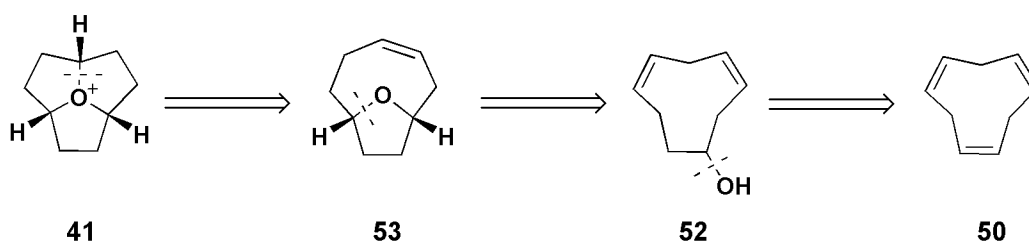
- 16) Breunig, H. J.; Mohammed, M. A.; Ebert, K. H. *Polyhedron* **1994**, *13*, 2471-2.
- 17) a) Meerwein, H.; Hinz, G.; Hofmann, P.; Kroning, E.; Pfeil, E. *J. Prakt. Chem. (Leipzig)* **1937**, *147*, 257-85.
- 18) a) Goodrich, R.A.; Treichel, P.M. *J. Am. Chem. Soc.*, **1966**, *88 (15)*, 3509–3511.
b) Olah, G.A.; Olah, J.A.; Svoboda, J.J. *Synthesis*, **1973**, 490-492.
- 19) Helmkamp, G. K.; Pettitt, D. J. *Org. Synth.* **1966**, *46*, 122-6.
- 20) Klages, F.; Jung, H. A. *Chem. Ber.* **1965**, *98*, 3757-64.
- 21) Etzkorn, M.; Aniszfeld, R.; Li, T.; Buchholz, H.; Rasul, G.; Prakash, G. K. S.; Olah, G. A. *Eur. J. Org. Chem.* **2008**, 4555-4558.
- 22) Umemoto, T.; Adachi, K.; Ishihara, S. *J. Org. Chem.* **2007**, *72*, 6905-6917.
- 23) Meerwein, H.; Hinz, G.; Hofmann, P.; Kroning, E.; Pfeil, E. *J. Prakt. Chem. (Leipzig)* **1937**, *147*, 257-85. b) Meerwein, H.; Florian, W.; Schon, N.; Stopp, G. *Justus Liebigs Ann. Chem.* **1961**, *641*, 1-39.
- 24) Meerwein, H.; Borner, P.; Fuchs, O.; Sasse, H. J.; Schrodtt, H.; Spille, J. *Chem. Ber.* **1956**, *89*, 2060-79.
- 25) Nesmeyanov, A. N.; Tolstaya, T. P. *Dokl. Akad. Nauk SSSR* **1957**, *117*, 626-8.
- 26) Ohkata, K.; Lee, Y. G.; Utsumi, Y.; Ishimaru, K.; Akiba, K. *J. Org. Chem.* **1991**, *56*, 5052-9.
- 27) a) Schneider, W.; Riedel, W. *Ber. Dtsch. Chem. Ges. B* **1941**, *74B*, 1252-78.
b) Shriner, R. L.; Johnston, H. W.; Kaslow, C. E. *J. Org. Chem.* **1949**, *14*, 204-9.
c) Balaban, A. T. *Org. Prep. Proced. Int.* **1977**, *9*, 125-30.
- 28) Kolling, O. W.; Smith, M. L. *Anal. Chem.* **1959**, *31*, 1876-9
- 29) Höfelschweiger, B. K. PhD Dissertation, University of Regensburg, 2005.
- 30) a) For flavanoids, see: Geissman, T. A.; Jorgensen, E. C.; Johnson, B. L. *Arch*

- Biochem Biophys* **1954**, *49*, 368-88. b) For anthocyanins, see: Karzel, R. *Österreichische Botan. Z.* **1909**, *56*, 348.
- 31) Arora, A.; Nair, M. G.; Strasburg, G. M. *Free Radic Biol Med* **1998**, *24*, 1355-63.
- 32) a) Ribereau-Gayon, J.; Ribereau-Gayon, P. *Am. J. Enol.* **1958**, *9*, 1-9. b) Afaq, F.; Syed, D. N.; Malik, A.; Hadi, N.; Sarfaraz, S.; Kweon, M.-H.; Khan, N.; Zaid, M. A.; Mukhtar, H. *J. Invest. Dermatol.* **2007**, *127*, 222-232.
- 33) Panchuk-Voloshina, N.; Haugland, R. P.; Bishop-Stewart, J.; Bhalgat, M. K.; Millard, P. J.; Mao, F.; Leung, W. Y. *J Histochem Cytochem* **1999**, *47*, 1179-88.
- 34) Belosludtsev, Y. Y.; Borer, B. C.; Taylor, R. J. K. *Synthesis* **1991**, 320-2
- 35) Tarbell, D. S.; Carman, R. M.; Chapman, D. D.; Cremer, S. E.; Cross, A. D.; Huffman, K. R.; Kuntsmann, M.; McCorkindale, N. J.; McNally, J. G., Jr.; Rosowsky, A.; Varino, F. H. L.; West, R. L. *J. Am. Chem. Soc.* **1961**, *83*, 3096-3113.
- 36) Shaw, J. T.; Woerpel, K. A. *Tetrahedron* **1999**, *55*, 8747-8756.
- 37) Kim, B.; Lee, M.; Kim, M. J.; Lee, H.; Kim, S.; Kim, D.; Koh, M.; Park, S. B.; Shin, K. J. *J. Am. Chem. Soc.* **2008**, *130*, 16807-16811.
- 38) a) Mascal, M.; Hext, N. M.; Shishkin, O. V. *Tetrahedron Lett.* **1996**, *37*, 131-4.
- 39) Hext, N. M.; Hansen, J.; Blake, A. J.; Hibbs, D. E.; Hursthouse, M. B.; Shishkin, O. V.; Mascal, M. *J. Org. Chem.* **1998**, *63*, 6016-6020.
- 40) Mascal, M.; Lera, M.; Blake, A. J. *J. Org. Chem.* **2000**, *65*, 7253-7255.
- 41) Mascal, M.; Ceron-Bertran, J. *J. Am. Chem. Soc.* **2005**, *127*, 1352-1353.

Chapter 2
Oxatriquinane

2.1 - Introduction

It became evident from the beginning of this endeavor that we could not adopt the same synthetic pathway used to obtain azatriquinane in preparing oxatriquinane. Thus, we explored a *de novo* synthetic route via retrosynthetic analysis. It was envisaged that the carbon-oxonium bond could be formed through an acid-induced attack of the double bond in **53** by the THF oxygen, since the driving force of the reaction would be the contraction of an eight-membered medium ring to form two energetically favorable five-membered rings (Scheme 2.1).¹



Scheme 2.1 – Retrosynthetic analysis for oxatriquinane.

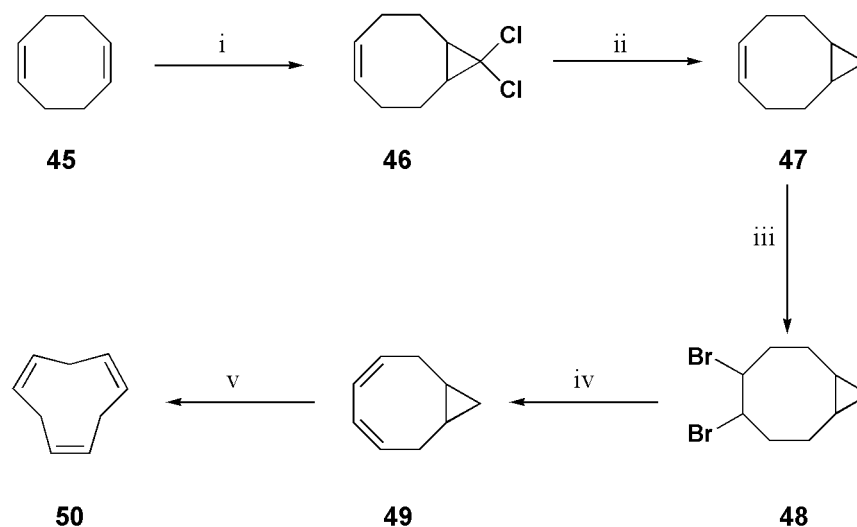
2.2 - Retrosynthetic Analysis for the Synthesis of Oxatriquinane

Intramolecular etherification could be accomplished either by acid-catalyzed addition of the alcohol across a double bond, oxymercuration-demercuration, or halo-etherification followed by hydro-dehalogenation. Lastly, the alcohol could conceivably be made from the known 1,4,7-cyclononatriene.

2.3 - Preparation of Cyclonona-3,6-dien-1-ol

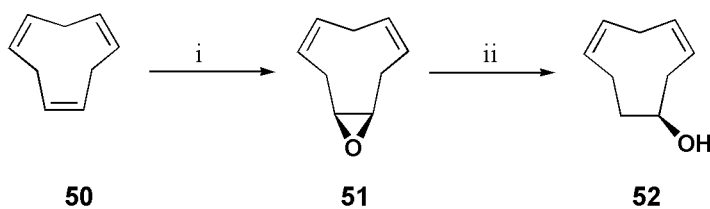
Starting from the commercially available 1,5-cyclooctadiene (**45**) and sodium trichloroacetate in 1,2-dimethoxyethane, we obtained **46** which was subsequently hydro-dehalogenated with sodium metal in isopropanol/THF to give **47**.²

Bromination of the resulting alkene in the presence of the cyclopropane ring was accomplished by carefully treating a solution of **47** in dichloromethane with a dilute bromine solution at 0 °C.² Regioselective elimination of the **48** could be accomplished by inducing a two-fold carbonate pyrolysis using LiBr/Li₂CO₃ in DMSO.² Finally, by heating neat **49**, it is possible to induce two 1,5-hydride rearrangements to obtain **50** in good yield (Scheme 2.2).³



Scheme 2.2 – Reagents and conditions: i) Cl₃CCO₂Na, glyme, reflux; 68% ii) Na⁰, iPrOH, THF; 85% iii) Br₂, CH₂Cl₂, 72%

From triene **50**, the mono-epoxide **51** can be prepared by treatment with *m*-CPBA according to the method of Thies *et al* in good yield (Scheme 2.3).⁴ The next step involved cleavage of the epoxide with a hydride source to obtain alcohol **52**. Unlike most epoxides, which are generally known to be labile towards hydrolysis and strong nucleophiles, epoxide **51** was found to be quite resilient toward cleavage.



Scheme 2.3 – Reagents and conditions: i) m-CPBA, CH₂Cl₂; 85% ii) LiAlH₄, ZnCl₂, Et₂O, 99%

Treatment of **51** with lithium aluminum hydride in refluxing THF resulted only in a 32% yield of alcohol **52** after 72 hours, the remainder of which was starting material. The difficulty in reduction stems from the crown-shaped conformation adopted by epoxide. This conformation restricts an aluminum hydride anion from approaching behind in the endospace (Figure 2.1)

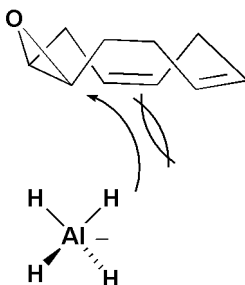
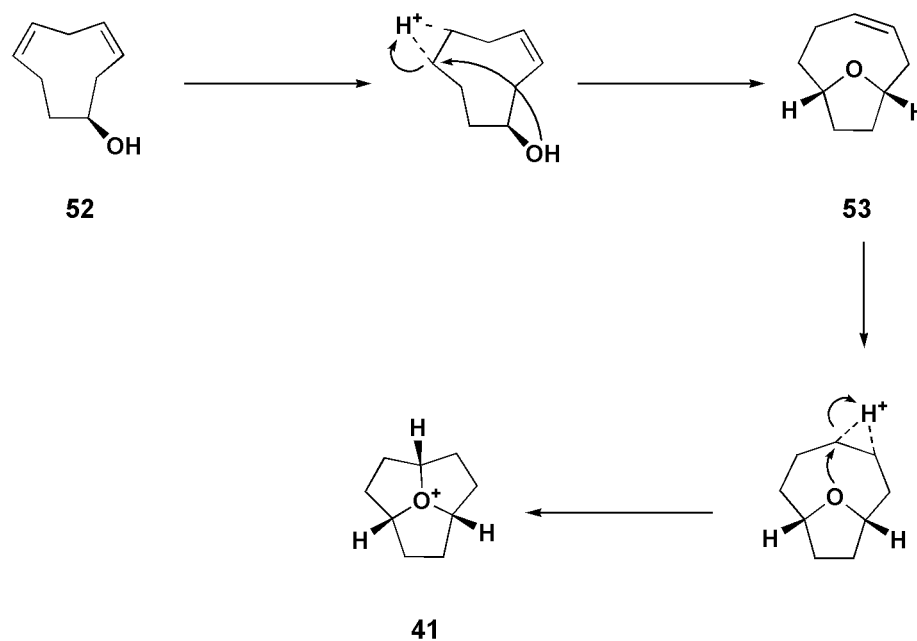


Figure 2.1 – The crown conformation of **51** prevents the tetrahydroaluminate ion from reacting in a S_N2-type manner.

Thus, we believed that by sufficiently activating the epoxide with a Lewis acid, we could push the reaction towards completion. The literature describes many ways of opening epoxides by reduction such as the use of DIBAL and selectrides.⁵ For epoxide **51**, the use of AlH₃ proved to be most effective means of reduction. Alane can be prepared by treating lithium aluminum hydride with either concentrated sulfuric acid, beryllium chloride, or aluminum trichloride in THF.⁶ Initially we chose to employ the latter, however the reaction was so exothermic that the solvent became prone to ignition. A milder method was found by using zinc chloride in diethyl

ether.⁷ A suspension of lithium aluminum hydride in a solution of epoxide **51** in diethyl ether was treated with zinc chloride in small portions and stirred for two hours to give **52** in quantitative yield.

With the alcohol **52** in hand, we initially hoped that we could get the target oxonium **41** simply by treating the alcohol with strong acid to induce an intramolecular alkoxylation of the double bond followed by electrophilic activation of the remaining double bond with acid and attack by the THF oxygen to give the target (Scheme 2.4).

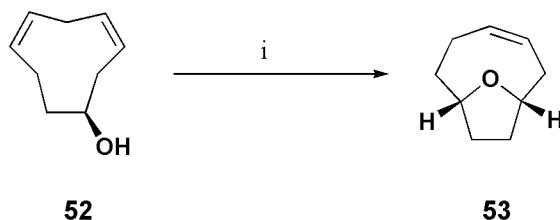


Scheme 2.4 – Suggested mechanism outlining the route towards **41** directly from **52**.

2.4 - Transannulation of Cyclonona-3,6-dien-1-ol

A solution of alcohol in deuterated chloroform was treated with triflic acid and the reaction was monitored by ¹H-NMR. Unfortunately, the acid was found to dehydrate the alcohol quantitatively to give back triene **50**. Although acid-catalyzed addition of

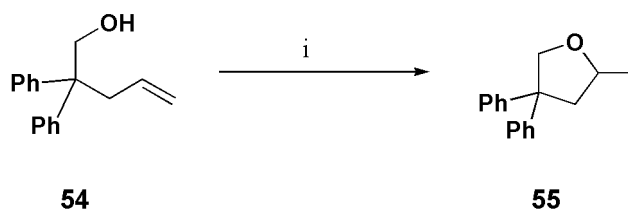
alcohols across double bonds are firmly established in the literature, most of the examples found involved the use of a primary alcohol, which are difficult to dehydrate.



Scheme 2.5 - Reagents and conditions: i) $\text{Hg}(\text{OAc})_2$, THF, H_2O , then NaBH_4 , $\text{NaOH}_{(\text{aq})}$, 28%

We then decided to re-examine the synthetic route towards oxatriquinane in a stepwise manner. Our goal now was to isolate the intermediate THF bicycle **53**. The classical route towards this target can be envisaged by performing oxymercuration/demercuration as it is a common method of adding an alcohol across a double bond.⁸ Thus, a solution of the alcohol in THF was treated with mercuric acetate and subsequently reduced with a basic solution of sodium borohydride to give the volatile **53** in a low yield (Scheme 2.5). According to TLC analysis, all the starting alcohol had been consumed and only one product could be observed. However, a satisfactory mass balance could not be established after examining both organic and aqueous phases. Attempts were also made to prepare and isolate the oxo-mercury intermediates, however the yields of those reactions were comparably low.

Few methods of intramolecular etherification are described in the literature, other than the aforementioned acid-catalyzed cyclization. One particularly attractive alternative was described by Widenhoefer *et al.*,⁹ who was able to induce an intramolecular cyclization of alcohols using a $[(\text{CH}_2=\text{CH}_2)_2\text{PtCl}_2]_2$ catalyst with phosphine ligands in tetrachloroethane (Scheme 2.6).



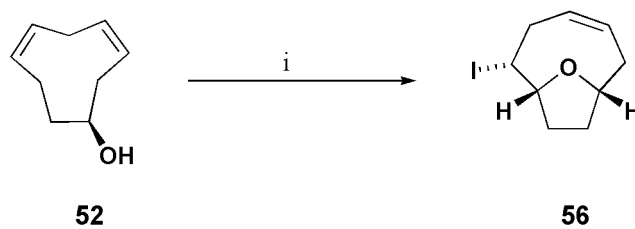
Scheme 2.6 – Reagents and conditions: $[(\text{CH}_2=\text{CH}_2)_2\text{PtCl}_2]$, $(4\text{-C}_6\text{H}_4\text{CF}_3)_3\text{P}$, 1,1,2,2-tetrachloroethane, 70°C .

The authors were able to induce an intramolecular hydroalkoxylation to get 2-methyl-3-diphenyl-tetrahydrofuran in a 76% yield with 100% regioselectivity for the five-membered ring (Scheme 2.6). Thus, a solution of alcohol was dissolved in tetrachloroethane and treated with 1 mol% $[(\text{CH}_2=\text{CH}_2)_2\text{PtCl}_2]$ and 2 mol% $(4\text{-C}_6\text{H}_4\text{CF}_3)_3\text{P}$ with heated to 70°C in a pressure vessel to avoid losing the volatile product. Unfortunately, the reaction resulted in complete recovery of the starting material. It is interesting to note that all the model alcohols used by the authors contained phenyl rings in close proximity to the reactive sites.

2.5 - Haloetherification

We then turned our attention towards haloetherification of alcohol **52**. This method was particularly attractive since it does not involve the use of toxic or precious metals such as mercury or platinum, respectively. The literature offers a plethora of examples on halolactonization.¹⁰ Haloetherification, although known, is far less common. The alcohol was tested for its reactivity towards various halonium sources such as bromine, NBS, and iodine. A solution of alcohol **52** in dichloromethane was treated with each of the mentioned reagents. Bromine was found to decompose the starting alcohol, while NBS gave some desired product,

along with the same distribution of TLC found in the reaction with bromine. On the other hand, reaction with iodine cleanly yielded the desired iodo-ether **56**. Iodine was found to be a superior reagent because it could be used in excess, without concern for dihalogenation of the olefin. Although the reaction worked well, it was very slow in dichloromethane. Other more polar solvents were tested in order to accelerate the reaction. THF was not suitable, since it was found to react readily with iodine to give 4-iodobutyl hypoiodite. Examination of the literature established that acetonitrile was the main solvent, other than dichloromethane, employed in reactions involving iodine.



Scheme 2.7 – Reagents and conditions: i) I₂, CH₃CN, 20 min, rt, 80%

Thus, a solution of alcohol in acetonitrile was treated with one equivalent of iodine and stirred for twenty minutes at room temperature (Scheme 2.7). According to TLC analysis, a substantial amount of starting material was present while a single new spot appeared with a higher R_f. It was discovered that the HI produced in the reaction combined with the remaining iodine to form HI₃ as a side product, which was observed as a black oil. By adding an additional equivalent of iodine, the reaction could be pushed to completion. Care was taken not to leave the reaction overnight, as it was found that light-sensitive hydrogen iodide, which is produced as a side product via disproportionation from HI₃, could hydrodehalogenate the desired

iodo-THF **56** to give **53** (Scheme 2.9). Although an intriguing observation, the reaction could not be utilized for practical purposes.

2.6 - Hydrodehalogenation of 6-Iodo-10-oxa-bicyclo[5.2.1]dec-3-ene (**56**)



Scheme 2.8 – Hydrodehalogenation of **56** to obtain **53**.

2.6.1 - Sodium and Zinc Metal in Protic Solvent

With **56** in hand, we began to explore methods of hydrodehalogenation (Scheme 2.8). We first attempted standard hydrodehalogenation conditions such as the use of sodium metal in ethanol. Upon exposure to sodium metal in ethanol, the THF ring was immediately cleaved to give the starting alcohol **52**. Milder conditions such as using zinc dust in acetic acid also lead to the formation of **52**.

2.6.2 - Hydrogen Iodide

As mentioned previously, hydrogen iodide can be used in hydrodehalogenation reactions, however it is a highly air-sensitive gas and could easily cleave the THF ether.

2.6.3 - Tributyltin Hydride

The most common method of hydrodehalogenation was employing tributyltin hydride in the presence of a radical initiator. Thus, a solution of **56**, tributyltin hydride, and the radical initiator AIBN was irradiated overnight in THF. Unfortunately, the resulting mixture only contained starting material. The same result was obtained by switching the radical initiator to benzoyl peroxide.

2.6.4 - Lithium Aluminum Hydride

Lithium aluminum hydride is also used to hydrodehalogenate alkyl halides and proceeds through a radical mechanism. A solution of **56** was treated with lithium aluminum hydride in diethyl ether overnight to give the desired product along with a minor amount of unreacted starting material according to TLC analysis. However, upon purification of the crude mixture with column chromatography, only a 28% yield of **53** was obtained.

2.6.5 - Raney Nickel

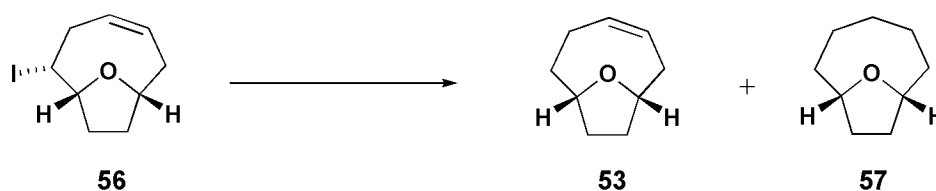
Hydrogenation is a well-established method of hydrodehalogenating alkyl halides. In the case of **56**, which possesses a double bond, hydrogenation, at first glance, does not appear to be a viable approach. Indeed, catalysts such as palladium or platinum on solid support are commonly used to hydrogenate double bonds. However, we began to entertain the possibility of a chemoselective metal catalyst capable of hydrodehalogenation without simultaneously hydrogenating a double bond. A thorough search of the literature yielded only one paper published by Barrero *et al.*,¹¹ which outlined the use of excess Raney Nickel in dehalogenation reactions. The

authors were able to chemoselectively hydrodehalogenate alkyl halides which possessed either nitriles or alpha-beta unsaturated esters. Encouraged by these results, we proceeded to treat a solution of **56** in THF with excess Raney Nickel at room temperature, which was agitated for twenty minutes to give **53** in a 54% yield. However, drawbacks to this method became evident in two respects. First, the reaction required a large excess of Raney Nickel to push the reaction to completion. A review of the literature revealed that Raney Nickel was susceptible to poisoning by halide ions, in the order of $I^- < Br^- \ll Cl^-$. This also makes the method difficult to employ on large scales as Raney Nickel is highly pyrophoric and must be disposed of with care. Second, an 1H -NMR spectrum of the crude product revealed that a minor impurity, ether **57**, was present. When allowing the reaction to stand overnight, **53** becomes fully hydrogenated to give **57**. Efforts were made to separate **53** from **57** using column chromatography. Despite all attempts, TLC analysis revealed that these two compounds were inseparable using various combinations of eluents. However, compounds **53** and **57** could be distinguished by permanganate dip, in which the former would appear immediately after being submersed into the dip, whereas compound **57** required the use of a heatgun to be visualized.

2.6.5.1 - Tuning the Reactivity of Raney Nickel with Poisons

The substantial reactivity of Raney Nickel towards unsaturated compounds was not fully appreciated. However, the fact that it was susceptible to poisoning made us consider whether the reactivity of Raney Nickel could be tuned with poisons in a similar manner to Lindlar's catalyst, which is poisoned to a point in which it can reduce alkynes but not alkenes. Whereas poisons for Raney Nickel are well

documented in the literature, none have been described to tune reactivity. Some poisons include salts of zinc, lead, mercury, as well as alkyl halides, hydrohalic acids and sulfides.¹² Quinoline was also included as it has been used before to tune metal catalysts. Thus, slurries of Raney Nickel were pretreated with 10 mol% of the following poisons outlined in Table and reacted with **56** in THF (Scheme 2.9).

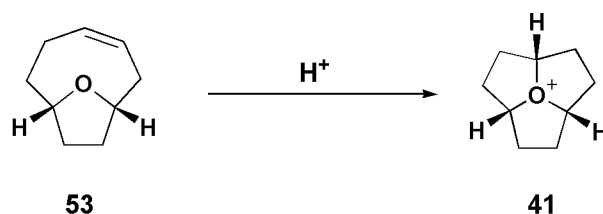


<u>Poison</u>	<u>Result</u>
-----	Over-reduction
ZnCl ₂	No Reaction
Pb(OAc) ₄	No Reaction
HgCl ₂	No Reaction
Bu ₄ N ⁺ Br ⁻	No Reaction
Quinoline	Over-reduction
ClCH ₂ CH ₂ Cl	Over-reduction

Scheme 2.9 – Reagents and conditions: i) Ra-Ni, THF, water, poison (see table above).

All reactions were monitored using TLC. Unfortunately, the poisons were found to either completely deactivate the catalyst or to be ineffective in suppressing reactivity. Similar observations were made by Choudhary and Chaudhari while measuring the rate of hydrogenation of styrene using Raney Nickel poisoned with hydrogen chloride gas.¹² Despite efforts, we were unable to separate the impurity from **53** and decided to carry over the contaminated precursor to prepare oxatriquinane (**41**).

2.7 - Endgame: Synthesis of Oxatriquinane



Scheme 2.10 – Treatment of **53** with acid to form oxonium **41**.

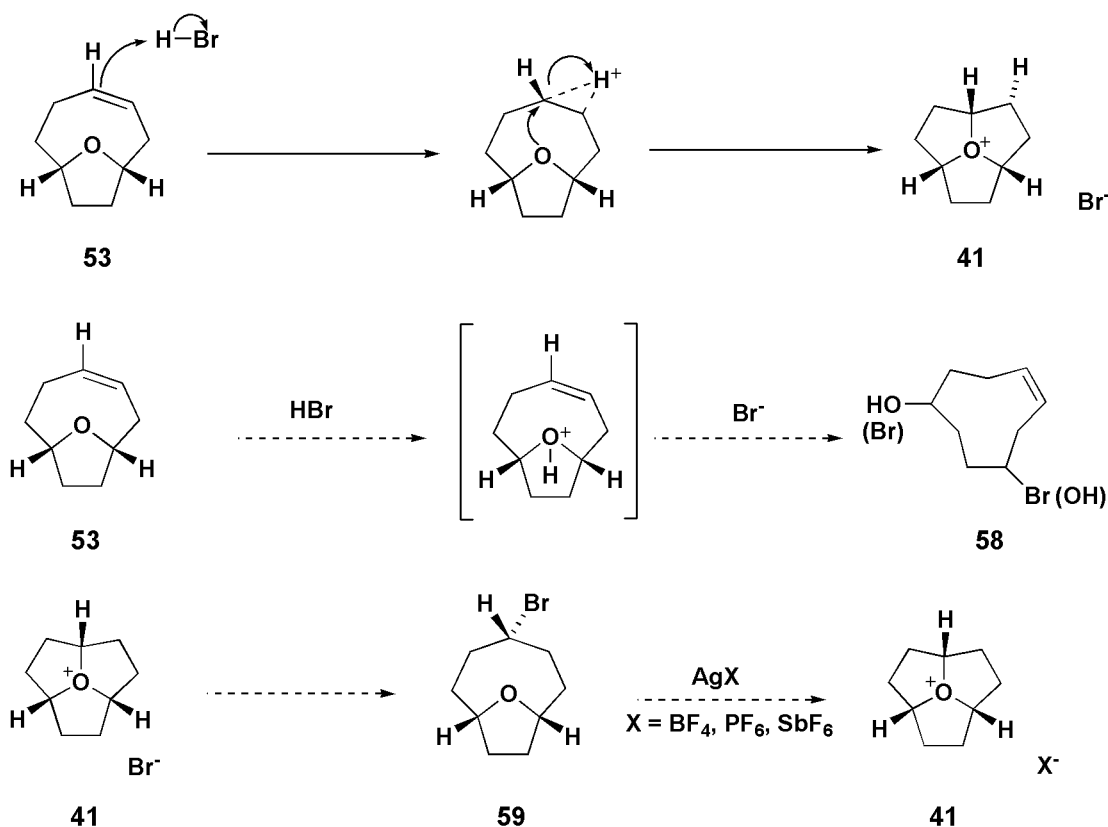
To accomplish the transformation of **53** to **41**, we needed a strong acid (Scheme 2.10). The first acid we employed was trifluoroacetic acid, which we supposed was strong enough since TFA has been known to add across double bonds. Thus a solution of **53** in chloroform was treated with one equivalent of TFA at room temperature. However, no reaction was observed. We then tried using sulfuric acid, which is 10^{10} times more acidic than TFA, but it too failed to induce ring closure. The resilience of **53** against protonation by common strong acids made us resort to using superacids, which are acids with pKas lower than sulfuric acid (pKa = -10). Two common superacids are triflic acid (pKa = \sim -16) and hexafluoroantimonic acid (pKa = \sim -31). We chose triflic acid, since hexafluoroantimonic acid contains a considerable amount of the Lewis acidic SbF₅, which could cleave the THF ring. Next, an appropriate solvent was needed to carry out the reaction, as it was found that triflic acid was sparingly soluble in chloroform. Solvents such as methanol, THF, and DMSO, form weaker conjugate acids with triflic acid. However, the pKa of protonated acetonitrile is -14, which is still ten thousand times stronger than sulfuric acid. Thus, a solution of **53** in acetonitrile was treated with triflic acid at room temperature to give oxatriquinane triflate in quantitative yield. The formation was

easily evidenced by the reduced complexity in the $^1\text{H-NMR}$ spectrum. Rather than forming a solid, the triflate salt of oxatriquinane was a brownish oil. We believed that by exchanging the triflate counterion with different ones, such as tetrafluoroborate, hexafluorophosphate, or hexafluoroantimonate, we could obtain a solid with which we could grow small crystals for x-ray crystallography. Despite our efforts, employing typical anion metathesis techniques followed by work-up failed to give **41** as a solid.

2.7.1 - The Bromide Salt of Oxatriquinane

Whereas the triflate anion was difficult to exchange due to its high affinity for polar aprotic solvents, halides such as the bromide ion are highly hydrophilic and can easily facilitate an anion exchange with more lipophilic anions such as hexafluorophosphate. Thus, we turned our attention towards preparing the bromide salt of **41**, which we could subsequently convert into a tetrafluoroborate, hexafluorophosphate, or hexafluoroantimonate salt through a biphasic exchange. This approach presented two significant challenges. First, the preparation of a bromide salt of oxatriquinane would require the use of hydrogen bromide gas, which is a standard condition for cleaving ethers and could lead to the formation of compound **58**. Second, the bromide ion has appreciable nucleophilicity, and oxonium ions such as Meerwein's salt would be expected to alkylate bromide. Thus, it could be predicted that a product equivalent to the hydrohalogenation of the double bond could be observed. However, the latter case would occur regioselectively to give **59** could then be treated with a silver salt of tetrafluoroborate, hexafluorophosphate, or

hexafluoroantimonate to give our target compounds **41** BF_4^- , PF_6^- , or SbF_6^- , respectively (Scheme 2.11).



Scheme 2.11 – Possible outcomes from the treatment of **53** with $\text{HBr}_{(g)}$.

When considering the preparation of oxatriquinane from **53**, one potential challenge becomes apparent. Compound **53** is an ambident base, in which protonation could occur either on the double bond or the more basic THF oxygen. Thus, it was possible that by treating **53** with a strong acid, simple protonation of the THF oxygen could occur to give protonated **53** (Scheme 2.11). On the other hand, molecular modeling suggests that the THF oxygen is poised closely on top of the double bond. Orbital arguments can then be made that electron density is transferred

to the double bond through a lone pair- π^* interaction, resulting in a more basic double bond (Figure 2.1).

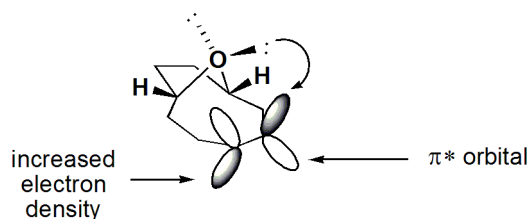


Figure 2.2 – The lone pair of the THF oxygen in **53** is thought to be poised directly over the π^* orbital of the double bond. This would lower electron density of the oxygen and increase electron density and basicity of the neighboring sp^2 carbon.

Thus, a solution of **53** in chloroform was treated with a steady stream of dry hydrogen bromide gas generated by heating a suspension of triphenyl phosphonium bromide in toluene. After ten minutes, a small droplet oiled out of solution and settled to the bottom of the flask, suggesting that the droplet had a higher density than chloroform and was not adventitious water. The supernatant chloroform was separated and the droplet was triturated with diethyl ether to give the bromide salt of oxatriquinane in excellent yield as a yellowish oil.

2.8 - Reactivity of Oxatriquinane

Heating **41** Br⁻ in neat conditions caused the bromide to attack oxatriquinane to give **59**. We then prepared the oxonium salt for hydrolysis in water by dissolving the salt in deuterated water and characterizing the product by ¹H-NMR. We were surprised, however, to observe that **41** persisted in water. No evidence of hydrolysis or attack by bromide was found. Given that it survived hydrolysis at room temperature, it appeared likely that a small activation barrier was blocking the hydrolysis pathway. So, we resorted to heating the solution in the NMR probe to 70

°C to induce a reaction. However, the oxonium remained intact. This is the first time a trialkyl oxonium ion was able to persist in water without *any* decomposition. The stability of oxatriquinane in water was formally established in an experiment to which a solution of **41** in deuterated water was refluxed and samples were analyzed by NMR over the span of 72 hours, showing no evidence of decomposition. The oxonium was also found to be stable in alcohols, acetone, acetonitrile, DMF, and DMSO. With regards to nucleophiles, **41** was found to react immediately with strong nucleophiles such as azide, cyanide, hydroxide, and triphenylphosphine. Treatment of **41** PF₆⁻ with either lithium bromide or iodide in methanol gave no reaction. Remarkably, treatment with Hünig's base gave no reaction, whereas DBU was slowly alkylated. An important question is raised from these observed results: what is the property that distinguishes the stability of oxatriquinane from typical alkyl oxonium ions?

2.8.1 - Explanation of the Unusual Stability of Oxatriquinane

The answer to the stability of **41** lies in a topological phenomenon called the medium-ring effect. Rings which consist of between three to six atoms primarily endure steric congestion from neighboring substituents, whereas rings consisting of more than nine atoms possess substantial torsional strain. Medium rings, which consist between seven and nine atoms, have to endure both types of strain as they are too small to avoid steric congestion and too large to avoid torsional strain. The summation of these properties make medium rings both difficult to form, and susceptible to ring contractions and expansions. In the case of **41**, a nucleophilic attack by water would result in the replacement of two, stable, five-membered rings,

with the formation of one, higher-energy, eight-membered ring. This barrier can be overcome, for example, in reactions between **41** and strong nucleophiles.

2.8.2 - Anion Exchange and X-Ray Crystal Structure Determination

Our efforts now turned towards anion exchange. Our first attempt was to “salt out” oxatriquinane by treating a solution of saturated MX (M=Na, K; X=BF₄, PF₆, SbF₆) in water with a concentrated solution of **41** Br⁻ in water. Our expectation was that a solid would precipitate and be isolated. In the case of sodium tetrafluoroborate, no precipitate was observed. The aqueous layer was extracted with dichloromethane and the combined organic layers were evaporated to give the tetrafluoroborate salt of oxatriquinane as an oil. However, when potassium hexafluorophosphate or hexafluoroantimonate was used, a white precipitate immediately formed. The solids were isolated and identified by NMR to be pure salts of **41**. Unfortunately, a substantial amount of **41** was soluble in the aqueous layer, so extractions were necessary to recover the remaining material. Unlike the triflate and bromide salts of oxatriquinane, which remain immobile on silica, the PF₆ and SbF₆ salts could be purified by flash column chromatography using dichloromethane as the eluent.

With the solid oxonium ion in hand, attempts were made to grow crystals suitable for x-ray crystallography. A biphasic approach was adopted since it was known that **41** was soluble in dichloromethane and insoluble in ether. Slow diffusion of ether into a solution of **41** SbF₆⁻ in dichloromethane gave a crystalline solid which was incapable of refracting polarized light. Different solvent combinations and diffusion techniques were found to give the same result. Using a more standard approach, a saturated solution of **41** SbF₆⁻ in water was heated to 100 °C and allowed to cool

slowly. However the precipitated crystals were not suitable for x-ray crystallography. Finally, a concentrated solution of **41** SbF₆⁻ in dichloromethane was allowed to slowly evaporate overnight. Unlike the biphasic systems, this method was able to yield crystals suitable for x-ray crystallography.

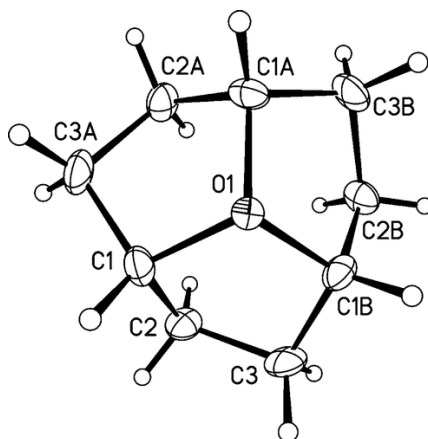


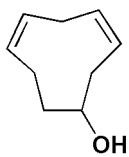
Figure 2.3 - X-ray crystal structure of cation of **41** SbF₆⁻ showing thermal ellipsoids at the 50% probability level. The counterion and a minor disorder component are omitted for clarity.

The x-ray crystal structure of the hexafluoroantimonate salt of oxatriquinane distinguishes itself from those of other trialkyl oxonium salts both in its long bond lengths (1.54 Å) and acute bond angles (109.8°) (Figure 2.3). The most accurate x-ray crystal structure of a trialkyl oxonium salt was that of Me₃O⁺ AsF₆⁻, which possessed bond lengths and C-O-C bond angles of 1.47 Å and 113.1°, respectively.¹³ The acute bond angles of **41** SbF₆⁻ are the result of the puckering caused by trefoil fusion of the three five-membered rings. The unusual C-O bond length is supported by gas phase computational modeling of the oxonium ion at the B3LYP/6-31+(g,d) level of theory.¹⁴

2.9 - Conclusion

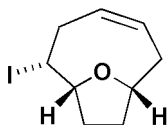
We have described herein the synthesis and characterization of oxatriquinane, an oxonium molecule with unprecedented stability towards nucleophiles. This work has established a number of firsts in the area of alkyl oxonium chemistry: the first bromide salt, the first NMR spectrum in D₂O, the first to be crystallized from and even refluxed in water, and the first to be chromatographed. The x-ray crystal structure showed the C-O bond lengths to be 1.54 Å, which to our knowledge are longer than any other oxonium ion reported in the literature. The unusual stability of **41** can be rationalized both in the rigid tricyclic framework and the large degree of angular strain accompanying the formation of a medium ring (an eight-membered ring in the present case.).

Experimental Procedures



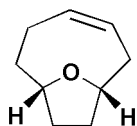
Cyclonona-3,6-dien-1-ol (**52**)

A mixture of 1,4,7-cyclononatriene oxide (**51**) (13.80 g, 0.101 mol) and LiAlH_4 (4.59 g, 0.121 mol) in freshly distilled ether (150 mL) was cautiously treated in small portions with anhydrous ZnCl_2 (6.90 g, 50.6 mmol) and the mixture was allowed to stir at rt for 2 h under argon. The reaction mixture was cooled to 0 °C and carefully quenched with 3N NaOH (5 mL). The resulting suspension was filtered and the filter cake was washed thoroughly with ether. The solvent was evaporated and the residue chromatographed on silica gel (2:1 hexane:ether) to give **52** as colorless crystals (13.70 g, 98%), mp 43–45 °C; $^1\text{H-NMR}$ (300 MHz, CDCl_3) δ 5.52 (m, 4H), 3.91 (m, 1H), 2.95(m, 2H), 2.62 (m, 4H), 2.33 (m, 2H); $^{13}\text{C-NMR}$ (75 MHz, CDCl_3) δ 131.9, 130.5, 127.5, 125.3, 73.5, 35.3, 31.6, 25.4, 19.4; $\nu\text{-max}$ (neat) 3260, 3009, 2927, 2859, 1636 cm^{-1} ; HRMS (EI) calcd for C_9H_{12} $[\text{M}-\text{H}_2\text{O}]^+$ m/z 120.0939, found 120.0936.



6-Iodo-10-oxa-bicyclo[5.2.1]dec-3-ene (56)

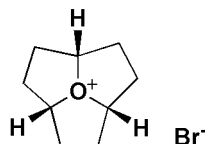
To a solution of **52** (2.07 g, 15.0 mmol) in CH₃CN (80 mL) was added iodine (6.85 g, 27.0 mmol) and the mixture was stirred for 15 min at rt. The mixture was diluted with CH₂Cl₂ (500 mL) and washed with 10% aq NaHSO₃ (100 mL), water (2 x 100 mL), and saturated aq NaCl (50 mL). The organic layer was dried over Na₂SO₄ and the solvent evaporated to give **56** as a yellow oil (3.17 g, 80%) which was used directly in the next step. ¹H-NMR (300 MHz, CDCl₃) δ 5.83 (m, 2H), 4.57 (m, 1H), 4.43 (m, 1H), 2.93 (m, 1H), 2.60 (quintet, *J* = 7.2 Hz, 1H), 2.35 (m, 1H), 2.20 (m, 1H), 2.07 (m, 4H), 1.73 (t, *J* = 9.5 Hz, 1H); ¹³C-NMR (100 MHz, CDCl₃) δ 131.8, 129.5, 82.2, 79.6, 34.3, 34.1, 33.0, 32.5, 30.0.



10-Oxa-bicyclo[5.2.1]dec-3-ene (53)

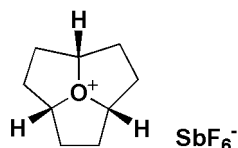
The general method of Barrero, *et al* was used:¹¹ A solution of **54** (3.15 g, 11.9 mmol) in THF (45 mL) was added to a slurry of Ra-Ni (32.3 g) in THF (45 mL). The heterogeneous mixture was agitated for 20 min after which ZnCl₂ (4.53 g) was added. The mixture was filtered through a pad of Celite and the filter cake washed with ether (3 x 60 mL). The combined filtrate was washed with water (2 x 100 mL) and brine (50 mL) and dried over Na₂SO₄. The solvent was carefully evaporated and residue chromatographed on silica gel (3:2 pentane/CH₂Cl₂) to give a ca. 7:1 mixture (by

NMR integration) of **53** and the saturated by-product 10-oxabicyclo[5.2.1]decane (**57**) (1.03 g, 54%). $^1\text{H-NMR}$ (300 MHz, CDCl_3) δ 5.82 (m, 1H), 5.67 (m, 1H), 4.42 (m, 1H), 4.35 (m, 1H), 2.35 (m, 2H), 1.99 (m, 6H), 1.67 (m, 1H), 1.48 (m, 1H); $^{13}\text{C-NMR}$ (75 MHz, CDCl_3) δ 134, 128, 80.0, 77.6, 34.1, 34.0, 31.9, 31.6, 22.1; HRMS (ESI) calcd for $\text{C}_9\text{H}_{15}\text{O}$ $[\text{M}+\text{H}]^+$ m/z 139.1117, found 139.1113.



10-Oxatriquinanium bromide (**41 Br⁻**)

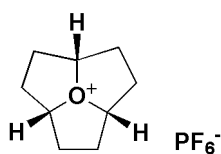
A steady stream of dry HBr gas was bubbled through a solution of **53** (484 mg, 3.50 mmol) in CHCl_3 (10 mL) for 10 min. The solvent was evaporated and the residue was triturated with benzene (2 x 2 mL) and dried under vacuum to give **41 Br⁻** as a yellow oil (723 mg, 94%). $^1\text{H-NMR}$ (600 MHz, CD_3CN) δ 5.40 (apparent quintet, $J = 4.4$ Hz, 3H), 2.44 (m, 6H), 2.18 (m, 6H); $^{13}\text{C-NMR}$ (150 MHz, CD_3CN) δ 101.8, 29.3.



10-Oxatriquinanium hexafluoroantimonate (**41 SbF₆⁻**)

A solution of **41 Br⁻** (221 mg, 1.01 mmol) in water (2 mL) was added to a cold, saturated, aq solution of NaSbF_6 (50 mL). The resulting precipitate was collected on a filter and the filtrate was washed with CH_2Cl_2 (5 x 10 mL). The organic phase was dried (Na_2SO_4) and the solvent was evaporated. The resulting solid was combined with the filtered product to give of **41 SbF₆⁻** for a total of 266 mg (70%) as a white

solid, mp 229-231 °C (dec). $^1\text{H-NMR}$ (300 MHz, D_2O) δ 5.34 (apparent quintet, $J = 5.0$ Hz, 3H), 2.37 (m, 6H), 2.19 (m, 6H).



10-Oxatriquinanium hexafluorophosphate (41 PF₆⁻).

Using the procedure described above, **41** Br⁻ (811 mg, 3.70 mmol) gave **41** PF₆⁻ (657 mg, 62%) as a white solid, mp 177-179 °C (dec). HRMS (ESI) calcd for C₉H₁₅O [M]⁺ m/z 139.1117, found 139.1116.

References

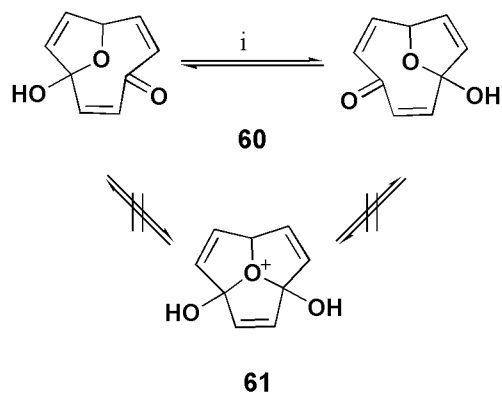
- 1) Mascal, M.; Hafezi, N.; Meher, N.K.; Fettinger, J.C. *J. Am. Chem. Soc.* **2008**, *130(41)*, 13532-13533.
- 2) Meier, H; Antony-Mayer, C.; Schulz-Popitz, C; Zerban, G. *Liebigs Annal.* **1987**, 1087-1094; Antony-Mayer, C; Meier, H. *Chem. Ber.* **1988**, 2013-2018;
- 3) Roth, W.R. *Liebigs. Annal.* **1964**, 10-25.
- 4) Thies, R. W., Gasic, M., Whalen, D., Grutzner, J. B., Sakai, M., Johnson, B., and Winstein, S. *J. Am. Chem. Soc.* **1972**, *94*, 2262.
- 5) Krishnamurty, S.; Schubert, R.M.; Brown, H.C.; *J. Am. Chem. Soc.* **1973**, *95*, 8486; Hutchins, R.O.; Taffer, I.M.; Burgoyne, W.; *J. Org. Chem.* **1981**, *46*, 5214; Katsuki, T.; Martin, V.S. *Org. React.* **1996**, *48*, 1.
- 6) Schmidt, D. L.; Roberts, C. B.; Reigler P. F.; *Inorg. Synth.*, **1973**, *14*, 47–52.
- 7) Brower, F.M.; Matzek, N.E.; Reigler, P.F.; Rinn, H.W.; Roberts, C.B.; Schmidt, D.L.; Snover, J.A.; Terada, K. *J. Am. Chem. Soc.*, **1976**, *98 (9)*, 2450–2453.
- 8) Bordwell, F.G.; Douglass, M.L.; *J. Am. Chem. Soc.* **1966**, *88*, 993-999; Larock, R.C. *Solvomercuration/Demercuration Reactions in Organic Synthesis*; Springer-Verlanger: New York, 1986; Brown, H.C; Geoghegan, P.J. Jr. *J. Org. Chem.* **1970**, *35*, 1844; Overman, L.E.; Campbell, C.B. *J. Org. Chem.* **1974**, *39*, 1474; Brown, H.C.; Lynch, G.J.; Hammar, W.J.; Liu, L.C. *J. Org. Chem.* **1979**, *44*, 1910.
- 9) Qian, H.; Han, X.; Widenhoefer, R.A. *J. Am. Chem. Soc.*, **2004**, *126 (31)*, 9536–9537.
- 10) Dowle, M.D.; Davies, D.I.; *Chem. Soc. Rev.* **1979**, 171; Mulzer, J. *In Organic Synthesis Highlights*, Mulzer, J.; Altenbach, H.J.; Braun, M.; Krohn, K.; Reissig, H.U.; Eds. VCH: Weinheim, **1991**, 158

- 11) Barrero, A.F.; Alvarez-Manzaneda, E.J.; Chahboun, R.; Meneses, R.; Romera, J.L.; *Synlett* **2001** No. 4, 485–488.
- 12) Choudhary, V.R.; Chaudhari, S.K. *React. Kinet. Catal. Lett.*, **1985**, 29 (1), 153-158; Pattinson, J.N.; Degering, E.F. *J. Am. Chem. Soc.*, **1951**, 73 (2), 611–613
- 13) Lork, E.; Gortler, B.; Knapp, C.; Mews, R. *Solid State Sci.* **2002**, 4, 1403.
- 14) Calculations were performed by Professor Mark Mascall using the Gaussian 03 program with default optimization parameters: Frisch, M. J.; et al. *Gaussian 03*, revision D.01; Gaussian, Inc.: Wallingford CT, 2004.

Chapter 3
Oxatriquinacene

3.1 - Introduction

Triquinacenes are tricyclic, bowl-shaped trienes, the parent hydrocarbon analogue of which was first synthesized by Woodward in the 1960s in order to probe the concept of neutral homoaromaticity and as a potential precursor to dodecahedrane.² The only reference to an oxatriquinacene was a postulated structure proposed over a decade ago by Prinzbach and co-workers in an acid-induced equilibrium of compound **60** (Scheme 3.1).³ This hemiacetal showed apparent C_s symmetry on the NMR time scale and thus could be considered a time-averaged oxatriquinacenium species as opposed to the formal oxatriquinacene **61**. This was determined based upon the lack of substantial change in chemical shifts as well as the size of the $^3J_{\text{H,H}}$ coupling constants. The synthesis of oxatriquinanes from this or related precursors in this paper was not further investigated.

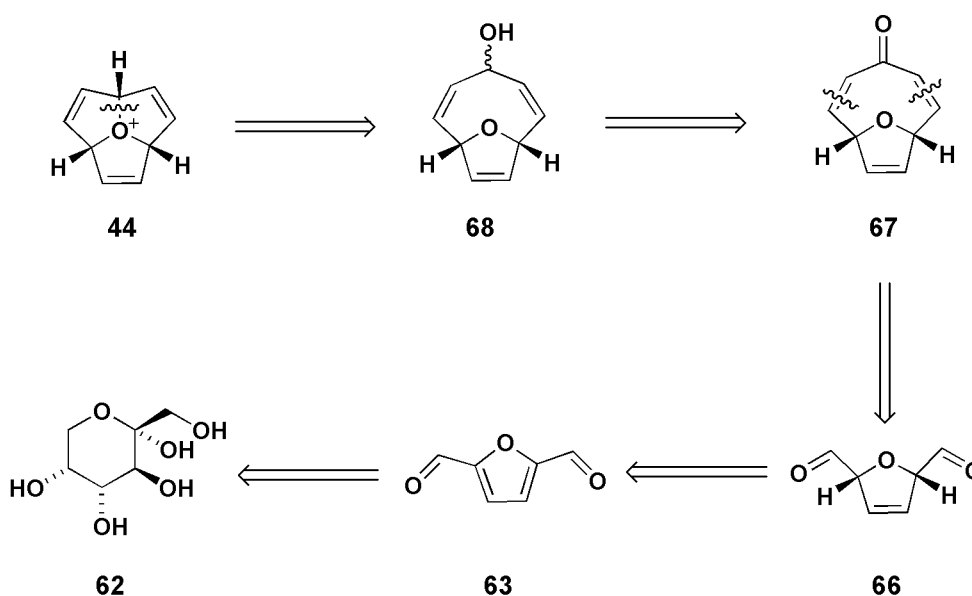


Scheme 3.1 – Reaction and conditions: i) TFA

3.2 - Proposed Synthesis from Fructose

With the successful synthesis of oxatriquinane behind us, we sought to synthesize its unsaturated counterpart, oxatriquinacene. The analogous route used to access **34** from **32**, i.e. irradiation of **41** in sulfuryl chloride to give perchloro oxatriquinacene, was not successful. Thus, we decided to engage a retrosynthetic analysis in an effort to create a *de novo* synthesis.

3.2.1 - Retrosynthetic Analysis

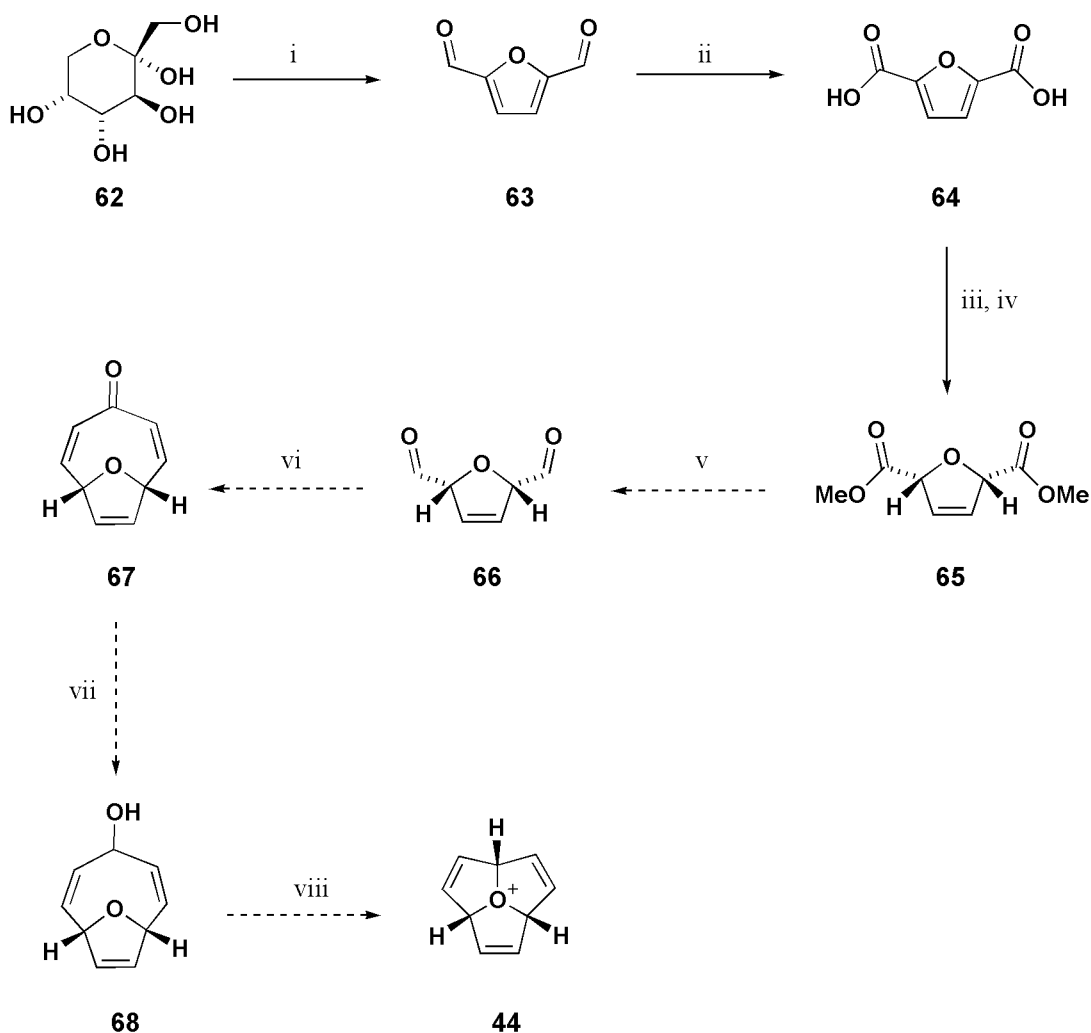


Scheme 3.2 – Retrosynthetic analysis for the preparation of oxatriquinacene.

The clear disconnection one must make first is the cleavage of the carbon-oxygen bond, which could be formed via an intramolecular S_N1 reaction of the precursor alcohol **68**, which could be obtained from a Luche reduction of ketone **67**. The ketone can be made by a two-fold aldol condensation of dialdehyde **66** with acetone, which could then be obtained from a dissolving metal reduction of diformyl furan. Ultimately, the known diformyl furan can be obtained from a sequential dehydration

and oxidation of fructose. The appeal of this synthetic approach stemmed from the use of a naturally-occurring, abundant and inexpensive sugar (Scheme 3.2).

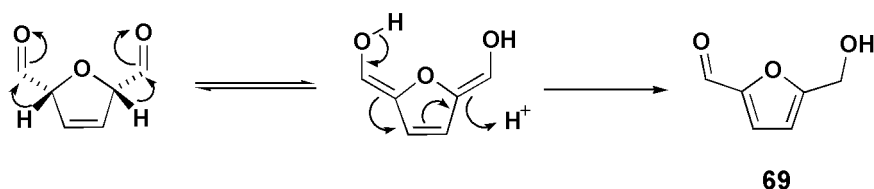
3.2.2 - Attempted Synthesis of Oxatriquinacene from Fructose



Scheme 3.3 - Reagents and Conditions: i) V_2O_5 , DMSO; 38% ii) Jones Reagent, acetone; 64% iii) Na^+ , NH_3 , $iPrOH$; 76% iv) cat H_2SO_4 , MeOH; 93% v) DIBAL, CH_2Cl_2 ; vi) Acetone, NaOH, H_2O ; vii) $NaBH_4$, $CeCl_3$, MeOH; viii) TFOH, CH_3CN .

The outline in Scheme 3.3 details a proposed synthesis of **44**. Fructose can be simultaneously dehydrated and catalytically oxidized with V_2O_5 in the presence of atmospheric oxygen to give diformyl furan (**63**).⁴ For the Birch reduction to be

accomplished, the aldehyde groups must be oxidized to the dicarboxylic acid **64**, with Jones reagent.⁵ Treatment of di-acid **64** with sodium metal in ammonia, followed by esterification gave diester **65** with modest diastereoselectivity and yield.⁵ Reduction of the esters down to the aldehyde was attempted using DIBAL. However, it was at this step where a flaw was encountered in the overall synthesis. Treatment of the diester with DIBAL apparently gave the desired alcohol, but this isomerized to hydroxymethylfurfural (**69**) by a tautomerization cascade shown in Scheme 3.4.



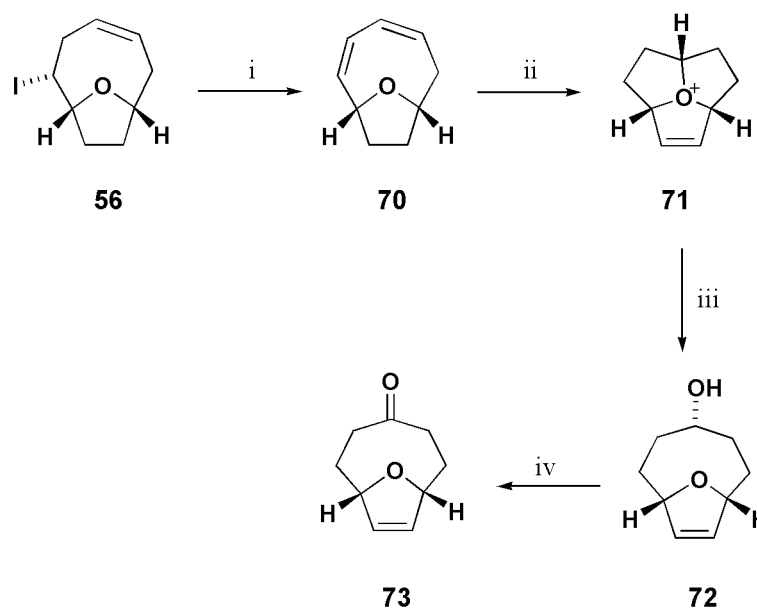
Scheme 3.4 – Proposed mechanism for the formation of hydroxymethylfurfural from dialdehyde **64**.

This result validated our previous suspicions as to the lack of precedents in the literature describing dihydrofurans with ketones or aldehydes at the 2 and 5 positions. While diesters and diacids of dihydrofurans are well documented, dialdehydes and diones were not. A protecting group for the double bond would be necessary for this route to be successful.

3.3 - Reassessment and New Approach Towards Oxatriquinacene

We decided to take a step back and reassess our approach and to explore modifying the synthesis of **41** for the preparation of **44**. We realized that **56** would be a good compound to branch off in the direction of the oxatriquinacene synthesis, because we could eliminate the halogen and treat the resulting diene **70** with an acid to make oxatriquinene (**71**). This synthesis would be part of a series of halogenations

and eliminations to introduce unsaturations and ultimately obtain oxatriquinacene (44).

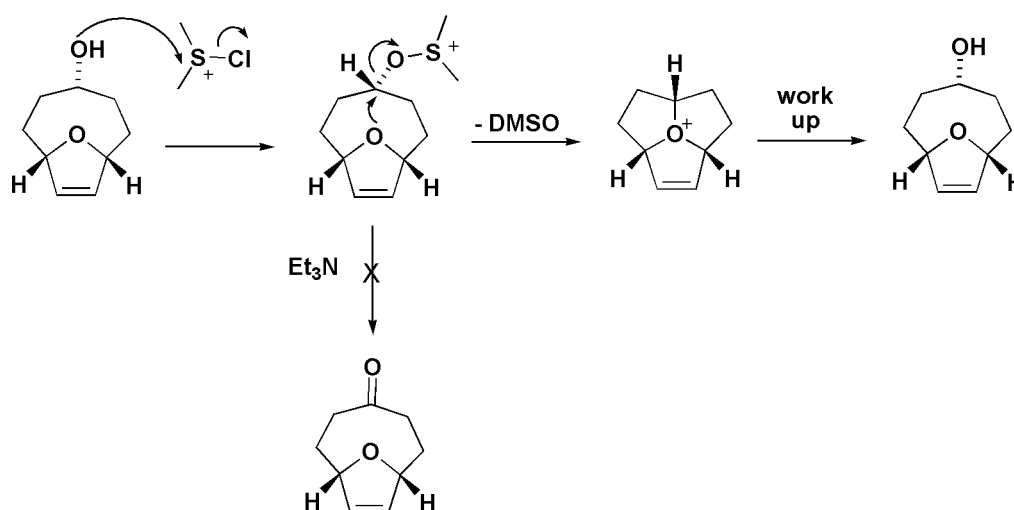


Scheme 3.5 – Reagents and conditions: i) DBU, benzene, reflux, overnight 49%; ii) TfOH, CH₃CN, 100%; iii) H₂O, CH₂Cl₂ 64%; iv) CrO₃, pyridine, CH₂Cl₂ 88%

Thus, a solution of **56** in benzene was treated with DBU and refluxed overnight to give **70** in moderate yield (Scheme 3.5). Subsequent treatment with triflic acid in dry acetonitrile gave **71**, the first formally allylic oxonium ion, in quantitative yield. Efforts towards making the bromide salt in a manner similar to the preparation of **41** Br⁻ led to decomposition. Unlike the parent triquinane **41**, which can remain in water indefinitely regardless of temperature, oxatriquinene **71** was found to immediately hydrolyze in water to give alcohol **72**. Remarkably, nucleophilic attack by water occurred mainly at the methine carbon opposite the double bond. This can be attributed to the inability of the double bond to stabilize the transition state of an S_N2 attack. Furthermore, the presence of a medium-ring endocyclic double bond would likely raise the transition-state energy, thus making the allylic attack pathway

less favorable. This presented us with an opportunity to pursue **44** in a more straightforward fashion.

Standard oxidation conditions such as PCC, and Jones reagent failed to oxidize **72** due to the acidic nature of the reagents, which result in transannulation back to **71**. The highly reliable Swern oxidation was also ineffective in inducing oxidation and resulted in quantitative recovery of starting material (Scheme 3.6). The failure of this oxidation stems from the formation of the oxo-sulfonium ion, which is normally eliminated by base to give the carbonyl. However, the oxo-sulfonium ion is also a good leaving group, and can be easily displaced by the THF oxygen to give back the oxonium ion after which, on aqueous workup, enol **72** is recovered. It soon became evident that the oxidation must be done in a basic system.



Scheme 3.6 – Mechanistic explanation for the failed Swern oxidation.

Oxidation reactions in basic conditions are less common than ones done under acidic conditions. Of those, we decided to employ the Collins oxidation which consists of a solution of bis-(pyridine)chromium(VI) oxide complex in

dichloromethane. Oxidation proceeded smoothly to give **73** in excellent yield (Scheme 3.5).

3.3.1 Introduction of Unsaturation in 10-Oxa-bicyclo[5.2.1]dec-8-en-4-one

Now that we had a concise route to the **73**, the significant challenge of introducing unsaturation was under way. A quick search of the literature revealed that introducing alpha-beta unsaturation to ketones and aldehydes was generally accomplished by functionalizing the alpha-position of the carbonyl with a halogen or selenyl group, followed by beta-elimination with base or by oxidation, respectively.⁶ We initially felt that performing stepwise halogenation and elimination would be problematic because of the difficulty in obtaining the **73** in large quantities. Thus we looked into various other approaches to introducing unsaturation.

3.3.1.1 Bromination with NBS

A common approach towards alpha-halogenation was to treat the carbonyl compound with NBS. However in the case of **73**, NBS was only able to introduce one halogen, while leaving a substantial amount of starting material.

3.3.1.2 Nicolaou's Oxidation Using IBX/NMO in DMSO

Nicolaou and co-workers were able to introduce unsaturation to enolizable ketones by treatment with IBX and NMO in DMSO.⁷ Unfortunately, applying Nicolaou's conditions to **73** gave no reaction.

3.3.1.3 - Exhaustive Bromination with Bromine

All of the previous reaction conditions employed were chosen to ensure that the double bond remained intact. However, this requirement was found to greatly limit our choices in employing various conditions. Furthermore, there are few known procedures for protecting double bonds. Many alpha-halogenations are accomplished by using molecular bromine in a halogenated solvent. If **73** was exhaustively brominated with Br₂, it should give the tetrabromo-ketone **77** (Scheme 3.7). Vicinal dihalides are often used as masks for double bonds, which can be reduced to give back the olefin.⁸ Thus, a solution of **73** was treated with a slight excess of bromine to give **77** as a crystalline solid in low yield.

Efforts were now geared towards eliminating the alpha halides. Although the reactions looked reasonable on paper, we soon encountered difficulties. Compound **77** was found to be remarkably stable against standard elimination conditions such as DBU/benzene and tBuOK in THF (Figure 3.1). Difficulties also stemmed from its poor solubility in a variety of organic solvents. The inertness of the **77** was epitomized by its ability to withstand elimination by LDA in THF, in temperatures ranging from -78 °C to reflux. All attempts gave back unreacted starting material. Photoelimination was also found to be ineffective.

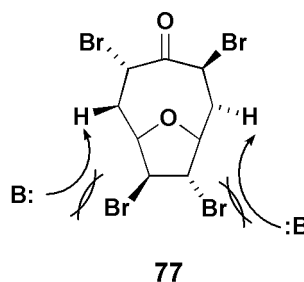


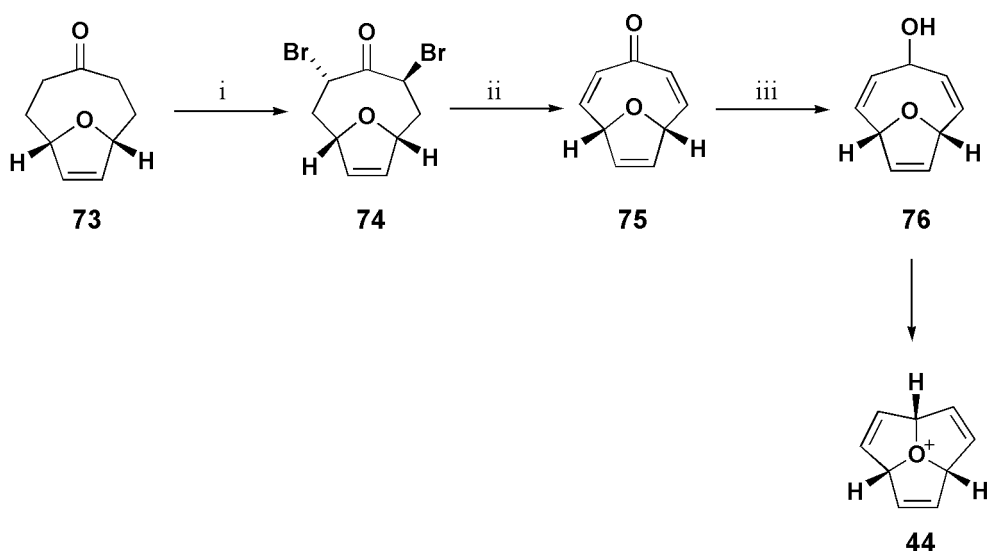
Figure 3.1 – Steric congestion presented by the bromines could explain the inability of **77** to undergo dehydrohalogenation.

3.3.1.4 - Selective Bromination of 10-Oxa-bicyclo[5.2.1]dec-8-en-4-one

The robustness of **77** forced us to re-evaluate the reactivity of **73** towards halogen electrophiles. Double bonds undergo facile halogenation in the presence of halides such as chlorine and bromine. However, in the case of **73**, the electronegative oxygen can pull electron density from the double bond and make it less reactive. This type of behavior has also been observed in the reactivity of the double bonds in azatriquinacene.⁹ Thus, we began to examine the stepwise halogenation of **73** by treating it with bromine in chloroform at 0 °C. We were able to form the α,α' -ketone **74** in 34% yield (Scheme 3.7).

3.3.2 - Elimination, Reduction and Endgame

The following work was all done by a postdoctoral researcher in the group.¹⁰ Preparation of **44** began with beta-elimination of **74** with DBU in toluene. Subsequent Luche reduction of the trienone **75** gave the trienol **76** in good yield. ¹H-NMR could not provide insight into the diastereoselectivity of the Luche reduction of **75**. Nevertheless, alcohol **76** was found to close down to form oxatriquinacene (**44**) in an 87% yield by treatment with triflic acid (Scheme 3.7).



Scheme 3.7 - Reagents and conditions: i) Br₂, CHCl₃, 0°C, 34%; ii) DBU, toluene, reflux, 65%; iii) NaBH₄, CeCl₃, MeOH, 88%; iv) TfOH, CH₃CN, 87%

3.4 - Reactivity of Oxatriquinacene

Oxatriquinacene (**44**) is the first formal triply bis-allylic oxonium ion. Apart from **44** and **71**, no other stable allyl oxonium ions have been reported to our knowledge. Oxatriquinacene (**44**) is more reactive than **41**, and is rapidly opened back to trienol **76** in water, although its NMR spectrum could be recorded in *d*₃-acetonitrile, which would otherwise be alkylated to the nitrilium salt by typical oxonium reagents. No evidence of S_N2' reactions were observed. The protons in the bridgehead positions show evidence of their extreme environment, appearing at 6.80 ppm, which is downfield even of the olefinic hydrogens.

3.5 - Conclusion

Oxatriquinacene was successfully synthesized from a common derivative shared in the oxatriquinane synthesis: the iodo-THF **56**. The synthesis as originally planned, involved the preparation of trienol **76** starting from fructose. However, an

intramolecular disproportionation of an earlier intermediate thwarted this approach. Efforts will be made in the future to isolate and characterize the ylide of oxatriquinacene (**78**), as well as preparing the 10π , bowl-shaped, *neutral*, aromatic species: oxaacceptalene (**79**) (Figure 3.2).¹¹

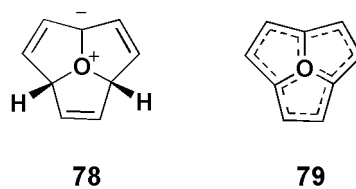
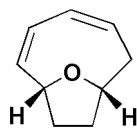


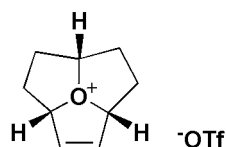
Figure 3.2 – Neutral trivalent oxygen compounds **78** and **79**.

Experimental Procedures



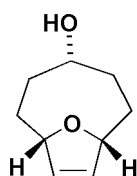
10-Oxa-bicyclo[5.2.1]deca-2,4-diene (**70**)

To a solution of alcohol **52** (4.80 g, 34.7 mmol) in CH₃CN (100 mL) was added iodine (15.9 g, 62.6 mmol) and the mixture was allowed to stir for 10 min. The solution was diluted with CH₂Cl₂ (100 mL) and decolorized by the addition of a minimum amount of 10% aq NaHSO₃, washed with water (3 x 100 mL), brine (50 mL), and dried over Na₂SO₄. The solvent was evaporated and the residue taken up in benzene (100 mL). DBU (5.00 mL, 5.09 g, 33.4 mmol) was added and the mixture was heated to reflux with stirring overnight. The reaction mixture was cooled and washed with saturated NH₄Cl (50 mL), NaHCO₃ (50 mL) and brine (50 mL). The solvent was evaporated and the residue chromatographed on silica gel (CH₂Cl₂) to give **70** (2.30 g, 49%) as a colorless oil. ¹H-NMR (300 MHz, CD₃CN) δ 6.07 (m, 1H), 5.67 (dt, J = 10.8, 8.1 Hz, 1H), 5.43 (d, J = 2.7 Hz, 2H), 4.74 (m, 1H), 4.06 (m, 1H), 2.50 (m, 2H), 2.08 (m, 6H); ¹³C-NMR (75 MHz, CD₃CN) δ 136.8, 131.3, 128.1, 121.4, 78.2, 76.0, 36.7, 34.1, 32.9; HRMS (ESI) calcd for C₉H₁₃O [M+H]⁺ m/z 137.0961, found 137.0955.



10-Oxatriquinenium trifluoromethanesulfonate (**71** OTf)

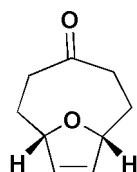
To a solution of **70** (115 mg, 0.844 mmol) in CH₃CN (0.5 mL) was added trifluoromethanesulfonic acid (75 μ L, 0.13 g, 0.85 mmol) and the resulting mixture was gently agitated. Evaporation of the solvent gave **71** OTf (242 mg, 100%) as a dark brown oil. ¹H-NMR (300 MHz, CD₃CN) δ 6.06 (apparent t, J = 5.9 Hz, 2H), 5.97 (s, 2H), 5.44 (quintet, J = 6.3 Hz, 1H), 2.61 (m, 2H), 2.40 (septet, J = 6.3 Hz, 2H), 2.34 (septet, J = 6.0 Hz, 2H), 2.14 (sextet, J = 6.6 Hz, 2H); ¹³C-NMR (75 MHz, CD₃CN) δ 126.7, 106.0, 105.0, 31.0, 29.1; HRMS (ESI) calcd for C₉H₁₃O [M]⁺ m/z 137.0961, found 137.0956.



10-Oxa-bicyclo[5.2.1]dec-8-en-4-ol (**72**)

A solution of **71** OTf was prepared as described above from **70** (136 mg, 1.00 mmol) and excess trifluoromethanesulfonic acid (0.20 mL) in CH₃CN (1.0 mL). The solvent was evaporated and water (20 mL) and CH₂Cl₂ (40 mL) were added. The resulting mixture transferred into a separatory funnel containing saturated aq NaHCO₃ (20 mL) and shaken. The organic layer was separated and aqueous layer was extracted with CH₂Cl₂ (2 x 15 mL). The combined organic layer was washed with brine (15 mL) and dried over MgSO₄. The solvent was evaporated and the residue was chromatographed on silica gel (ether) to give **72** (99 mg, 64%) as a white solid, mp 86-87 °C. ¹H-NMR (300 MHz, CDCl₃) δ 5.78 (s, 2H), 4.99 (s, 2H), 3.95-3.89 (m, 1H), 2.19-2.07 (m, 2H),

1.89-1.64 (m, 6H), 1.18 (d, $J = 3.3$ Hz, 1H); ^{13}C -NMR (75 MHz, CDCl_3) δ 130.4, 84.9, 74.5, 36.9, 34.1; HRMS (EI) calcd for $\text{C}_9\text{H}_{13}\text{O}_2$ $[\text{M}-\text{H}]^+$ m/z 153.0916, found 153.0916. A minor component, (10-oxabicyclo[5.2.1]dec-2-en-4-ol) (14 mg, 9%), was also isolated as a colorless oil. ^1H -NMR (300 MHz, CDCl_3) δ 5.47–5.41 (m, 1H), 5.27–5.21 (m, 1H), 5.18–5.15 (m, 1H), 4.65–4.62 (m, 1H), 4.34–4.26 (m, 1H), 2.07–1.92 (m, 2H), 1.87–1.66 (m, 6H), 1.64–1.53 (m, 1H); ^{13}C -NMR (75 MHz, CDCl_3) δ 134.0, 131.5, 79.4, 77.5, 70.2, 34.5, 31.6, 31.3, 27.0.



10-Oxa-bicyclo[5.2.1]dec-8-en-4-one (73)

To a suspension of CrO_3 (3.07 g, 30.7 mmol) in CH_2Cl_2 (150 mL) at 0 °C under nitrogen was added pyridine (7.20 mL). The mixture was stirred for 5 min at 0 °C and then for 1 h at rt. A solution of **72** (788 mg, 5.11 mmol) in CH_2Cl_2 (40 mL) was added and the mixture was stirred for 30 min. The reaction mixture was filtered and the filtrate was successively washed with 3N NaOH (2 x 60 mL), 1N HCl (2 x 75 mL), water (2 x 60 mL) and brine (60 mL) and dried over MgSO_4 . Evaporation of the solvent gave **73** as a white solid (681 mg, 88%), mp 55 °C. ^1H -NMR (400 MHz, CDCl_3) δ 5.94 (s, 2H), 5.04 (s, 2H), 2.60–2.48 (m, 4H), 2.13–2.06 (m, 2H), 2.05–1.99 (m, 2H); ^{13}C -NMR (75 MHz, CDCl_3) δ 218.3, 130.5, 85.3, 38.9, 37.9; HRMS (ESI) calcd for $\text{C}_9\text{H}_{13}\text{O}_2$ $[\text{M}+\text{H}]^+$ m/z 153.0916, found 153.0900.

References

- 1) Mascial, M.; Hafezi, N.; Meher, N.K.; Fettinger, J.C. *J. Am. Chem. Soc.* **2008**, *130(41)*, 13532-13533.
- 2) Woodward, R. B.; Fukunaga, T.; Kelly, R. C. *J. Am. Chem. Soc.* **1964**, *86*, 3162.
- 3) Person, G.; Keller, M.; Prinzbach, H. *Liebigs Ann.* **1996**, 507; Pleschke, A.; Geier, J.; Keller, M.; Wörth, J.; Knothe, L.; Prinzbach, H. *Eur. J. Org. Chem.* **2007**, 4867.
- 4) Halliday, G.A.; Young, R.J. Jr.; Grushin, V.V. *Org. Lett.*, **2003**, *5 (11)*, 2003–2005.
- 5) Hultin, P.G.; Mueseler, F. J.; Jones, J. B. *J. Org. Chem.*, **1991**, *56 (18)*, 5375-5380.
- 6) Lightner, D.A.; Crist, B.V.; Kalyanam, N.; May, L.M.; Jackman, D.E. *J. Org. Chem.* **1985**, *50 (20)*, 3867-78; Engman, L. *J. Org. Chem.*, **1988**, *53(17)*, 4031-7.
- 7) Nicolaou, K.C.; Montagnon, T.; Baran, P.S. *Angew. Chem. Int. Ed.* **2002**, *41(6)*, 993-996.
- 8) Husstedt, U.; Schäfer, H.J. *Tett. Lett.* **1981**, 22(7),
- 9) Mascial, M.; Mollard, P.M. Unpublished results.
- 10) This portion of the project was completed by Dr. Nabin K. Meher.
- 11) Compound **79** has been determined by NICS1 calculations to be at least as aromatic as benzene. See Mascial, M. *J. Org. Chem.*, **2007**, *72 (12)*, 4323–4327.

Chapter 4

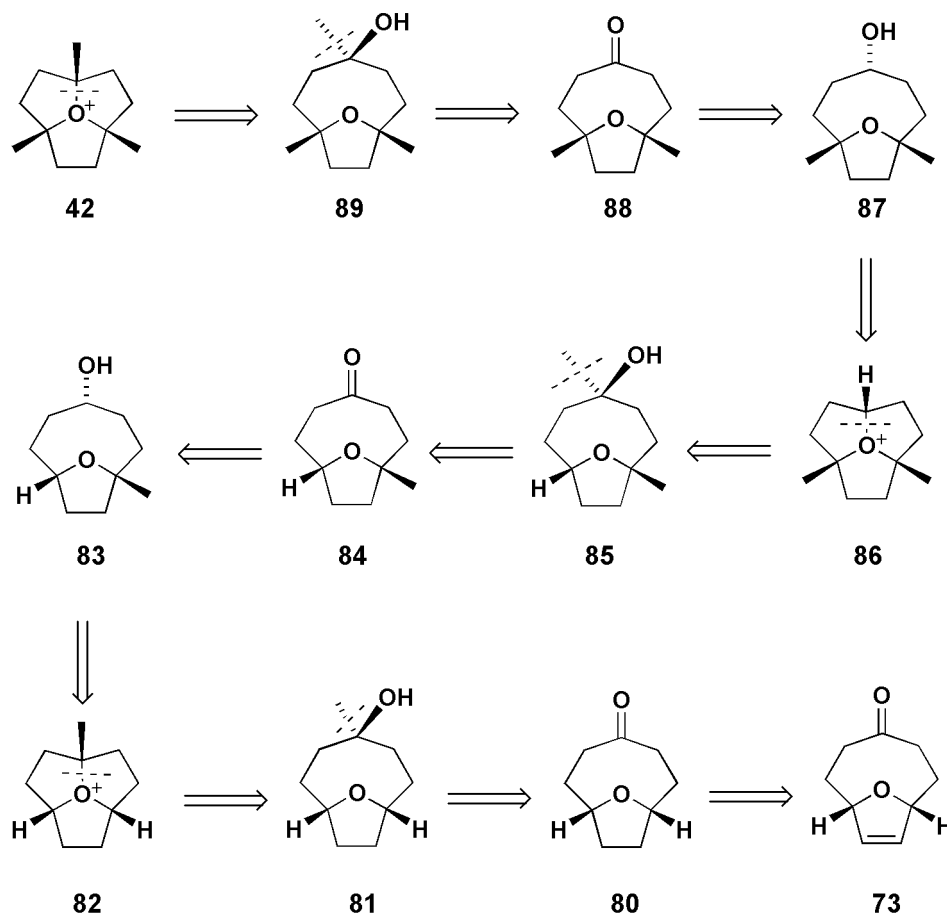
1,4,7-trimethyloxatriquinane

4.1 - Introduction

Oxatriquinane **41** was found to be exceptionally stable under reaction conditions which would decompose typical Meerwein-type oxonium ions. Despite this stability, it was found to readily alkylate strong nucleophiles such as azide, cyanide, and hydroxide by an S_N2 pathway.^{1,2} This observation, coupled with the inertness of **41** towards solvolytic conditions, led us to speculate on how **41** would behave if the protons α to the oxygen were replaced with alkyl groups, giving a threefold tertiary oxonium ion. This would presumably render trimethyl oxatriquinane inert towards S_N2 substitution. However, we were fully aware that both S_N1 and E2 pathways could be established as a result. Here, we describe the synthesis, characterization, and reactivity of 1,4,7-trimethyl oxatriquinane (**42**).³

4.2 - Retrosynthetic Analysis

A carbon-oxonium bond formation could stem from an acid-induced dehydration of tertiary-alcohol **89**. This tertiary alcohol could easily be formed by treating the corresponding ketone **88** with a methyl Grignard or lithium reagent. Ketone **88** would result from an oxidation of an alcohol, which was previously formed by nucleophilic attack on dimethyl-oxatriquinane (**86**). The attack of the hydroxide nucleophile should be regioselective at the secondary position over the tertiary position. This cycle can be repeated twice over and eventually lead us to **80**, which can be acquired from hydrogenation of **73**, an intermediate in the synthesis of oxatriquinacene (Scheme 4.1).



Scheme 4.1 – Retrosynthetic analysis for the preparation of **42**.

4.3 - Preparation of 1,4,7-trimethyloxatriquinane

Starting with enone **73**, hydrogenation gave **80** in good yield (Scheme 4.2). High pressure (5 atm) was required to promote the reaction due to the low reactivity of the double bond, attributed to the electron-withdrawing THF oxygen. The ketone was dissolved in ether and treated with a solution of MeMgBr in THF to give the tertiary alcohol **81**. Unlike the ene-THF **53**, which required the use of triflic acid to induce transannulation, the tertiary alcohol **81** could be easily converted to oxatriquinane **82** using concentrated HCl. Subsequent treatment with saturated aqueous KPF₆ solution caused the PF₆ salt of **82** to precipitate from solution as a white solid. Extractions

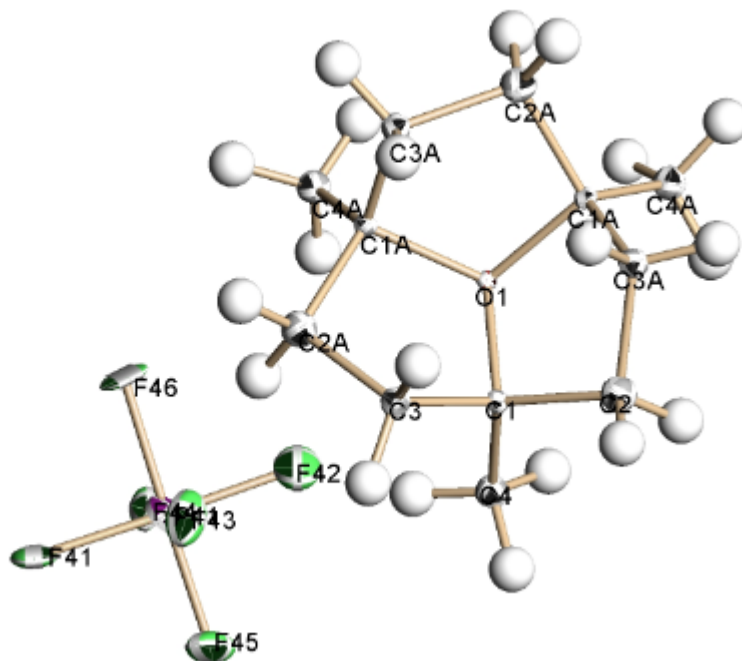
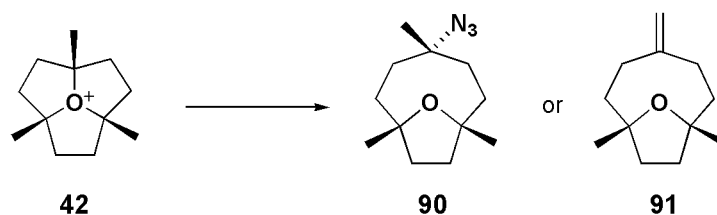


Figure 4.1 - X-ray crystal structure of cation of **42** PF_6^- showing thermal ellipsoids at the 50% probability level. A minor disorder component is omitted for clarity.

Crystals suitable for x-ray crystallography were grown by slow evaporation of a solution of **42** PF_6^- in dichloromethane. The x-ray crystal structure of **42** PF_6^- distinguishes itself from **41** SbF_6^- both in its longer C-O bond lengths (1.56 Å) and more acute C-O-C bond angles (103.9°) (Figure 4.1).

4.4 - Reactivity of 1,4,7-trimethyloxatriquinane

We first subjected **42** to classic solvolysis conditions (refluxing ethanol), and found no trace of reaction, even after several hours. It quickly became clear that **42** was not going to traverse a reaction pathway involving a unimolecular mechanism, whether substitution or elimination. Reaction with basic nucleophiles, such as methoxide, cyanide, or acetate, led to the anticipated elimination product **91** while other less basic nucleophiles were unreactive (Table 4.1).



Entry	Nucleophile	Solvent	Result
1	NaSMe	MeCN	Elimination and substitution
2	Bu ₄ N ⁺ CN ⁻	MeCN	Elimination
3	Et ₄ N OAc ⁻	MeCN	Elimination
4	NaOMe	MeOH	Elimination
5	Bu ₃ P	MeCN	Elimination
6	Ph ₃ P	MeCN	No reaction
7	LiBr	MeCN	No reaction
8	EtOH	EtOH	No reaction
9	(EtO) ₃ P	MeCN	No reaction
10	NaI	MeOH	No reaction
11	Cl ⁻	HCl	No reaction
12	Bu ₄ N ⁺ N ₃ ⁻	CHCl ₃	Substitution

Table 4.1 – Details regarding the reactivity of **42** towards various nucleophiles.

Entry 7 was thought to be the representative example of an attempt at an S_N2 attack, in which the bromide ion failed to be alkylated in acetonitrile. This was an expected result. However, our concept to the reactivity of **42** was challenged when it was found that azide was able to attack **42** to give the alkyl azide **90** as the sole product. Furthermore, when the reaction was carried out in methanol, a protic solvent, the rate significantly decreased, but the product was the same. The addition of a salt, LiBF₄,

was found to further suppress the reaction rate. All of these observations were indicative of a bimolecular process, despite the electrophile being a tertiary carbon.

4.4.1 - S_N2 Bimolecular Displacement at a Tertiary Carbon: A Brief Review

A widely-taught concept in undergraduate organic chemistry courses is that S_N2 displacements do not occur at tertiary carbon centers. This is attributed to steric repulsion from the three alkyl groups against the incoming nucleophile. To provide a context for the above result, we looked to the literature for examples of S_N2 reactions at a tertiary carbon. Whereas mechanistic ambiguity can be argued under some circumstances at arylated C(sp³) centers, literature claims for bimolecular reactions at tertiary alkyl carbons have been infrequent.⁴ In one of the earliest papers dealing with this subject, Ingold and co-workers concluded that halide exchange at *tert*-butyl centers in acetone was, to a considerable extent, a bimolecular process.⁵ This finding was criticized by Winstein and co-workers, who elucidated an elimination-addition pathway for the reaction.^{6a} Later, Cook and Parker published a detailed analysis of halide exchange with *tert*-butyl bromide and tetraethylammonium chloride in DMF and the presence of tetraethylammonium perchlorate, which provided evidence for about 5% of the reaction occurring via the S_N2 mechanism while the remaining 95% occurred via E2 elimination to isobutene.^{6b}

The small fraction of S_N2 at a tertiary center can be enhanced by replacing the alkyl groups with more electron withdrawing substituents. For example, Miotti and Fava studied the halide exchange reaction of triphenylmethyl chlorides with either two or three rings substituted with a *p*-nitro group, which strongly destabilizes positive charge at the reaction center.⁷ This disfavoring of the S_N1 pathway, with its

carbocation intermediate, forces the reaction to occur through the S_N2 mechanism. Similarly, tertiary α -bromolactones and α -bromoketones are substituted through the S_N2 pathway.⁸ Examples of intramolecular substitution at tertiary centers have also been proposed as concerted, non-synchronous reactions at the S_N1-S_N2 borderline.⁹

4.4.2 - The Case for the S_N2 Mechanism

Thus, the reaction of **42** with azide had the appearance of a bimolecular substitution, despite the fact that the center of attack is a tertiary carbon. In order to demonstrate unequivocally that the kinetics were second order, the concentration dependence with respect to the nucleophile was determined. Reactions were conducted in a solution of 0.003 M **42** and 0.2 M LiBF₄ in CD₃OD. The role of the lithium salt was added to slow the reaction rate so that NMR data could be collected over a reasonable period of time. The appearance of **90** was monitored by ¹H-NMR at three different concentrations of NaN₃ (0.024, 0.030, and 0.036 M). Figure 4.2A presents the fits of the NMR integration data to a single exponential equation. These conditions give good pseudo-first order behavior, as evidenced by the good fit of the kinetic data (NMR integration values for the methyl group vicinal to the azido group in **90**) to the equation. Figure 4.2B is a plot of the observed pseudo-first order rate constants vs. azide concentration. The results presented in Figure 4.2B can be interpreted in no other way than describing a second order reaction mechanism. The slope of the fitted line in Figure 4.2B provides the value of the second order rate constant of $0.0235 \pm 0.0011 \text{ M}^{-1} \text{ s}^{-1}$ for this reaction.

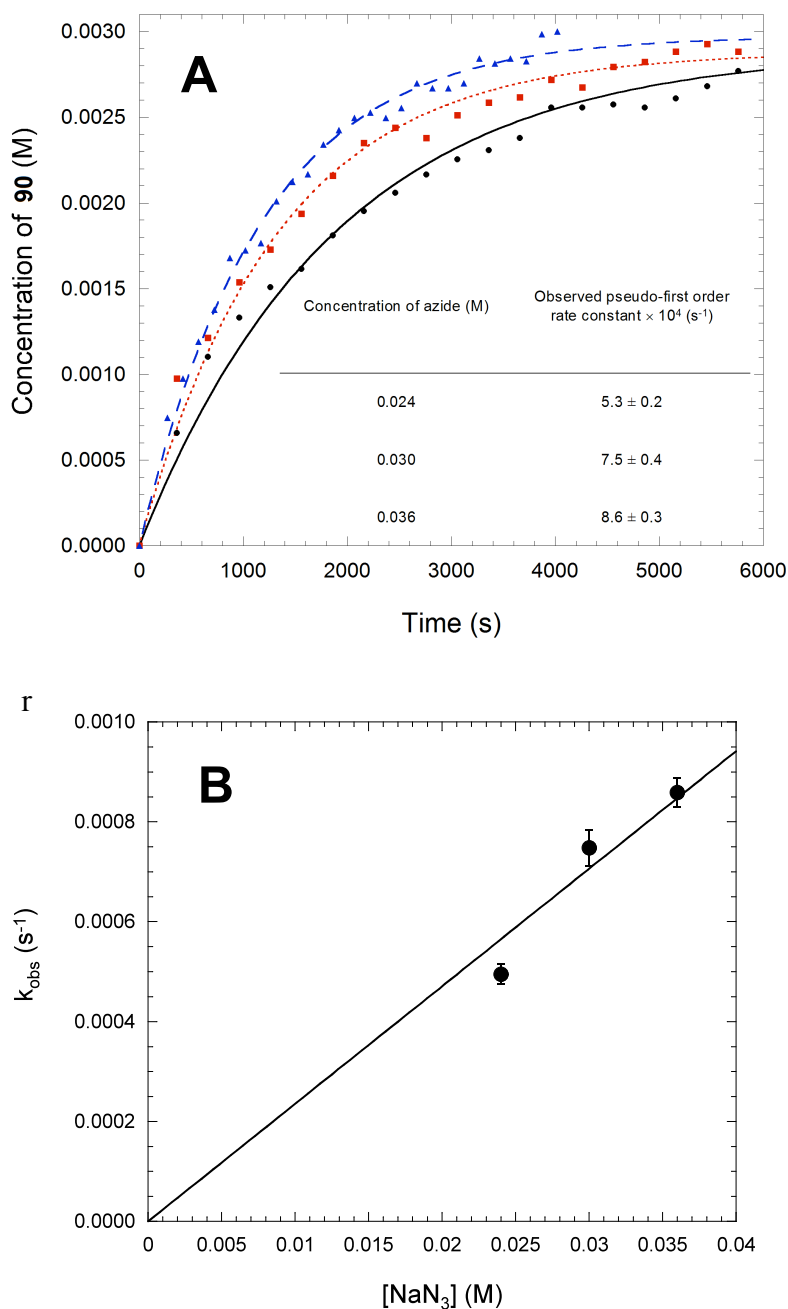
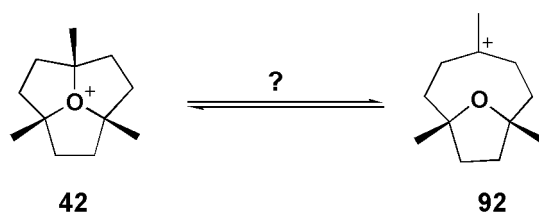


Figure 4.2 - A. Plot of $[90]$ versus time for the reaction of 0.003 M **42** and NaN_3 at three different concentrations (black, 0.024 M; red, 0.030 M; and blue 0.036 M), with observed pseudo-first order rate constants (inset). B. Plot of k_{obs} versus NaN_3 concentration.

4.4.3 - Existence of a Possible Equilibrium

The question arises as to whether it is possible that **42** might exist in equilibrium with a ring-opened, carbocationic intermediate, the formation of which is not rate-determining (Scheme 4.3). This intermediate could undergo a reversible reaction with

solvent but an irreversible, apparent S_N2 reaction with azide. To investigate this possibility, we attempted to model a bicyclic species of general structure **92** using DFT computational methods.¹⁰ However, no minimum energy structure, or stationary point of any description, was located for **92** starting from a range of reasonable initial geometries. In each case, the oxygen and α -carbon simply reunite to give back **42**. It could, however, be argued that this would be a solvent-assisted process and that such an intermediate may not be observable in a continuum solvent model. But the experimental observation is that the substitution reaction is much faster in chloroform than it is in methanol, and if a discrete intermediate like **92** existed, its preferred formation in chloroform is difficult to rationalize. The observed solvent effect and the fact that the reaction is decelerated in the presence of an inert salt (LiBF_4)^{11,12} speak strongly in favor of the proposed S_N2 mechanism.

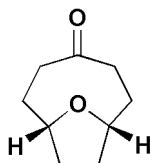


Scheme 4.3 – DFT calculations were unable to detect a transition state or a local energy minimum belonging to cation **90** for the following equilibrium.

4.5 - Conclusion

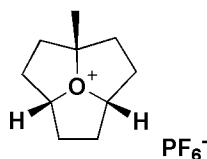
In conclusion, we have successfully prepared trimethyloxatriquinane (**42**), which bears three tertiary carbon substituents,¹³ and has been shown to be even less reactive than **41**. With the exception of unusual cases in which carbocation formation is electronically disfavored, there are no previous examples of substitution reactions at tertiary alkyl centers that proceed exclusively with second order kinetics. This is, to our knowledge, the first report of such a reaction.

Experimental Procedures



10-Oxabicyclo[5.2.1]decan-4-one (**80**)

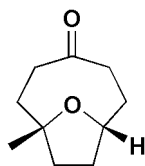
A mixture of 10-oxabicyclo[5.2.1]dec-8-en-4-one (**73**) (1.75 g, 11.5 mmol) and 5% Pd/C (500 mg) in methanol (30 mL) was shaken overnight in a Parr hydrogenator pressurized with 5 atm of hydrogen gas. The mixture was filtered through a pad of Celite and the filter cake was washed with methanol. Evaporation of the filtrate gave **80** as a white solid (1.56 g, 88%). Recrystallization from hexane gave long colorless needles, mp 53-54 °C; $^1\text{H-NMR}$ (300 MHz, CDCl_3) δ 4.18 (m, 2H), 2.44 (m, 2H), 2.14 (m, 4H), 1.95 (m, 2H), 1.82 (m, 4H); $^{13}\text{C-NMR}$ (75 MHz, CDCl_3) δ 215.1, 76.8, 76.4, 34.0, 29.6; HRMS (ESI) calcd for $\text{C}_9\text{H}_{14}\text{O}_2$ $[\text{M}+\text{H}]^+$ m/z 155.1057, found 155.1067.



2-Methyloxatriquinanium hexafluorophosphate (**82**)

To a stirring solution of **80** (1.0 g, 6.5 mmol) in THF (30 mL) was added dropwise a solution of 3M MeMgBr (4.0 mL, 12 mmol) in diethyl ether. The mixture was allowed to stir for 1 h before being quenched with a minimum amount of water. The solvent was evaporated and the resulting solid was treated with conc. aq. HCl (20

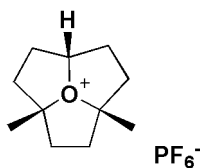
mL). The homogeneous solution was allowed to stir for 15 min before being diluted with sat. aq. KPF_6 (100 mL). The precipitated white product was collected and the supernatant was extracted with CH_2Cl_2 (5 x 20 mL). The organic layer was separated and evaporated to give a white solid. The combined solids were washed once with 10 mL of ice-cold water, and then thoroughly with ether to give **82** (1.2 g, 62%), mp 210 °C (dec.); $^1\text{H-NMR}$ (300 MHz, CD_3CN) δ 5.27 (apparent quintet, $J = 6.1$ Hz, 2H), 2.5-2.05 (m, 12H), 1.60 (s, 3H); $^{13}\text{C-NMR}$ (75 MHz, CD_3CN) δ 101.7, 36.3, 30.9, 30.2, 25.1; HRMS (ESI) calcd for $\text{C}_{10}\text{H}_{17}\text{O}^+$ $[\text{M}]^+$ m/z 153.1274, found 153.1273.



1-Methyl-10-oxa-bicyclo[5.2.1]decan-4-one (**84**)

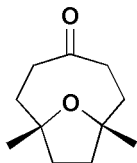
A solution of **82** (929 mg, 3.12 mmol) in acetone (20 mL) was treated with 3N aq. NaOH (10 mL). The biphasic mixture was stirred vigorously for 20 min. The organic phase was separated and the aqueous phase was diluted with brine (100 mL) and extracted with ether (5 x 20 mL). The combined organic extracts were washed with brine (50 mL) and dried (Na_2SO_4). The solvent was evaporated and the residue was taken up in CH_2Cl_2 (10 mL) and added to a stirring solution of Collin's reagent, which had been prepared from pyridine (2.04 g, 25.7 mmol) and CrO_3 (1.26 g, 12.6 mmol) in CH_2Cl_2 (50 mL). After stirring for 1 h, the reaction mixture was washed once with 3N NaOH (30 mL), once with 3N HCl (30 mL), once with brine (30 mL), and dried (Na_2SO_4). The solvent was evaporated and the residue was chromatographed (ether) to give **84** (624 mg, 62%) as a colorless oil; $^1\text{H-NMR}$ (300

MHz, CDCl₃) δ 5.27 (apparent quintet, 2H), 2.5-2.05 (m, 12H), 1.60 (s, 3H); ¹³C-NMR (75 MHz, CDCl₃) δ 101.7, 36.3, 30.9, 30.2, 25.1; HRMS (ESI) calcd for C₁₀H₁₇O⁺ [M]⁺ *m/z* 153.1274, found 153.1273.



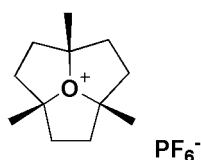
2,4-Dimethyloxatriquinanium hexafluorophosphate (**86**)

To a stirring solution of **84** (380 mg, 2.26 mmol) in THF (5 mL) was added dropwise a solution of 3M MeMgBr (1.5 mL, 4.5 mmol) in diethyl ether. The mixture was allowed to stir for 1 h before being quenched with a minimum amount of water. The solvent was evaporated and the remaining solid was treated conc. aq. HCl (5 mL). The homogeneous solution was allowed to stir for 20 min before being diluted with sat. aq. KPF₆ (30 mL). The precipitated white product was collected and the supernatant was extracted with CH₂Cl₂ (5 x 20 mL). The organic layer was separated and evaporated to give a white solid. The combined solids were washed once with ice-cold water (10 mL), and then thoroughly with ether to give **86** (444 mg, 63%). mp 200 °C (dec.); ¹H-NMR (300 MHz, CD₃CN) δ 5.34 (apparent quintet, *J* = 6.1 Hz, 1H), 2.48-2.12 (m, 12H), 1.63 (s, 6H); ¹³C-NMR (75 MHz, CD₃CN) δ 115.7, 100.0, 36.2, 35.6, 30.1, 25.2. HRMS (ESI) calcd for C₁₁H₁₉O [M]⁺ *m/z* 167.1430, found 167.1427



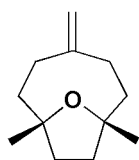
1,7-Dimethyl-10-oxa-bicyclo[5.2.1]decan-4-one (88)

A solution of **86** (444 mg, 1.42 mmol) in acetone (20 mL) was treated with 3N NaOH (10 mL). The biphasic mixture was stirred vigorously for 20 min. The organic phase was separated and the aqueous phase was diluted with brine (100 mL) and extracted with ether (5 x 20 mL). The combined organic extracts were washed with brine (50 mL) and dried (Na₂SO₄). The solvent was evaporated and the residue was taken up in CH₂Cl₂ (5 mL) and added to a stirring solution of Collin's reagent, which had been prepared from pyridine (882 mg, 11.2 mmol) and CrO₃ (567 mg, 5.67 mmol) in CH₂Cl₂ (15 mL). After stirring for 1 h, the solution was washed once with 3N NaOH (30 mL), once with 3N HCl (30 mL), once with brine (30 mL), and dried (Na₂SO₄). The solvent was evaporated and chromatographed (ether) to give **88** (159 mg, 61%) as a white solid, mp 65 °C. ¹H-NMR (300 MHz, CDCl₃) δ 2.42 (ddd, *J* = 4.2, 8.2, 13.9 Hz, 2H), 2.13-2.04 (m, 2H), 2.00-1.88 (m, 6H), 1.71-1.65 (m, 2H), 1.12 (s, 6H); ¹³C-NMR (75 MHz, CDCl₃) δ 215.1, 82.6, 39.2, 36.7, 36.1, 27.9. HRMS (ESI) calcd for C₁₁H₁₉O₂⁺ [M+H]⁺ *m/z* 183.1380, found 183.1369.



1,4,7-Trimethyloxatriquinanium hexafluorophosphate (42)

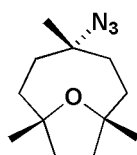
To a stirring solution of **88** (125 mg, 0.687 mmol) in THF (5 mL) was added dropwise a solution of 3M MeMgBr (500 μ L, 1.5 mmol) in diethyl ether. The mixture was allowed to stir for 2 h before being quenched with a minimum amount of water. The solvent was evaporated and the remaining solid was treated conc. aq. HCl (5 mL). The homogeneous solution was allowed to stir for 15 min before being diluted with sat. aq. KPF₆ (30 mL). The precipitated white product was collected and the supernatant was extracted with CH₂Cl₂ (5 x 10 mL). The organic layer was separated and evaporated to give a white solid. The combined solids were washed once with ice-cold water (5 mL), and then thoroughly with ether to give **42** (128 mg, 57%), mp 210-225 °C (dec.); ¹H-NMR (300 MHz, CD₃OD) δ 2.52-2.27 (ddq, $J = 7.4, 9.4, 12.1$ Hz, 12H), 1.71 (s, 9H); ¹³C-NMR (75 MHz, CD₃CN) δ 114.6, 36.2, 25.9; HRMS (ESI) calcd for C₁₂H₂₁O⁺ [M]⁺ m/z 181.1587, found 181.1586



1,7-Dimethyl-4-methylene-10-oxa-bicyclo[5.2.1]decane (91)

A solution of **42** (20 mg, 61 μ mol) and tetraethylammonium acetate tetrahydrate (17 mg, 65 μ mol) was stirred in acetonitrile (2 mL). The reaction mixture was diluted with water (20 mL) and extracted with pentane (5 x 5 mL). The combined organic layers were washed with water and brine and then dried (Na₂SO₄). The solvent was

evaporated and the residue was chromatographed (CH₂Cl₂) to give **91** as a colorless oil (10 mg, 92%). ¹H-NMR (600 MHz, CD₃OD) δ 4.72 (s, 2H), 2.32-2.27 (m, 2H), 2.24-2.19 (m, 2H), 2.13-2.06 (m, 2H), 1.83-1.78 (m, 2H), 1.75-1.73 (m, 2H), 1.70-1.64 (m, 2H), 1.21 (s, 6H); ¹³C-NMR (125 MHz, CD₃CN) δ 153.81, 110.5, 84.7, 42.5, 37.0, 31.7, 30.0; HRMS (ESI) calcd for C₁₂H₂₁O⁺ [M+H]⁺ *m/z* 181.1587, found 181.1579



4-Azido-1,4,7-trimethyl-10-oxa-bicyclo[5.2.1]decane (**90**)

A solution of **42** (92 mg, 0.28 mmol) and NaN₃ (21 mg, 0.32 mmol) in methanol (5 mL) was stirred for 30 min. The solvent was evaporated under a steady stream of argon and the solid residue was triturated with ether. The triturate was dried (Na₂SO₄) and the solvent was evaporated under a steady stream of argon to give **90** (44 mg, 70%) as a colorless oil. ¹H-NMR (400 MHz, CD₃OD) δ 1.96-1.92 (m, 4H), 1.83-1.81 (m, 2H), 1.71-1.69 (m, 4H), 1.58-1.52 (m, 2H), 1.34 (s, 3H), 1.21 (s, 6H); ¹³C-NMR (100 MHz, CD₃OD) δ 82.5, 66.0, 39.9, 36.3, 35.3, 29.0, 28.9; IR (film) ν_{\max} : 2931, 2927, 2097 cm⁻¹; HRMS (ESI) calcd for C₁₂H₂₁O⁺ [M-N₃]⁺ *m/z* 181.1587, found 181.1579.

General Procedure for the Analysis of Rate Dependence of [NaN₃] in the Formation of **90 Using ¹H-NMR:** An NMR tube was charged with a freshly prepared solution of 6 mM **42** in 0.2 M LiBF₄ in CD₃OD (500 μL), to which was added the internal standard CHCl₃ (10 μL) and a solution of 48, 60, or 72 mM NaN₃ in 0.2 M LiBF₄ in CD₃OD (500 μL). The mixture was quickly agitated and immediately placed into an NMR probe equilibrated to 298 K. ¹H-NMR spectra were obtained once every 30 s using the "array" parameter on a Varian MercuryPlus-400 NMR spectrometer. The resulting concentration versus time data were corrected for the time interval between injection of azide solution and the acquisition of the first data point (approximately 60-80 s). Pseudo-first order rate constants were obtained by plotting ln [**90**] versus time (s) giving linear plots up to 90% conversion.

References

- 1) Mascial, M.; Hafezi, N.; Meher, N. K.; Fettinger, J. C. *J. Am. Chem. Soc.* **2008**, *130*, 13532
- 2) Review: Haley, M. M. *Angew. Chem., Int. Ed.* **2009**, *48*, 1544.
- 3) Mascial, M.; Hafezi, N.; Toney, M.D. *J. Am. Chem. Soc.*, **2010**, *132* (31), 10662–10664
- 4) Phan, T. B.; Nolte, C.; Kobayashi, S.; Ofial, A. R.; Mayr, H. *J. Am. Chem. Soc.* **2009**, *131*, 11392.
- 5) Hughes, E. D.; Ingold, C. K.; Mackie, J. D. H. *J. Chem. Soc.* **1955**, 3173.
- 6a) Winstein, S.; Smith, S.; Darwish, D. *Tetrahedron Lett.* **1959**, 24.
- 6b) Cook, D.; Parker, A. J. *J. Chem. Soc. B* **1968**, 142.
- 7) Miotti, A.; Fava, A. *J. Am. Chem. Soc.* **1966**, *88*, 4274.
- 8) Edwards, O. E.; Grieco, C. *Can. J. Chem.* **1974**, *52*, 3561.
- 9) Grob, C. A.; Seckinger, K.; Tam, S. W.; Traber, R. *Tetrahedron Lett.* **1973**, 3051.
- 10) Calculations were performed by Professor Mark Mascial using the density functional B3LYP method with the 6-31G(d,p) basis set. Optimizations were done both in the gas phase and in a polarizable continuum solvent model (methanol, $\epsilon = 32.63$) using the CPCM method with United Atom Topological Model radii. Default optimization parameters in the Gaussian03 program were applied: Frisch, M. J.; et al. *Gaussian 03*, revision D.01; Gaussian, Inc.: Wallingford CT, 2004
- 11) Bordwell, F. G.; Mecca, T. G. *J. Am. Chem. Soc.* **1972**, *94*, 2119.
- 12) Winstein, S.; Savedoff, L. G.; Smith, S. *Tetrahedron Lett.* **1960**, 24, and references therein.

- 13) It must be noted that **42** is not the only example of a tertiary oxonium ion. Gargiulo and Tarbell in 1969 described 1,2,2,5-tetramethyltetrahydrofuran, which was stable enough to be isolated. It did, however, show reactivity that would be expected of a tertiary oxonium salt, solvolyzing with ethanol by exclusive attack at the 2-position: Gargiulo, R. J.; Tarbell, D. S. *Proc. Natl. Acad. Sci. U.S.A.* **1969**, *62*, 52.

Chapter 5
Future Work

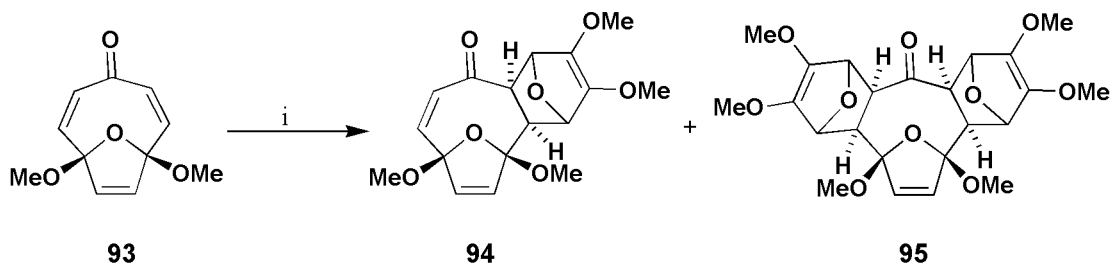
5.1 - Introduction

It is evident from the results discussed in the preceding chapter that the presence of a methyl group attached to the alpha fails to block an incoming nucleophile from attacking the oxatriquinane ring system in **42**, despite the electrophile being a tertiary carbon. We therefore began to explore the possibility of blocking the alpha carbon by introducing substituents on the neighboring beta carbons. An example of this was observed by Cook and Parker,¹ who found that while sodium azide reacted with *tert*-butyl bromide to give S_N2 and E2 products, no reaction occurred when employing the same conditions to sodium azide and neopentyl bromide.

5.2 – The Diels-Alder Reaction

The Diels-Alder reaction is a powerful method of forming carbon-carbon bonds in a diastereoselective fashion. Trienone **75**, an intermediate in the synthesis of oxatriquinacene, could serve as an ideal dienophile due to its electron-poor double bonds stemming from conjugation with the carbonyl group. Although we were confident that a Diels-Alder reaction would occur on the alpha-beta unsaturated double bonds, it was uncertain as to whether the double bond opposite the ether oxygen satisfied the electron demand of the diene.

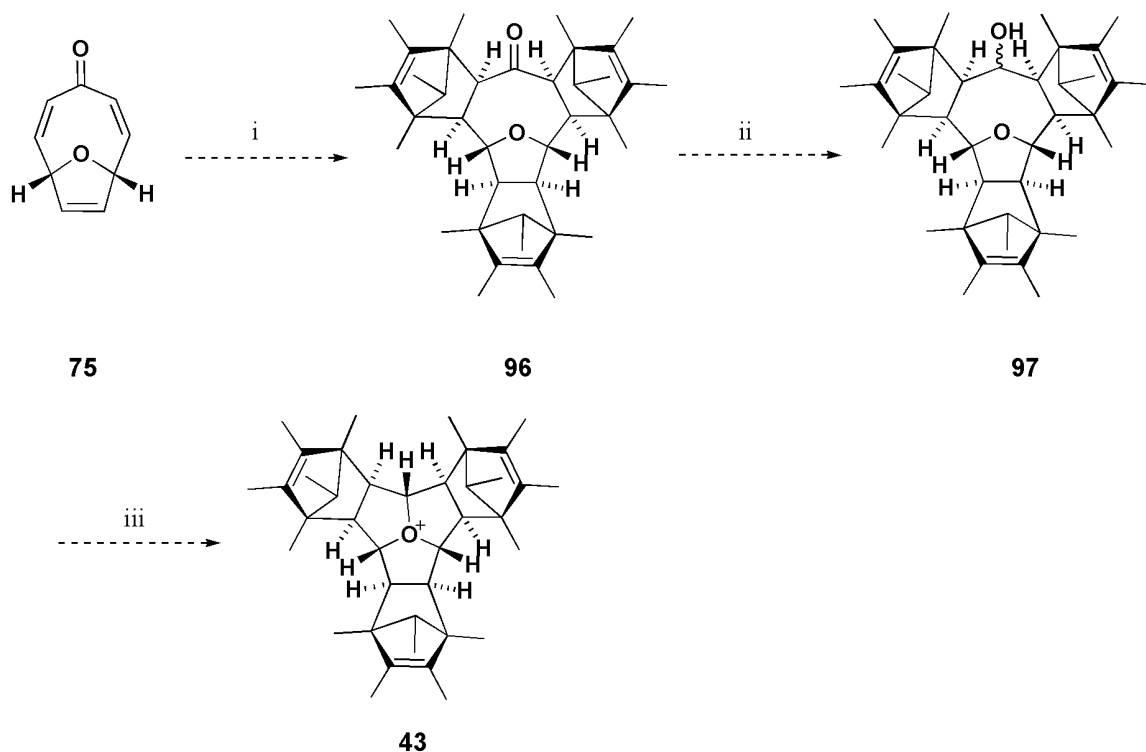
A similar synthetic approach was pursued by Prinzbach and co-workers.² It was found that only electron-rich furans would undergo a Diels-Alder reaction with **93** at high temperatures and pressures, for a prolonged amount of time, and in poor yield. Although this precedent appeared to be discouraging, we believed that the poor reactivity was due to steric constraints attributed to the methoxy groups and not to orbital interactions or electron demand (Scheme 5.3).



Scheme 5.1 - Reagents and conditions: i) 3,4-dimethoxyfuran, diethyl ether, 60 °C, 15 kbar, 11 days, 26% (4:1)

5.3 – Preparation of Diels-Alder Adducts of Trienone **75**.

It is critical that the 1- and 4-positions of the dienes be substituted to ensure optimal steric congestion while preserving structural integrity. The dienes that fit this criteria were the following: 2,5-dimethylfuran, 1,4-dimethyl-1,3-cyclohexadiene, and 1,2,3,4,5-pentamethylcyclopentadiene (Cp*). Upon treatment of **75** in neat 2,5-dimethylfuran heated to 250 °C in a pressure vessel, only the starting material was observed from TLC and mass spectrometry. Likewise, treatment of **75** with 1,4-dimethyl-1,3-cyclohexadiene in toluene, heated to 270 °C also failed to form any adducts. However, trienone **75** reacted successfully with the bulky Cp* to give mono-, di-, and tri-adducts, which could be observed by TLC and mass spectrometry. The successful formation of these Diels-Alder adducts along with their potential to form novel oxonium ions merits further investigation, as shown in Scheme 5.2.

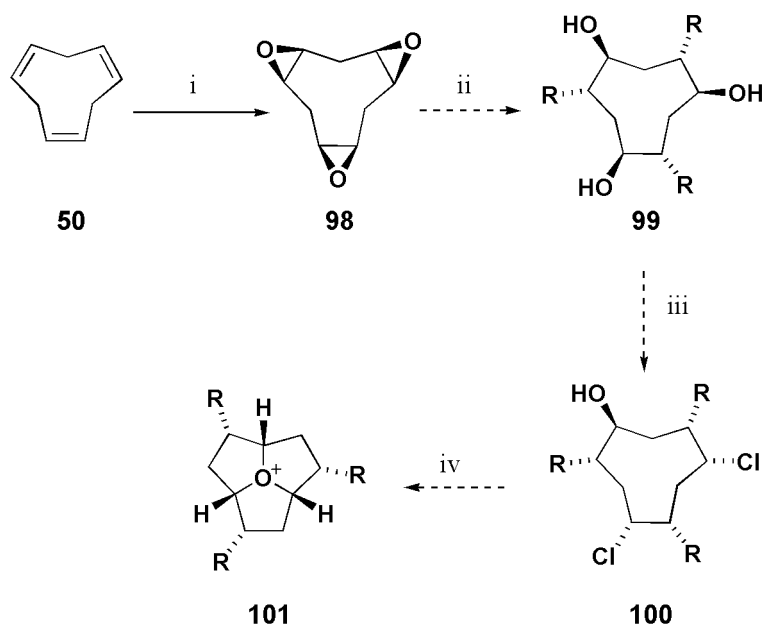


Scheme 5.2 – Proposed reagents and conditions: i) Cp*, toluene, reflux; ii) LiAlH₄, ether; iii) TfOH, CH₃CN

5.4 – Formation of Beta-substituted Oxatriquinanes Through 1,4,7-Cyclonatriene Trioxide

An alternative route to beta-substituted oxatriquinanes can be accomplished by reaction of an organometallic reagent and 1,4,7-cyclonatriene trioxide (**98**) (Scheme 5.3). This known epoxide can be prepared by treatment of triene **50** with three equivalents of *m*-CPBA.² Exposure of **98** to an organometallic reagent would ideally result in three-fold alkylation to give triol **99**. It is presumed that the oxygen from the first ring opening could facilitate regioselective attack of the two remaining epoxides. Stoichiometric halogenations of **99** with two equivalents of thionyl chloride would invert the stereochemistry to give dichloro alcohol **100** and

subsequent treatment with silver hexafluorophosphate could facilitate backside displacement of the two chlorides by the alcohol to give oxonium **101**.



Scheme 5.3 – Proposed reagents and conditions: i) 3 eq. *m*-CPBA, CH_2Cl_2 ; ii) R-M ($\text{M} = \text{MgX}$, CeCl_2 , $\text{Ti}(\text{O}i\text{Pr})_3$), THF; iii) 2 eq. SOCl_2 , CH_2Cl_2 ; iv) AgPF_6 , CH_3CN

5.5 - Conclusion

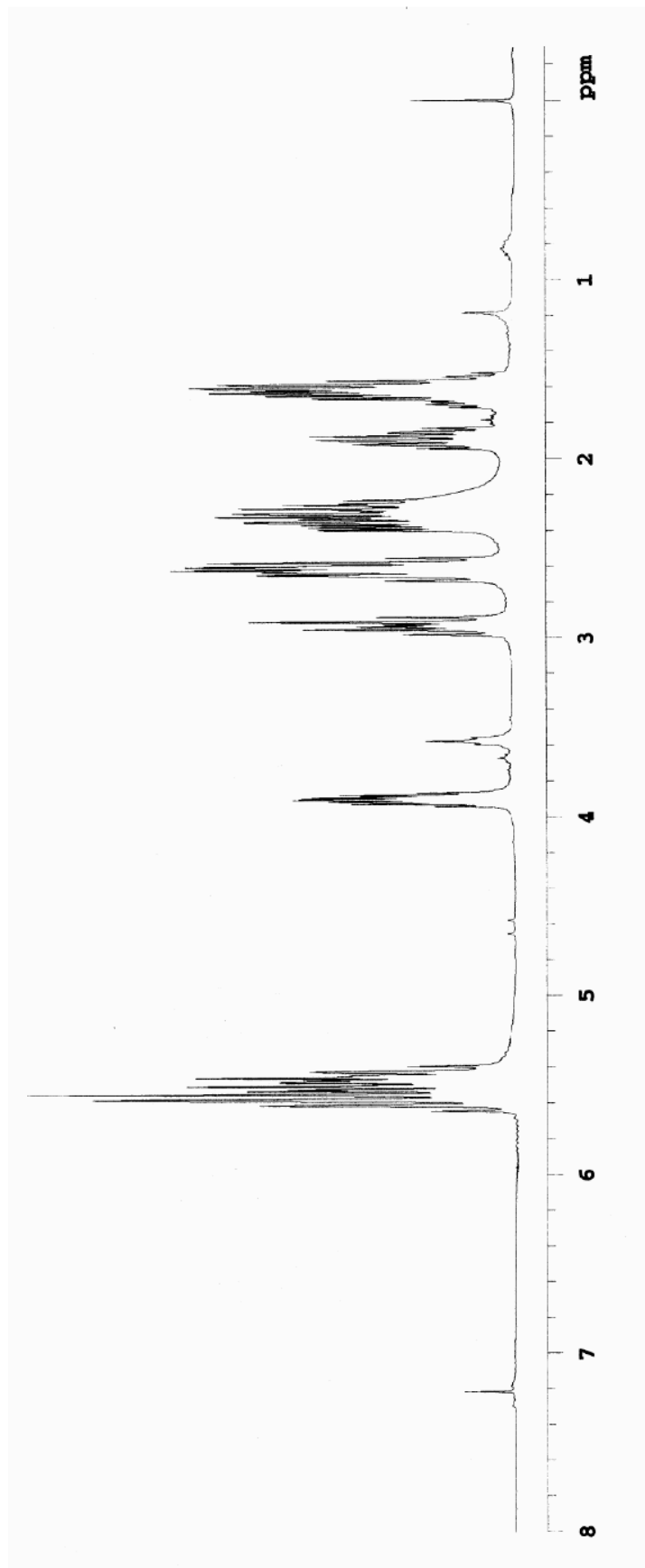
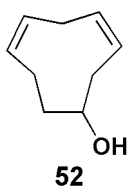
In conclusion, different strategies toward obtaining beta-substituted oxatriquinanes are discussed. By utilizing trienone **75** in the Diels-Alder reaction, bulky dienes, such as Cp^* may be introduced. Beta-substitution can also occur by treating triepoxide **98** with organometallic reagents. These synthetic pathways could pave the way towards an “indestructible” oxonium ion.

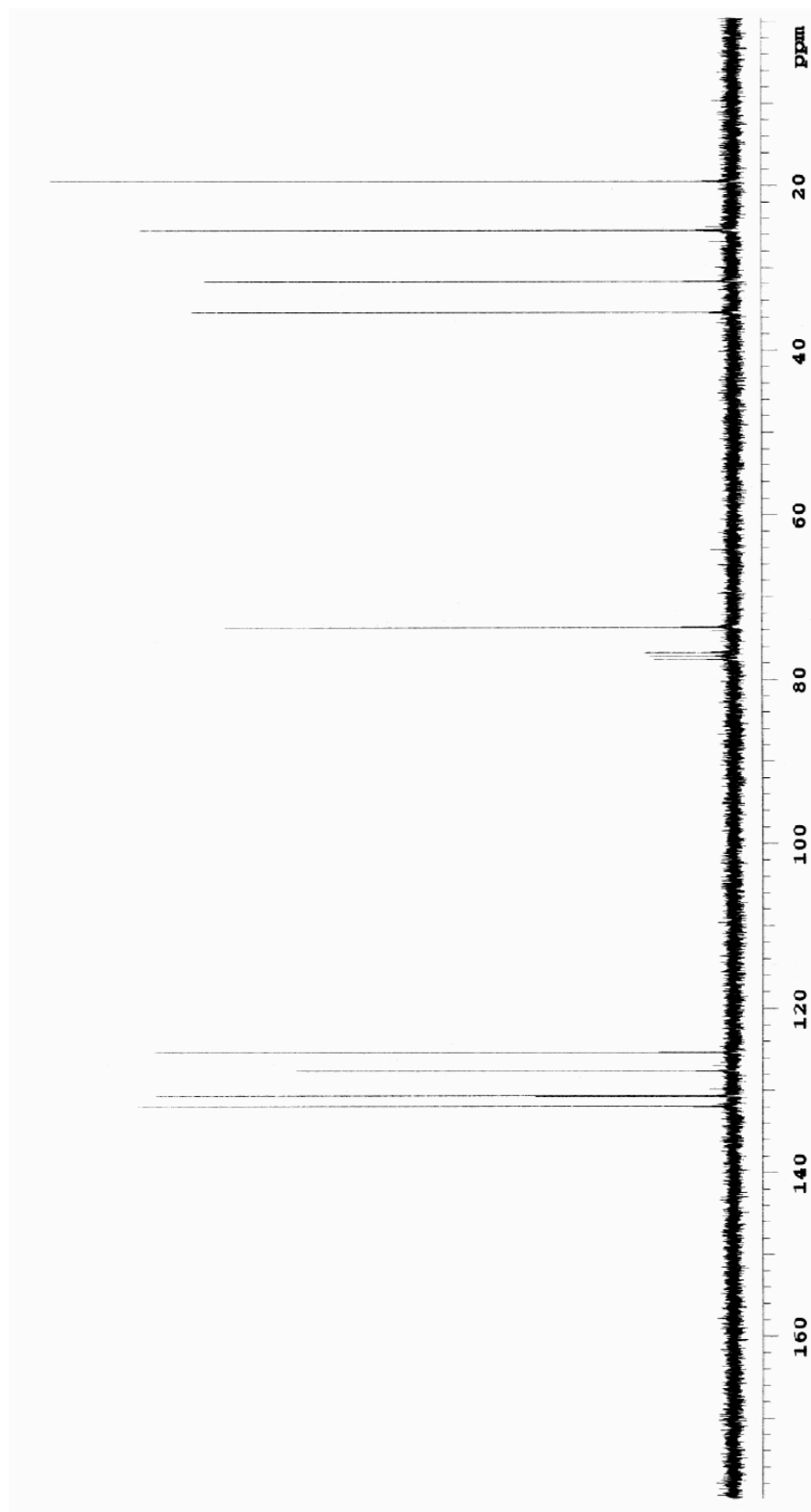
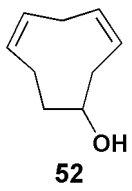
References

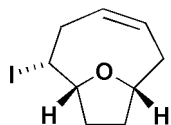
- 1) Cook, D.; Parker, A. J. *J. Chem. Soc. B* **1968**, 142.
- 2) Person, G.; Keller, M.; Prinzbach, H. *Liebigs Ann.* **1996**, 507; Pleschke, A.; Geier, J.; Keller, M.; Wörth, J.; Knothe, L.; Prinzbach, H. *Eur. J. Org. Chem.* **2007**, 4867.

Appendix

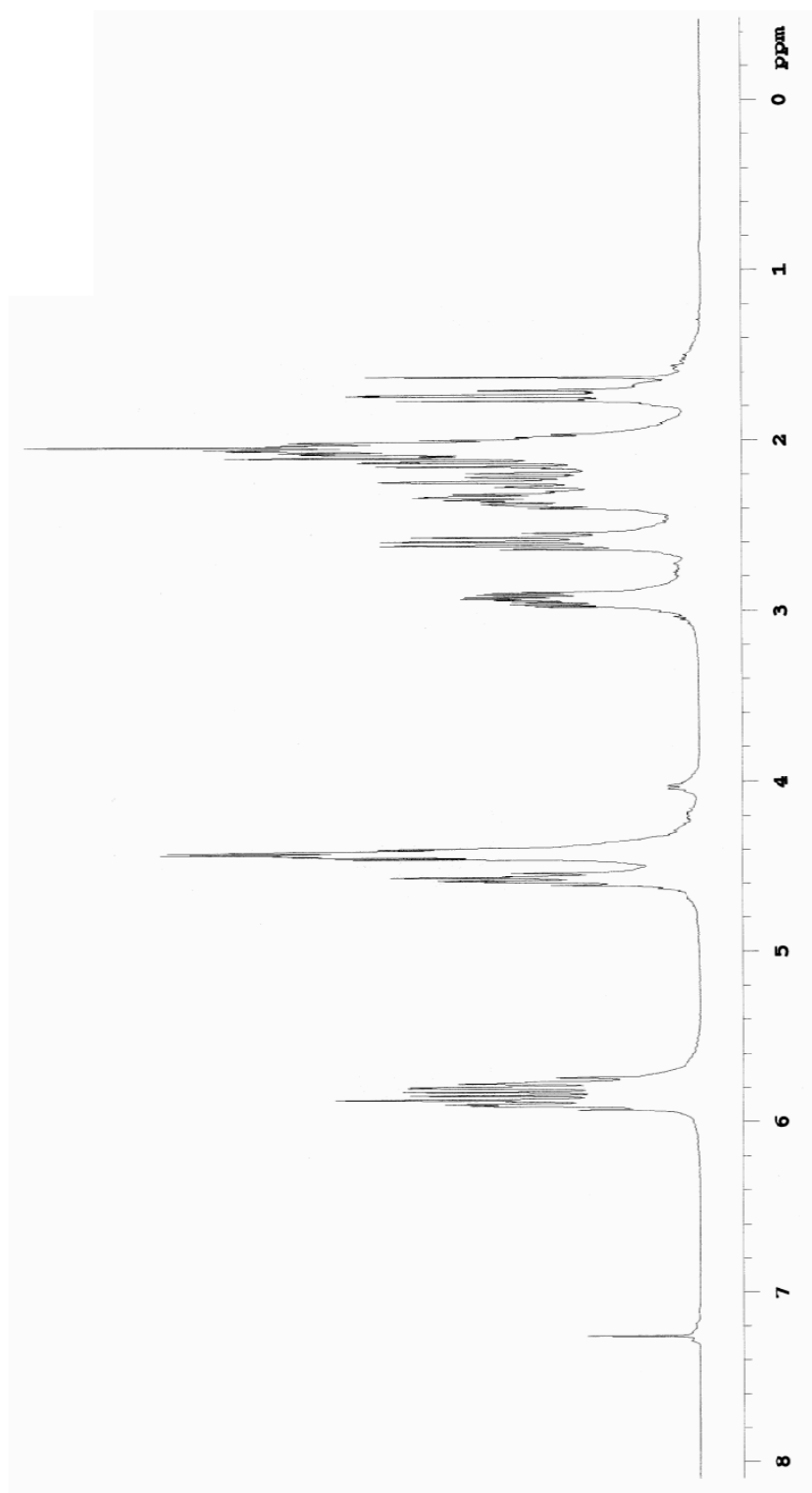
Representative NMR spectra are present

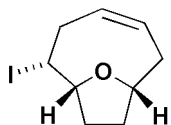




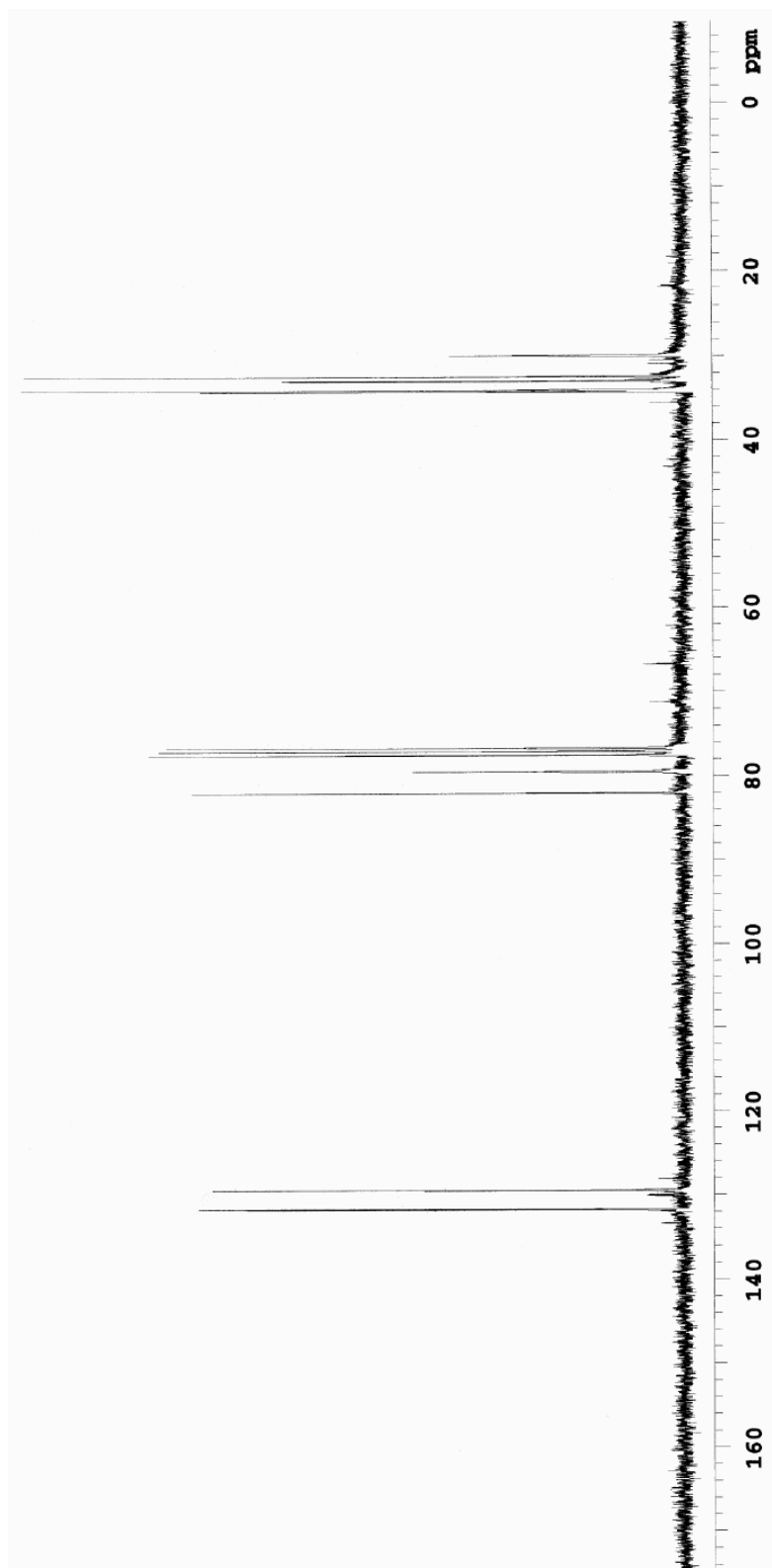


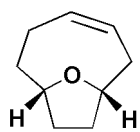
56



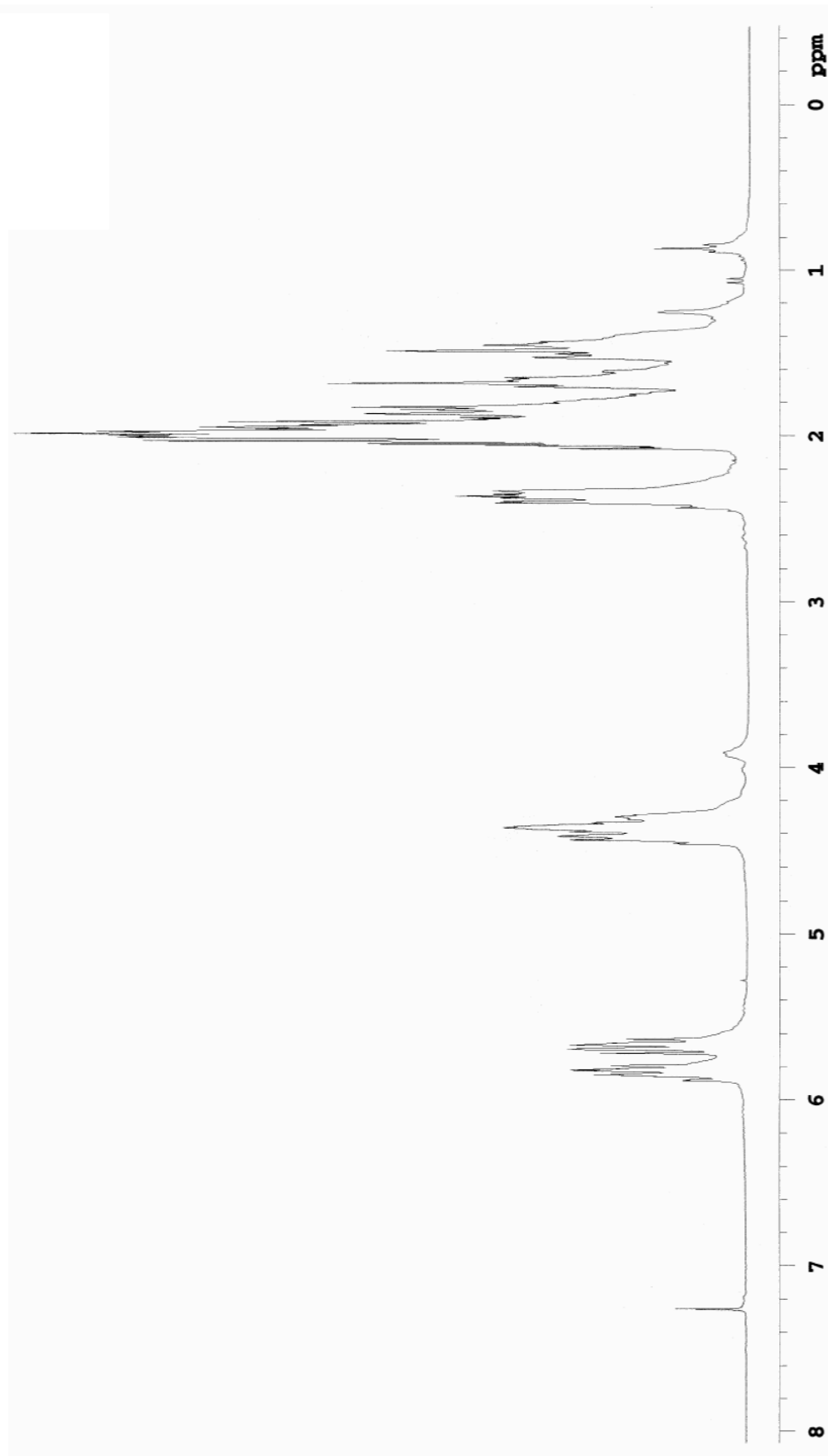


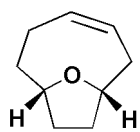
56



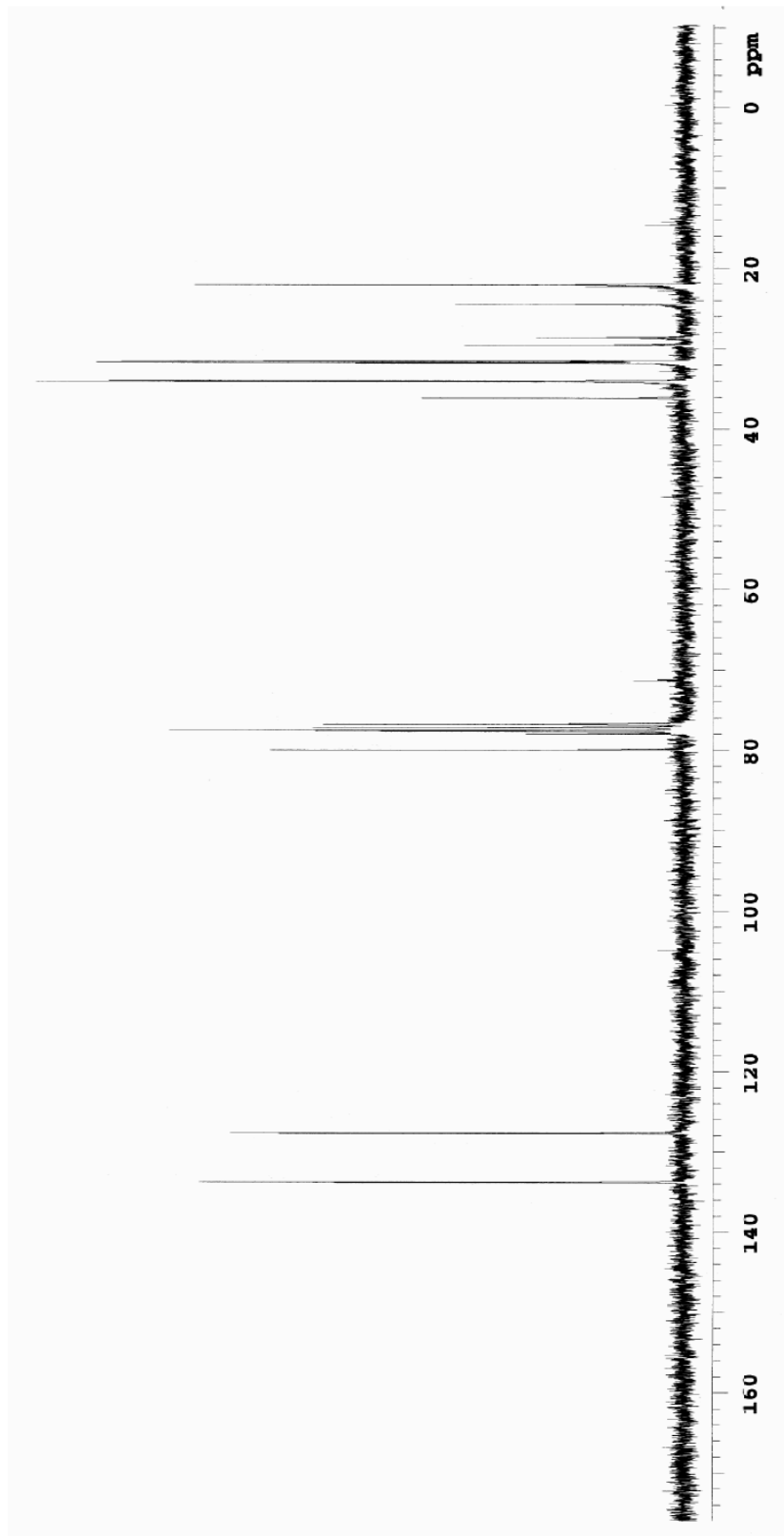


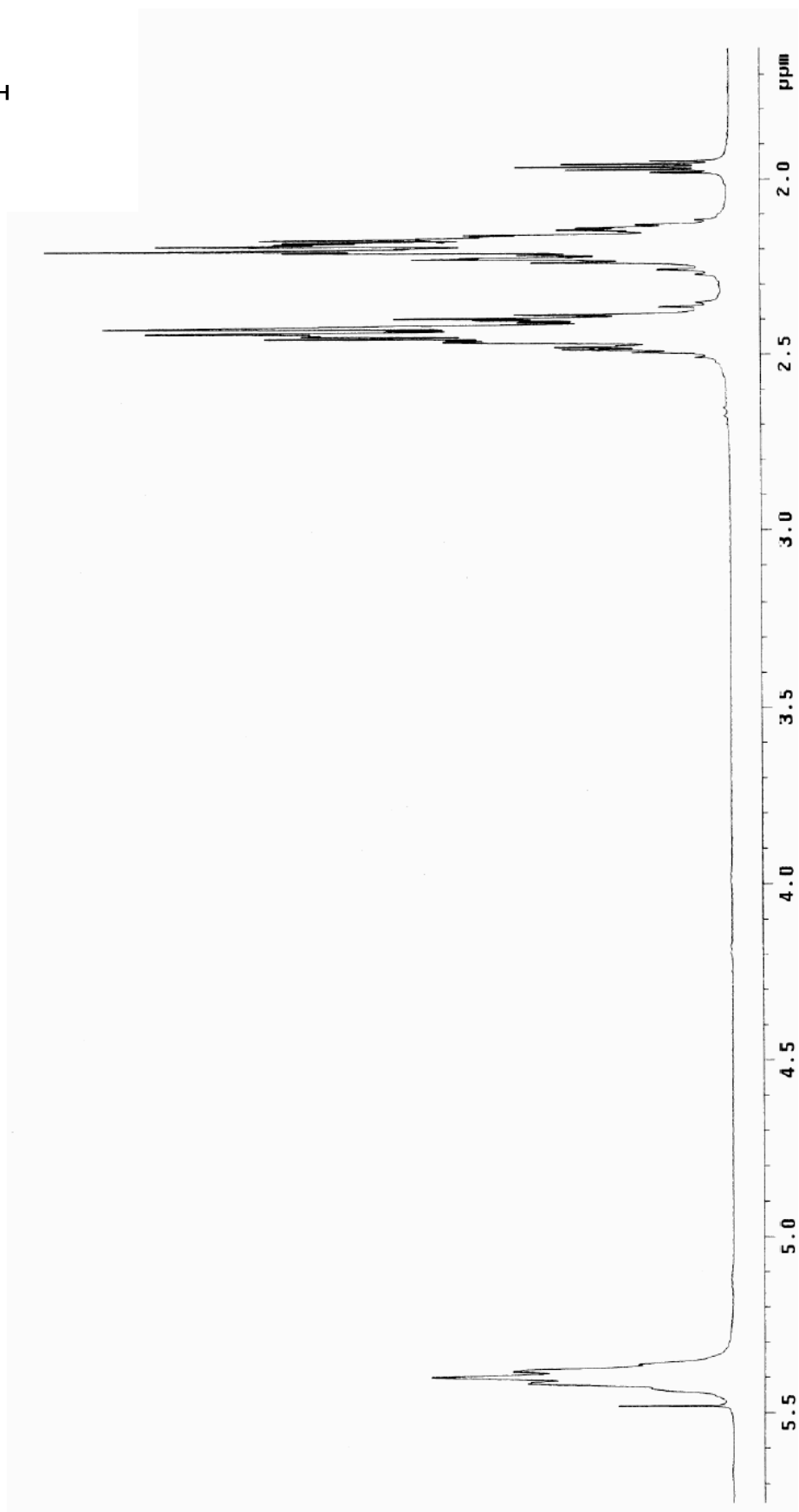
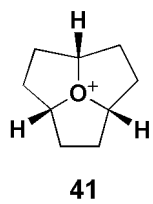
53

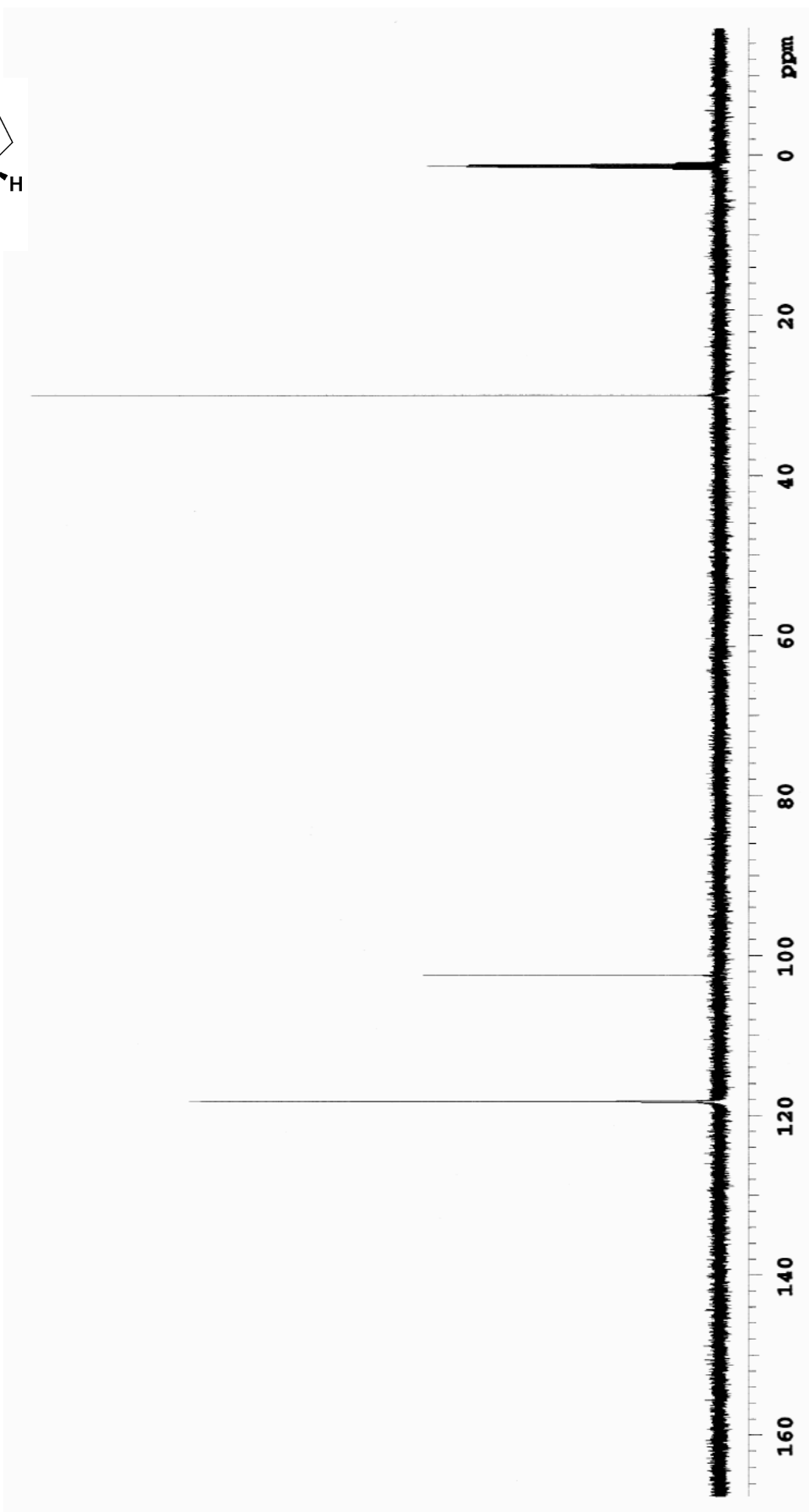
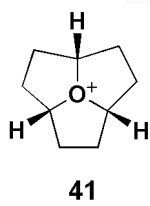


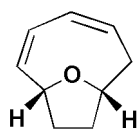


53

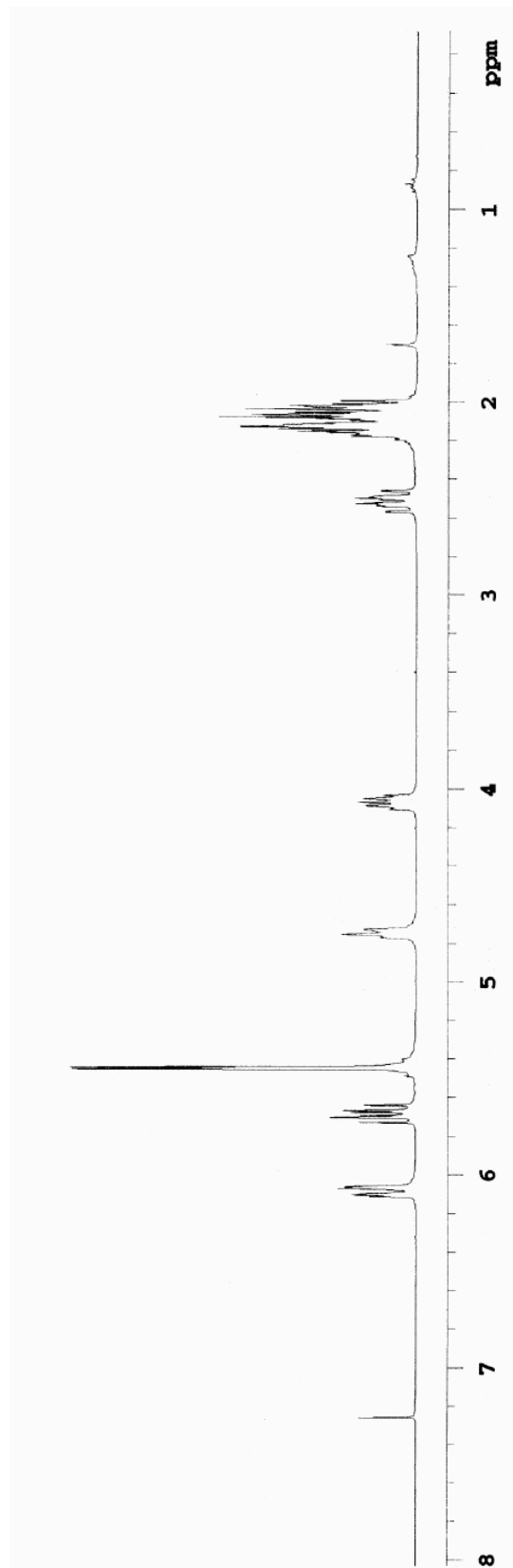


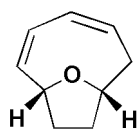




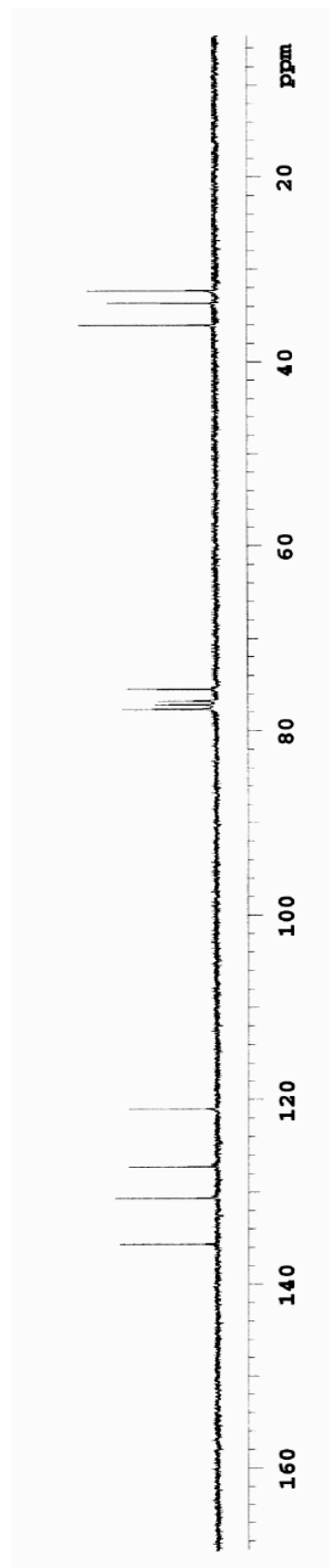


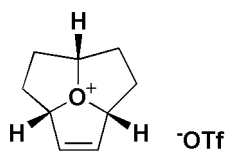
70



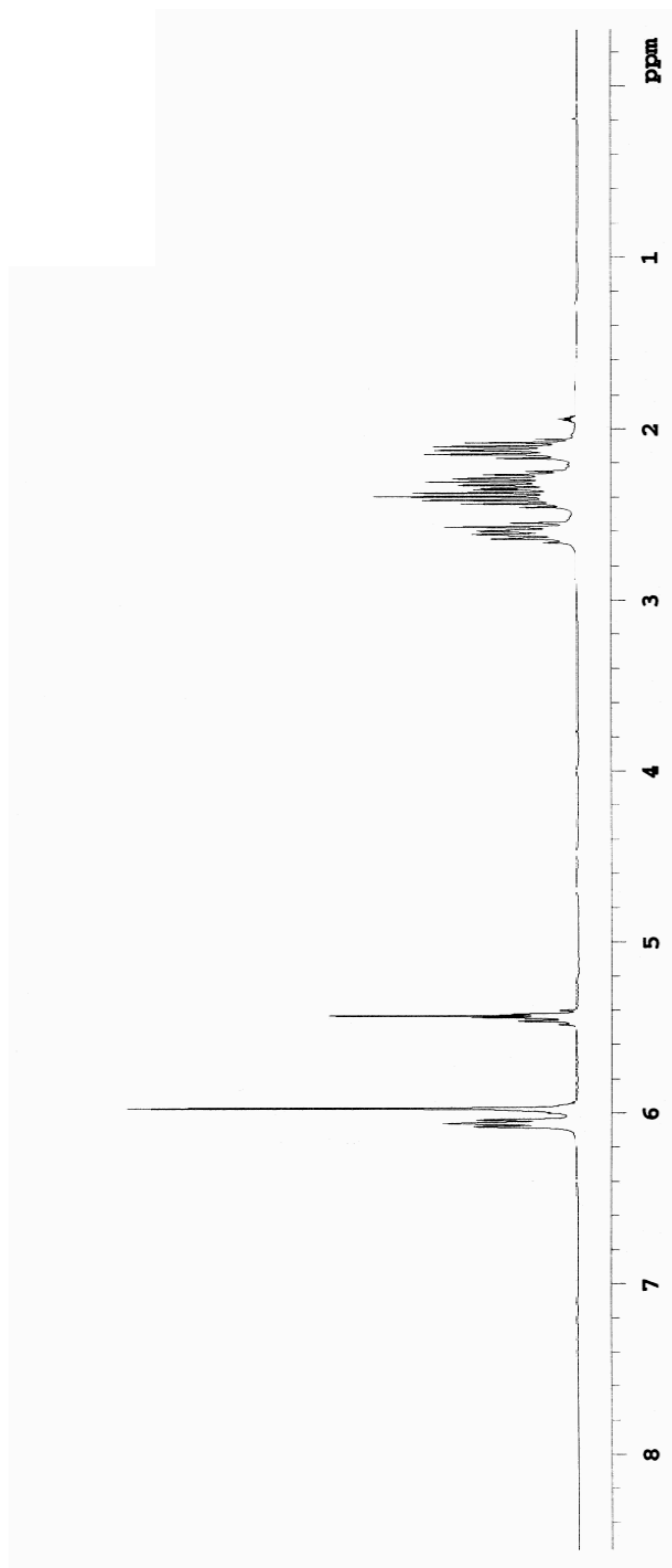


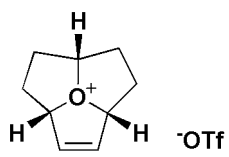
70



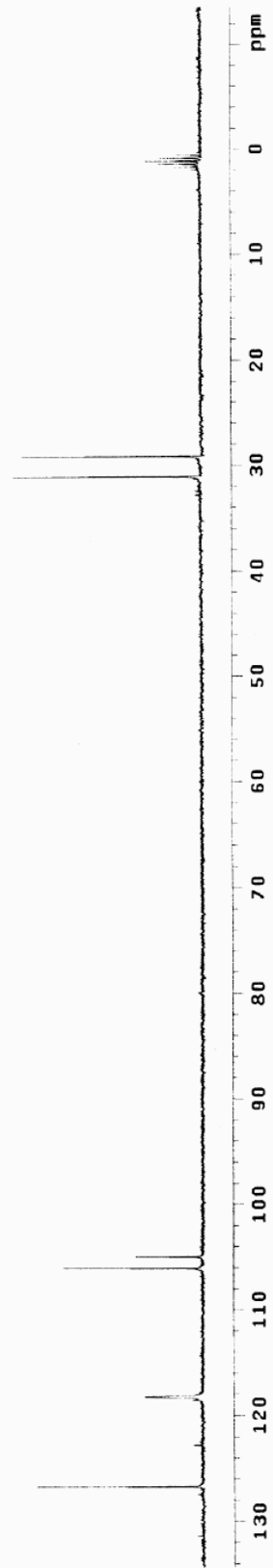


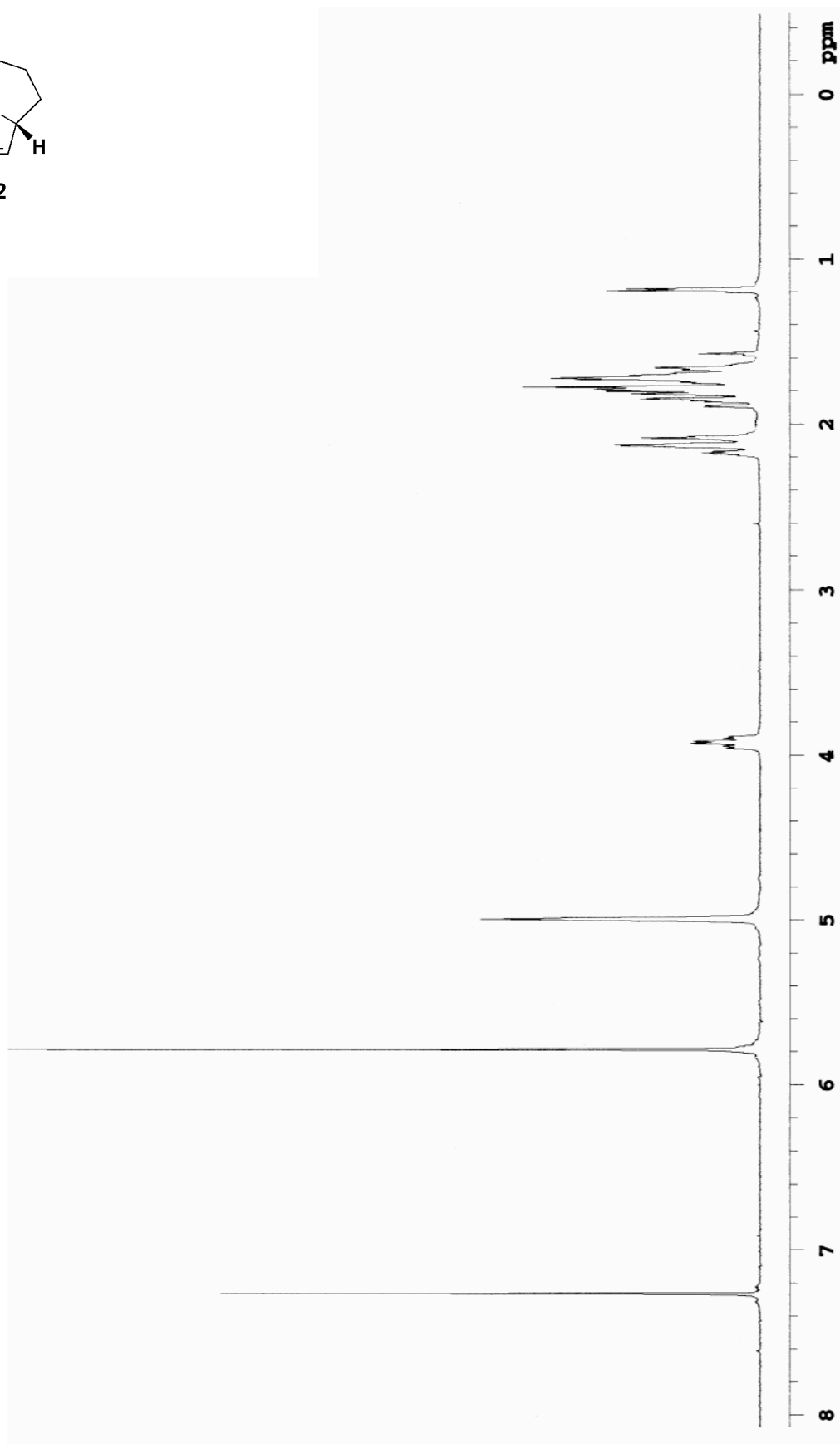
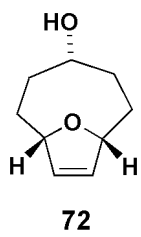
71

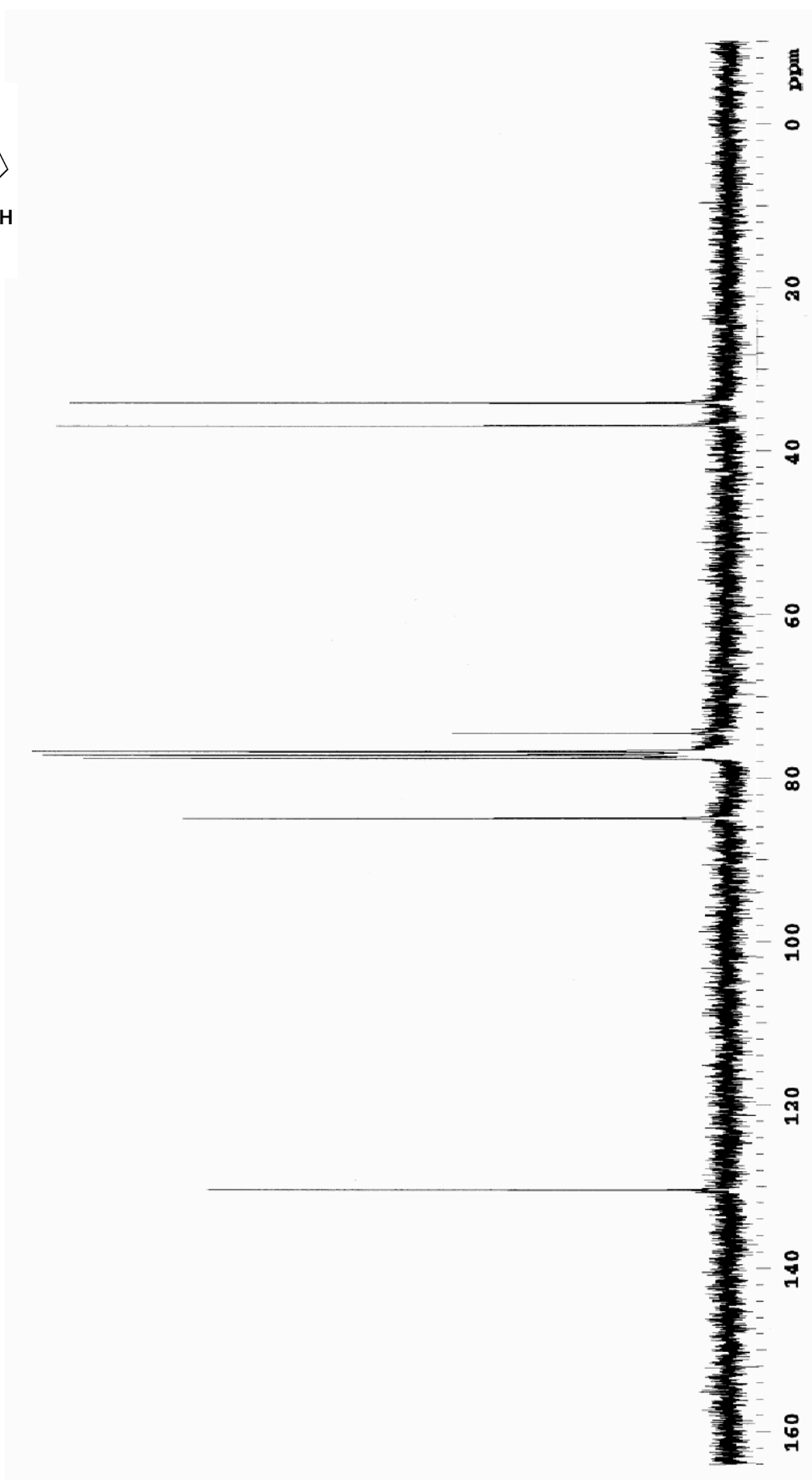
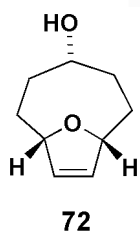


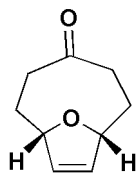


71

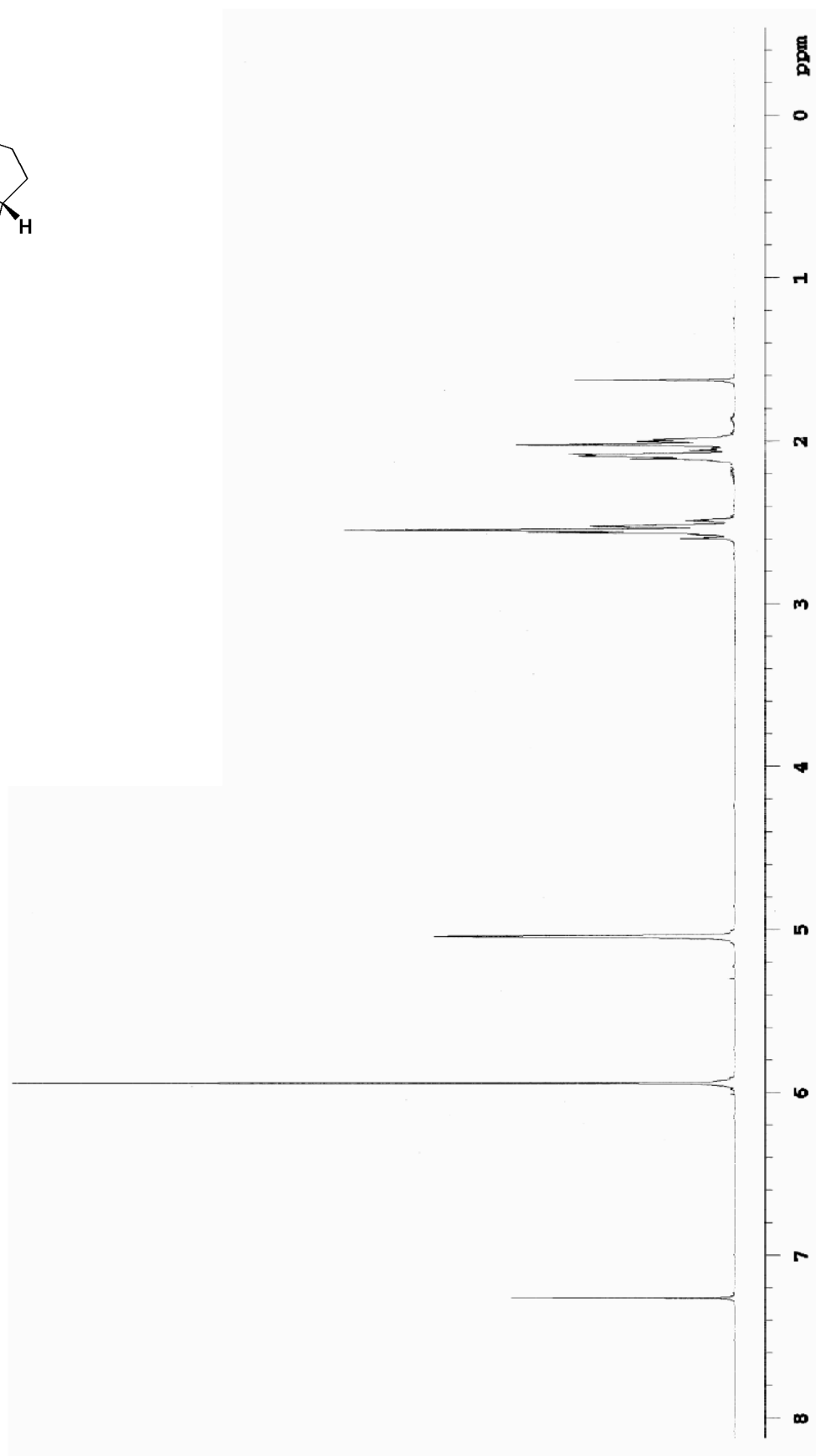


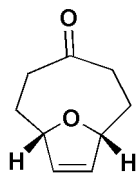




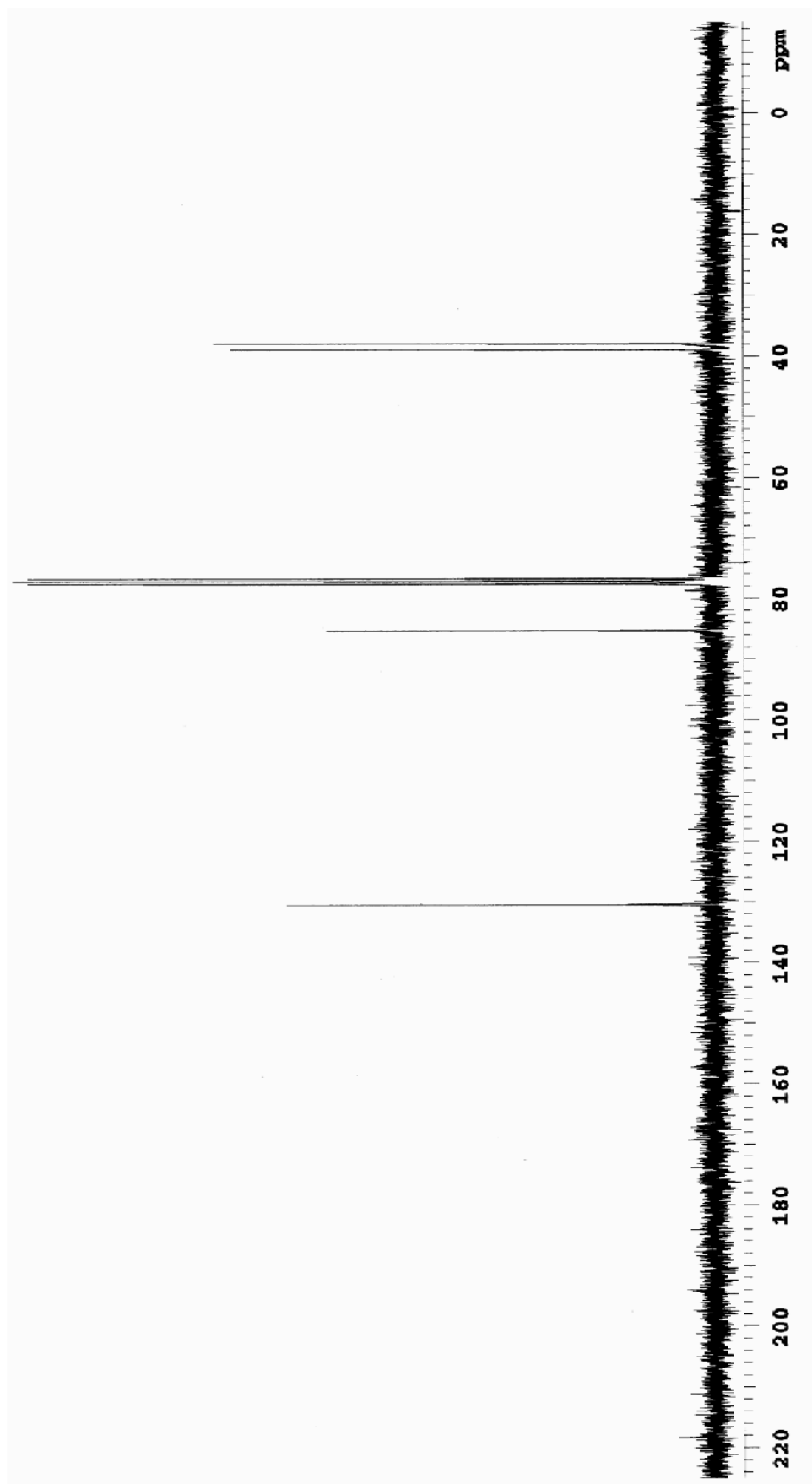


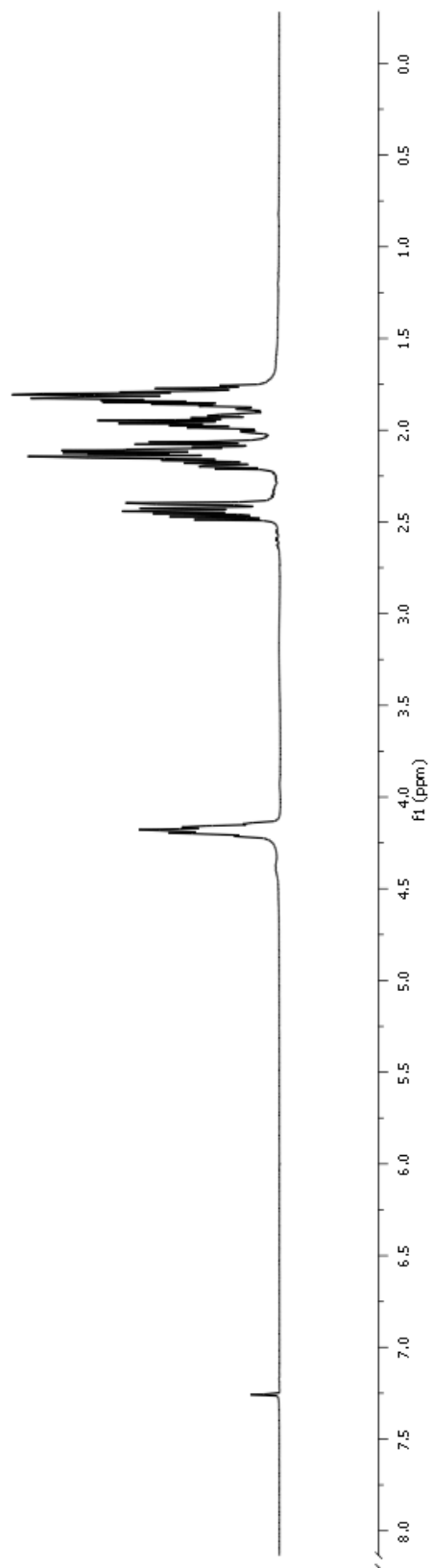
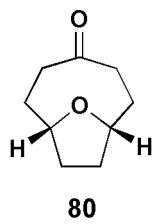
73

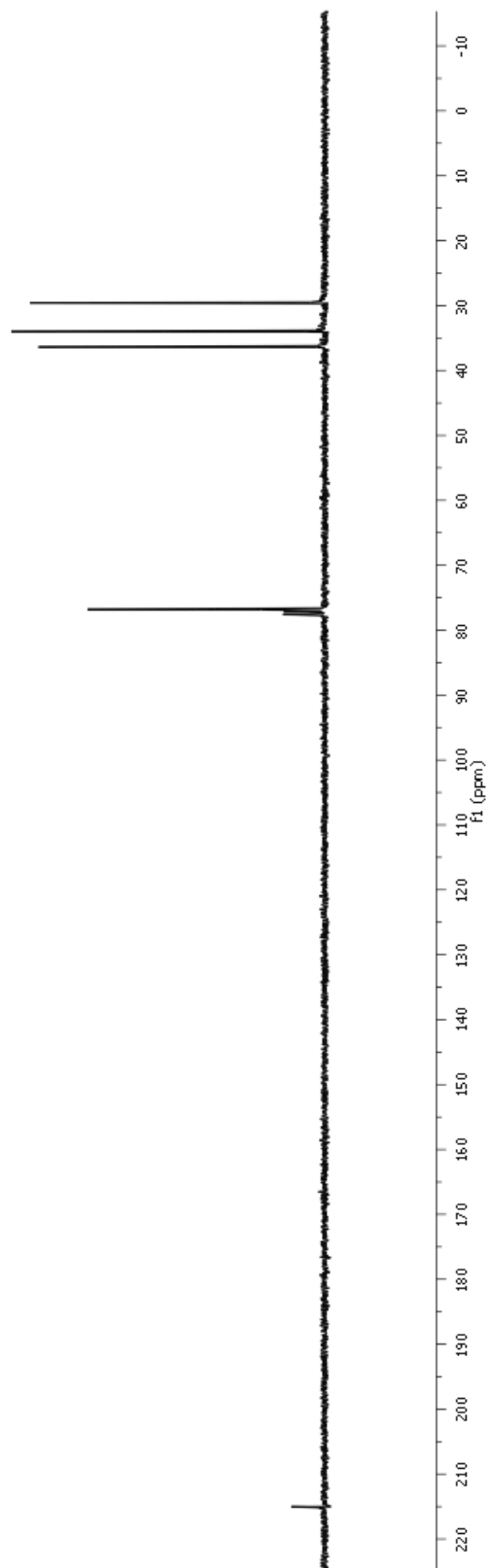
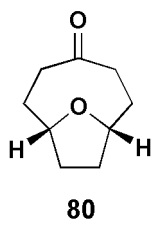


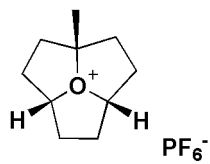


73

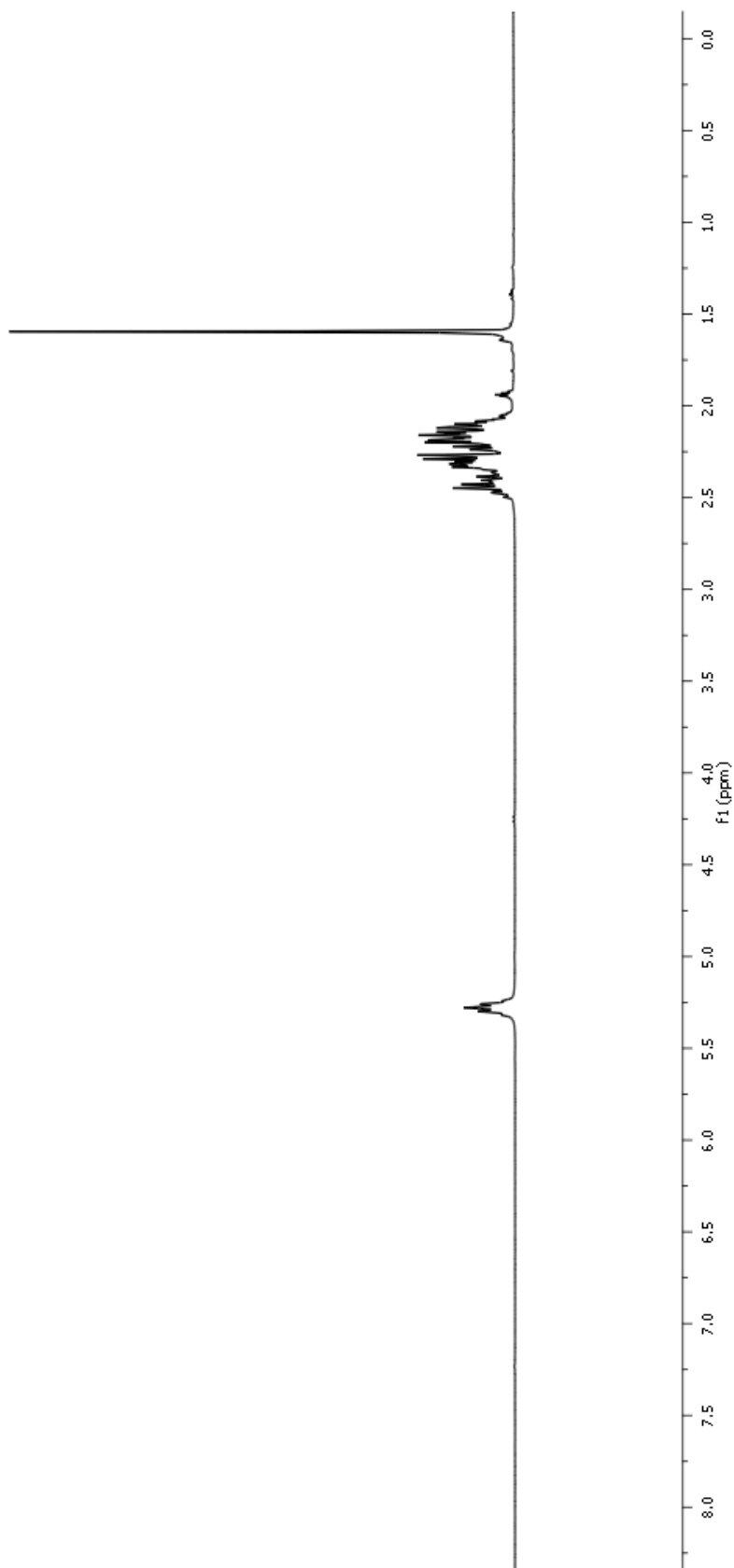


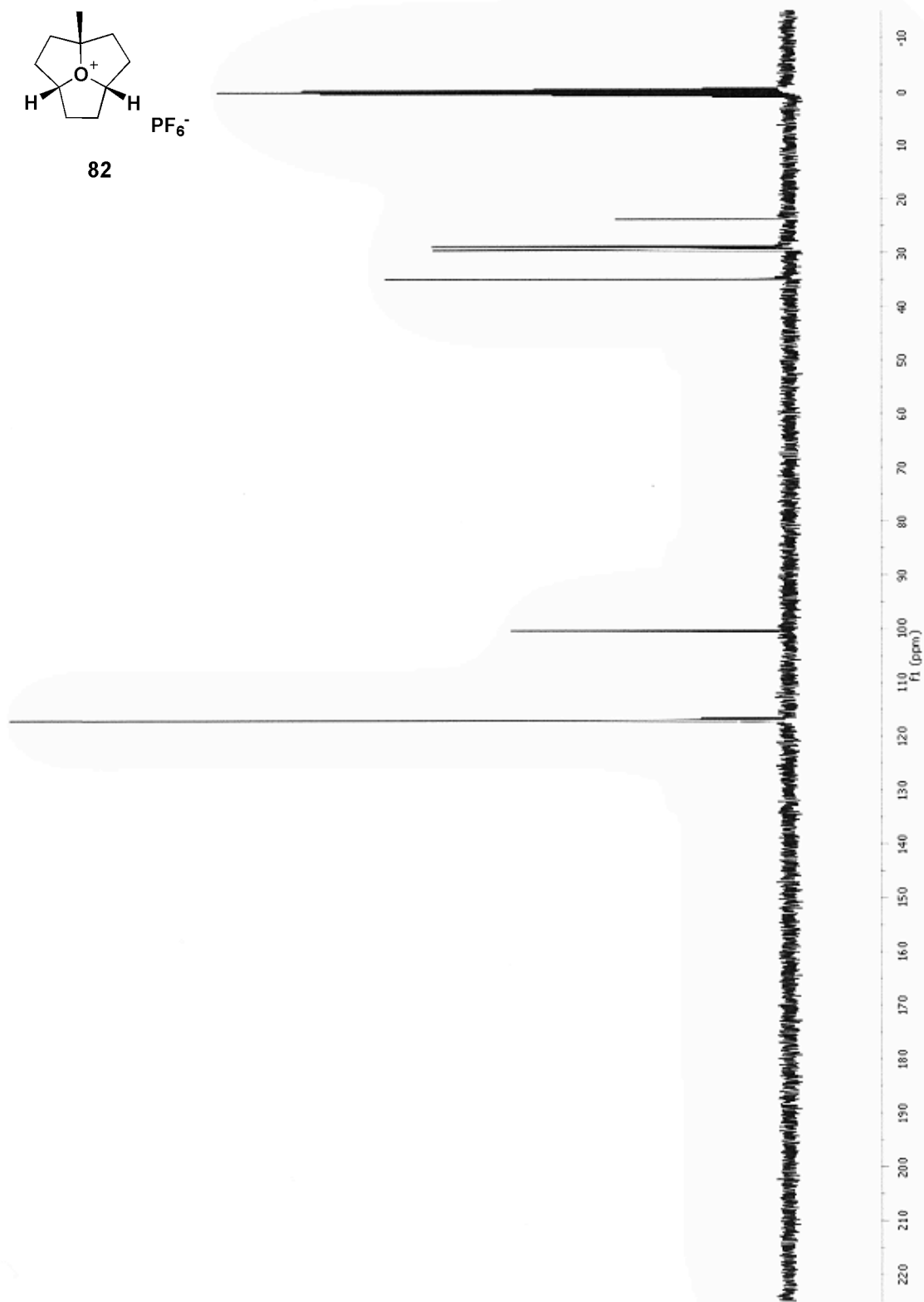
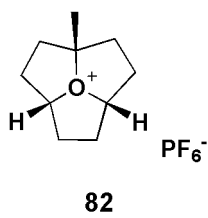


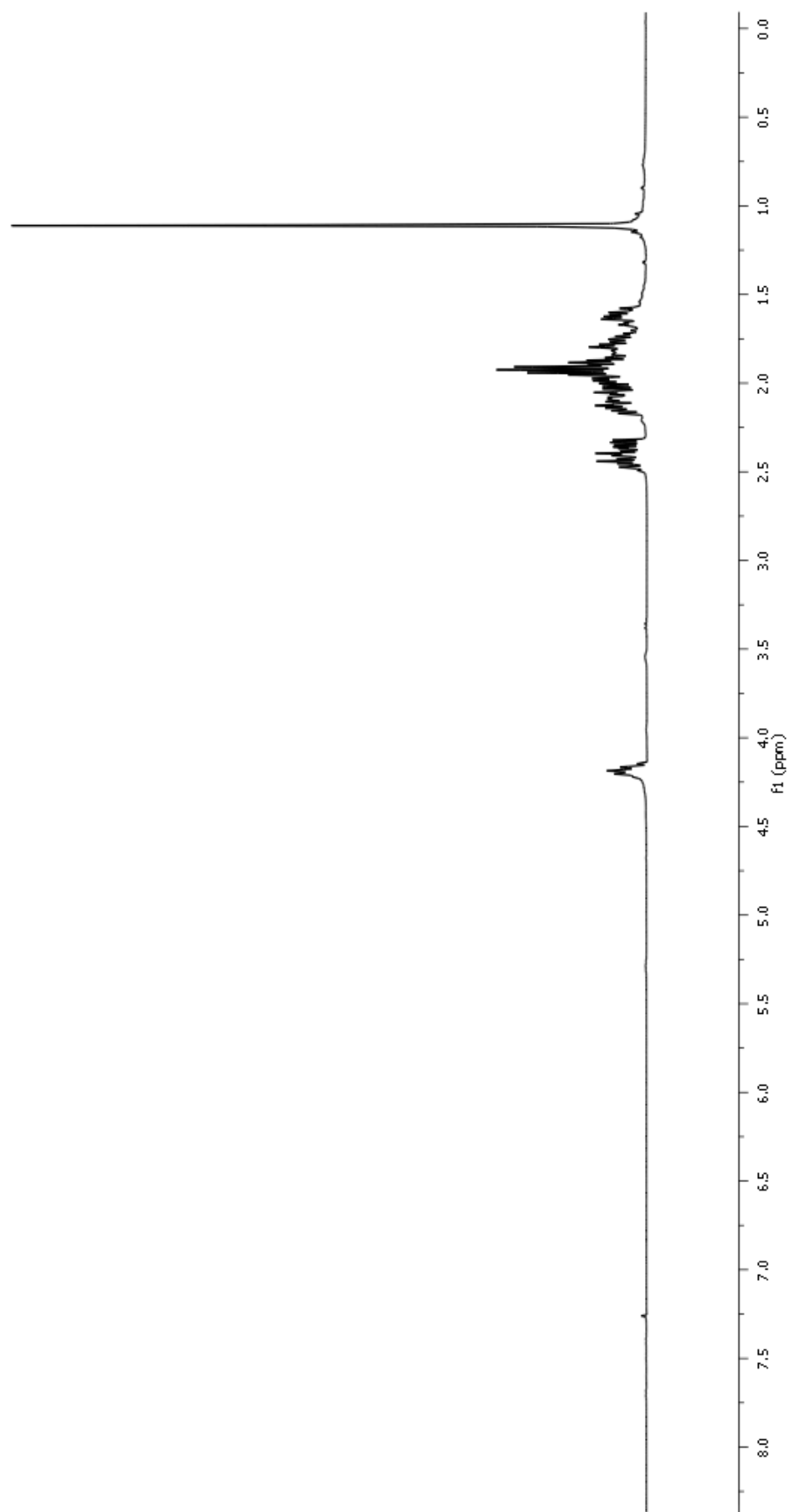
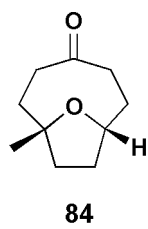


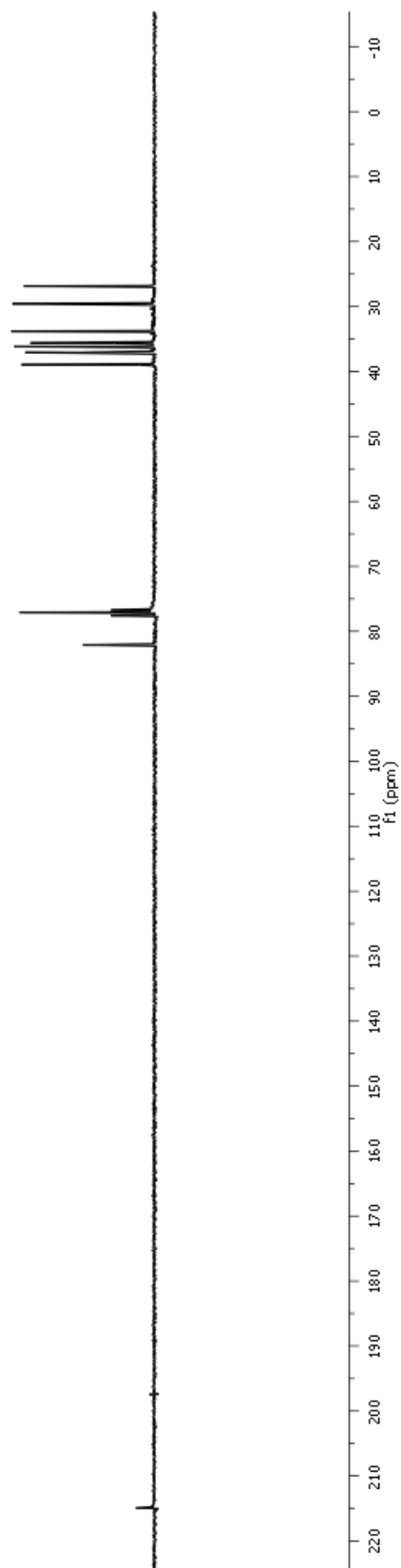
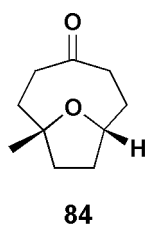


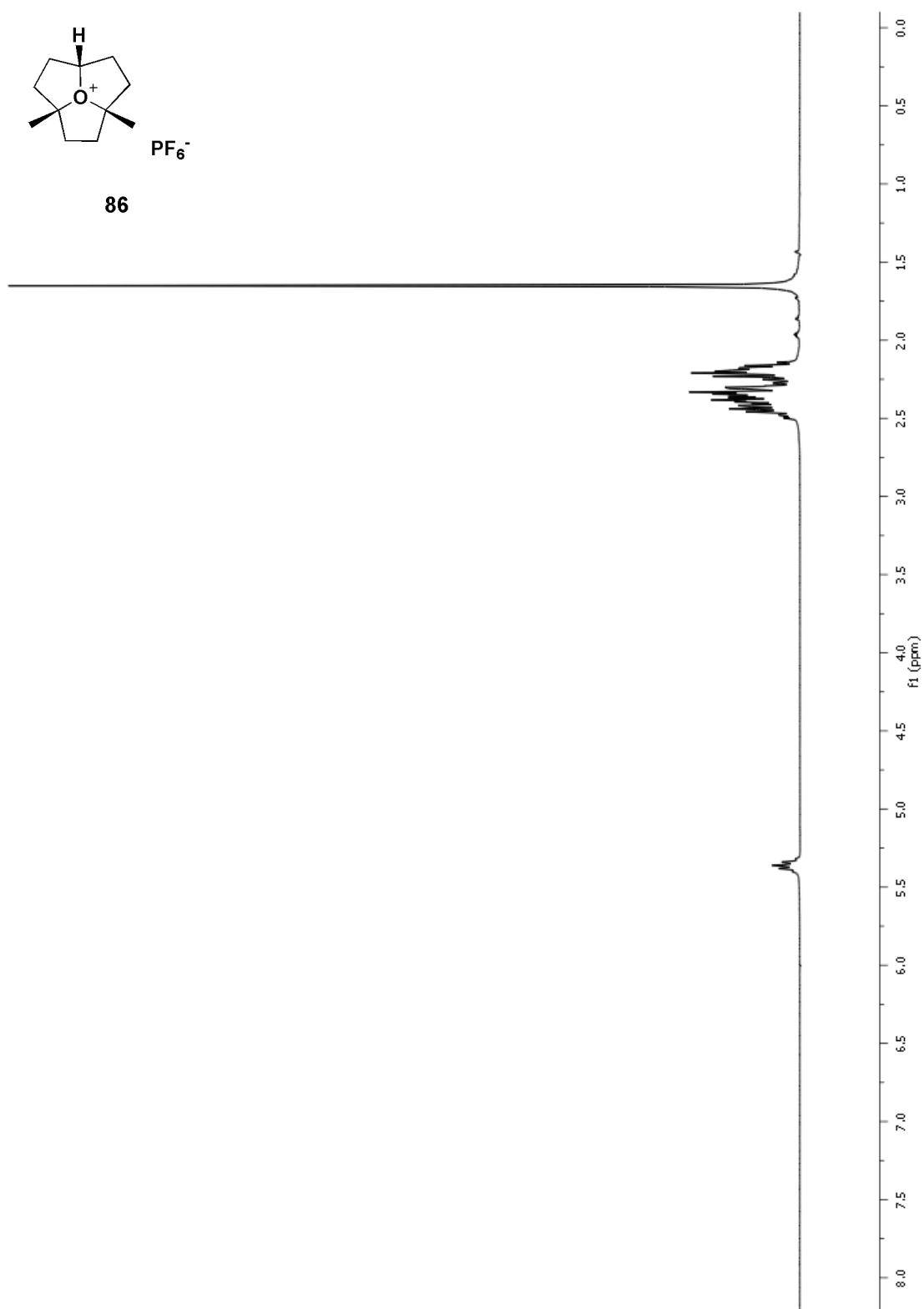
82

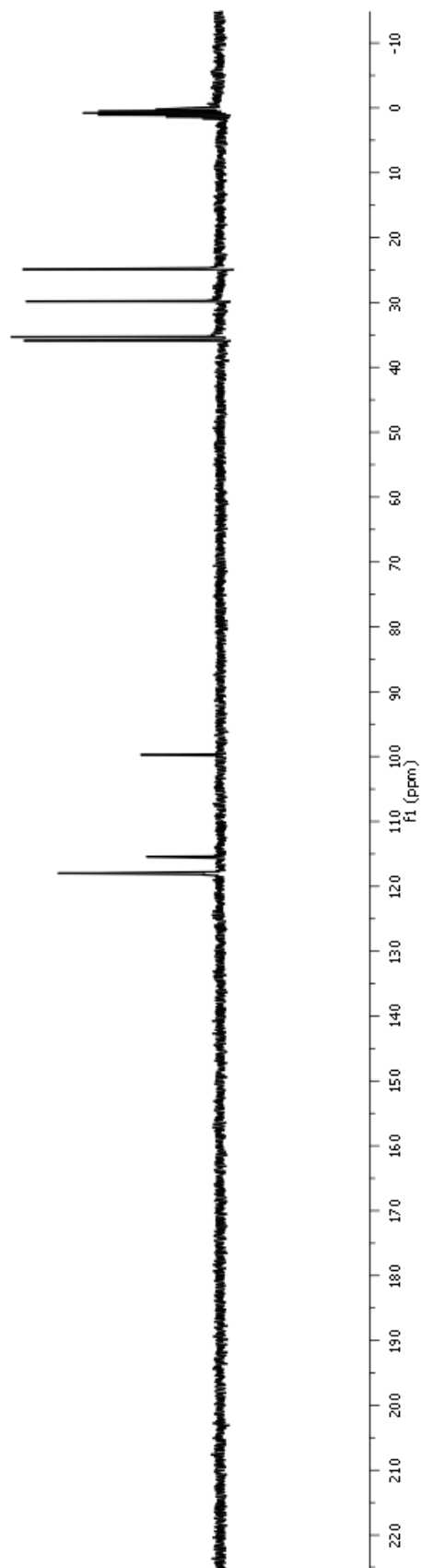
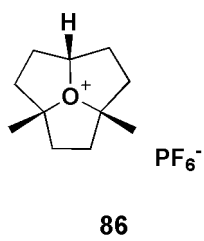


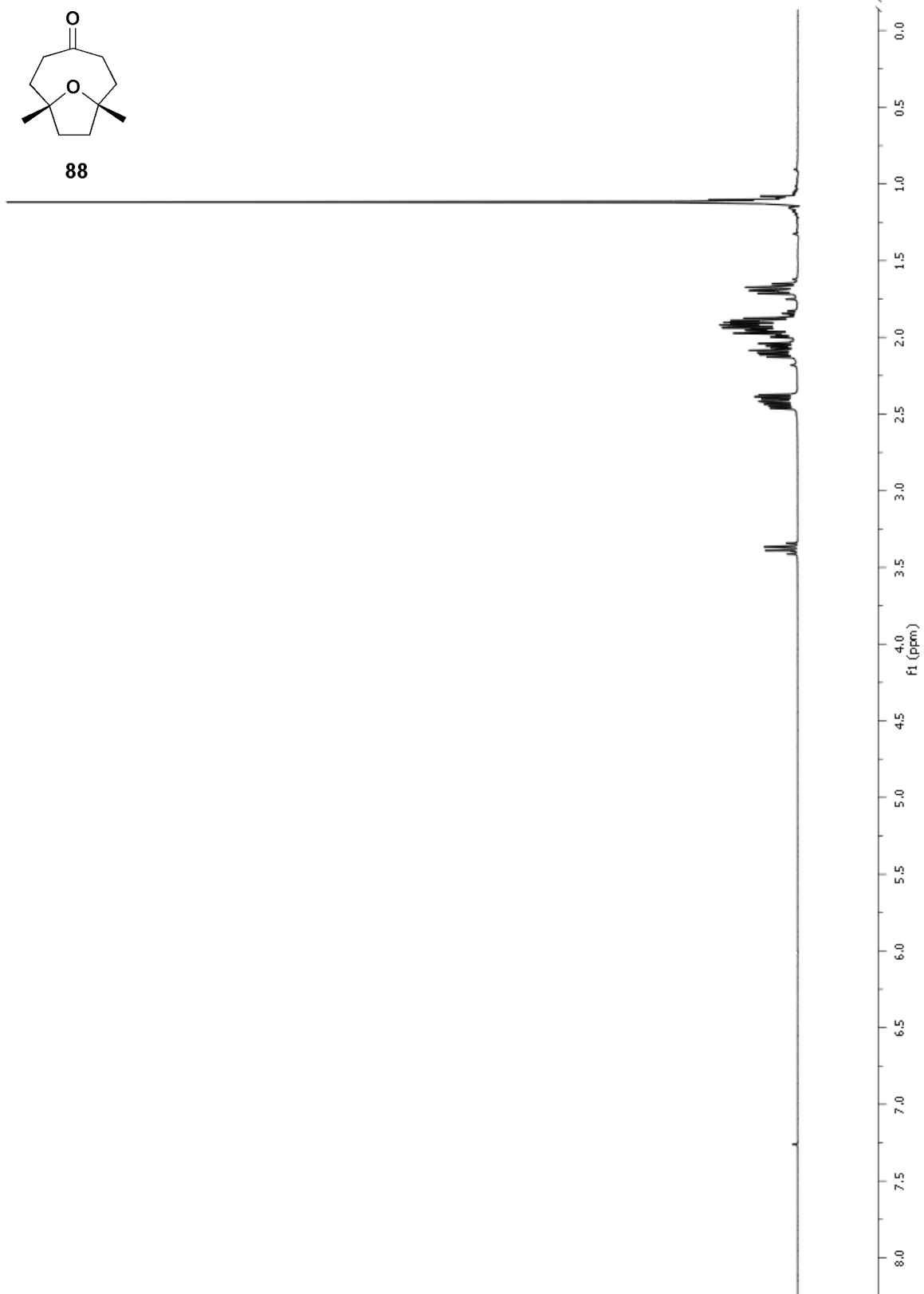


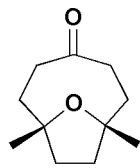




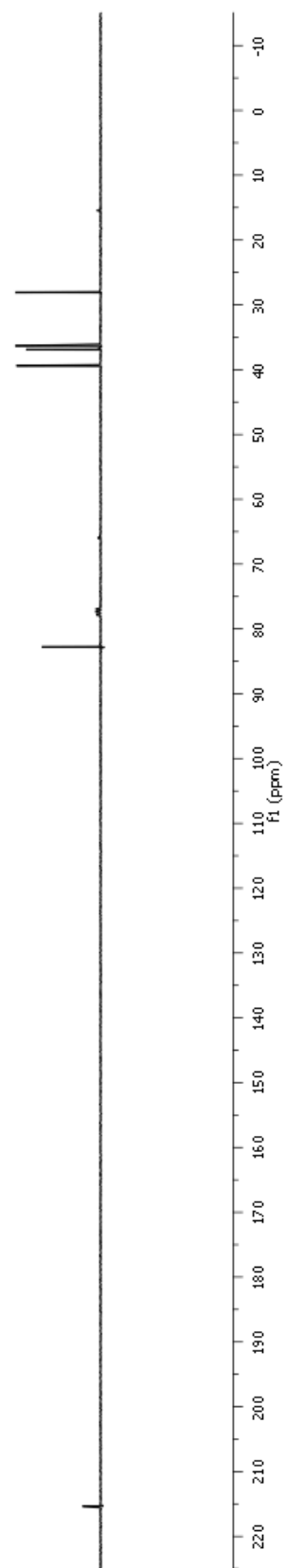


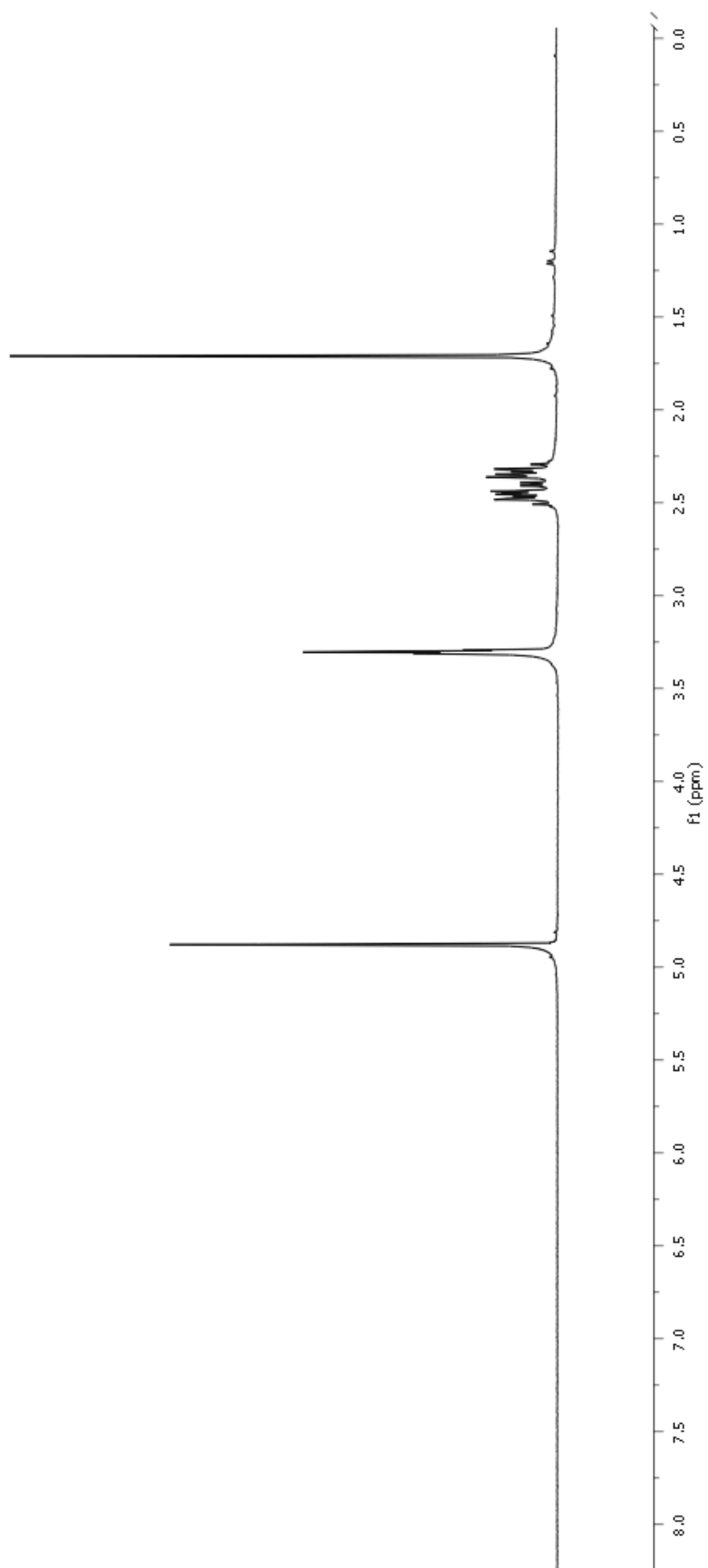
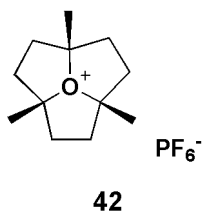


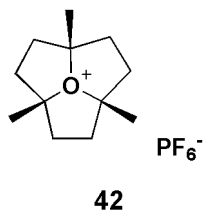




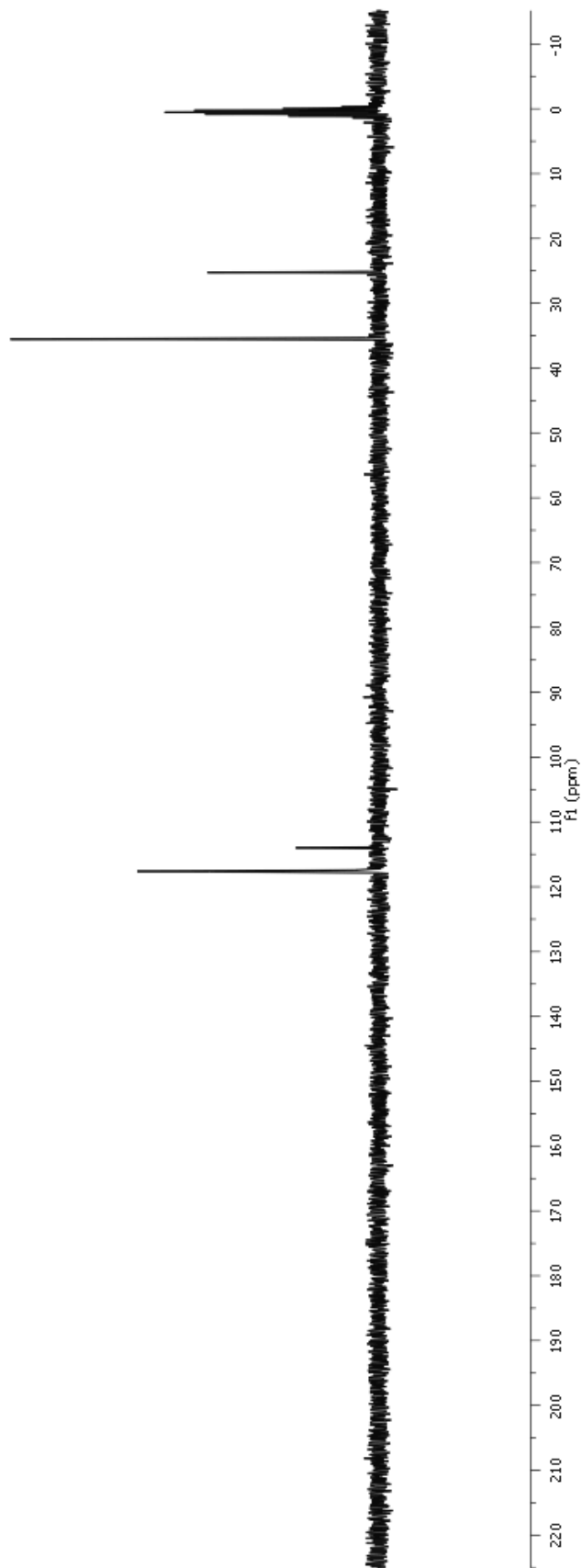
88

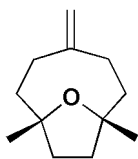




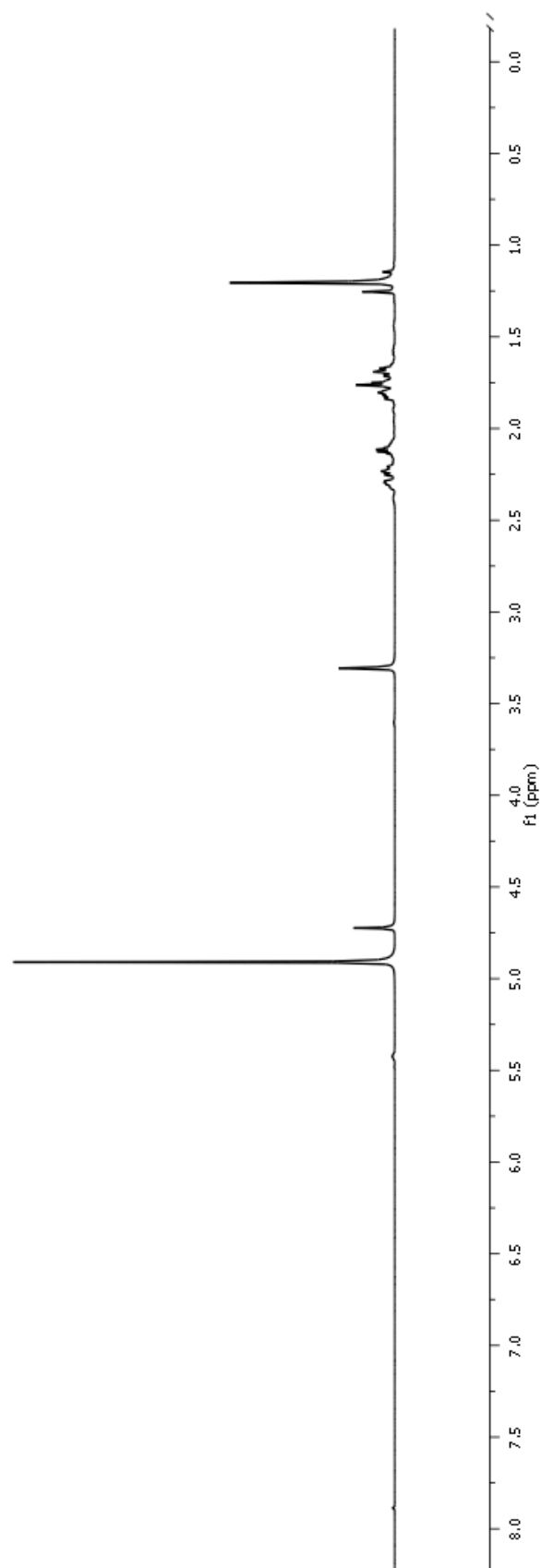


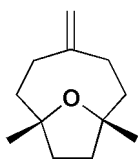
42



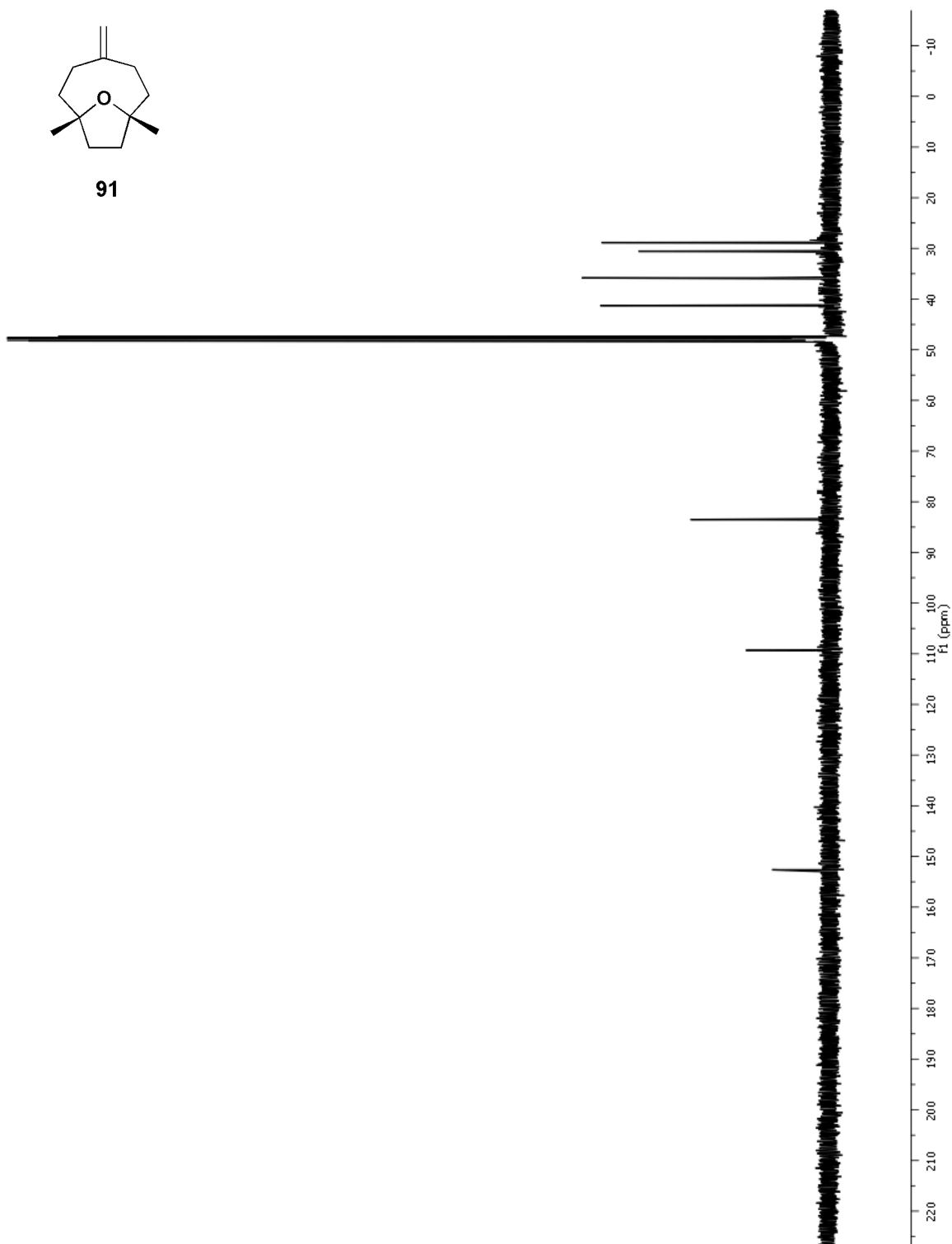


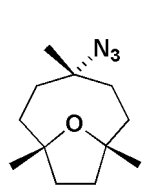
91



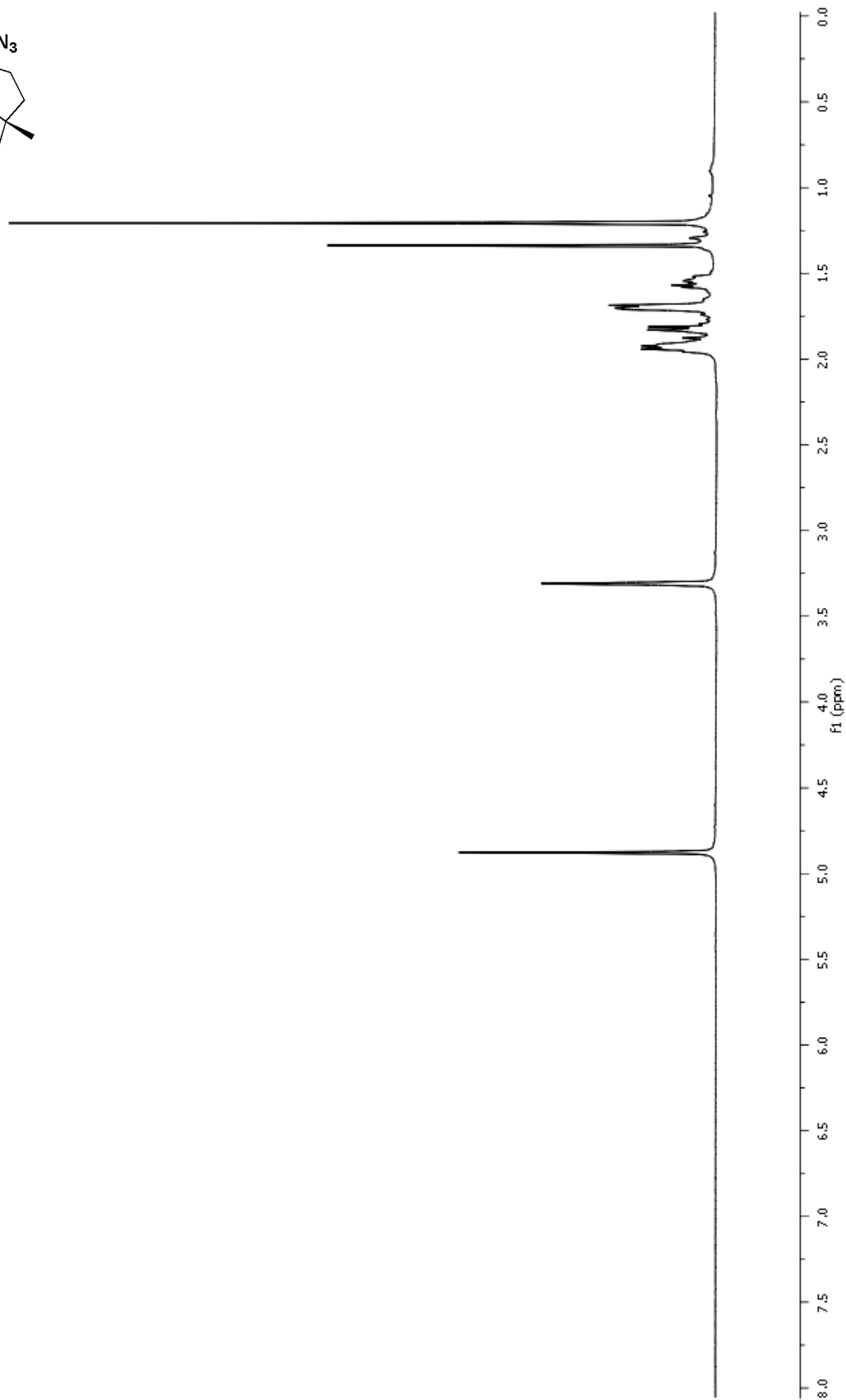


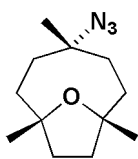
91



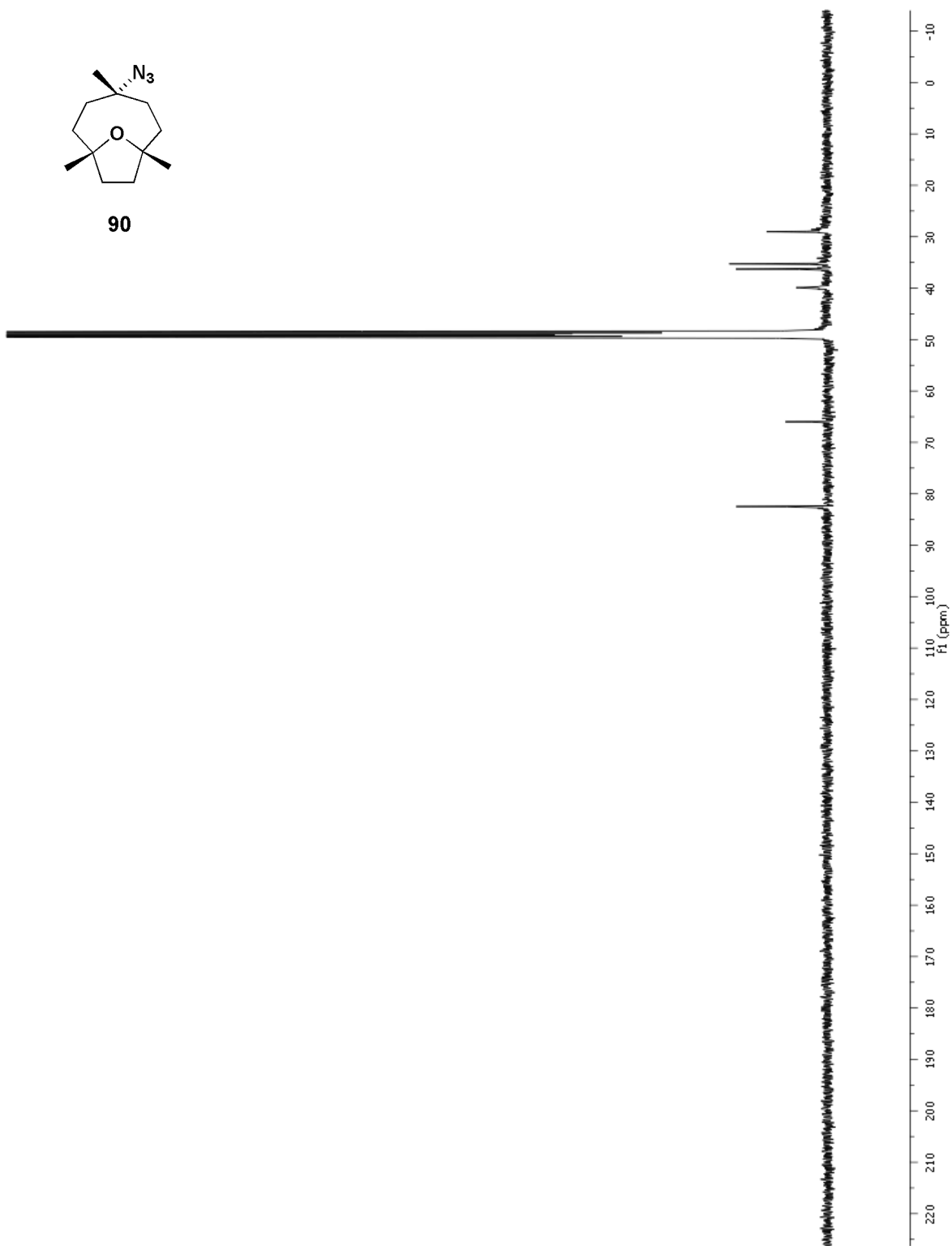


90





90



Crystal Structure Determination and Refinement for Oxatriquinane SbF_6^- (41)*

A colorless rod with approximate orthogonal dimensions 0.099x0.111x0.498 mm³ was placed and optically centered on a Bruker APEXII₂ CCD system at 90(2)K. The initial unit cell was indexed using a least-squares analysis of a random set of reflections collected from three series of 0.3° wide ω -scans, 10 seconds per frame, and 30 frames per series that were well distributed in reciprocal space. Four ω -scan data frame series were collected [MoK α] with 0.3° wide scans, 25 seconds per frame and 606 frames per series at varying ϕ angles ($\phi=0^\circ, 90^\circ, 180^\circ, 270^\circ$). The crystal to detector distance was 5.23 cm, thus providing a complete sphere of data to $2\theta_{\text{max}}=61.05^\circ$. A total of 9246 reflections were collected and corrected for Lorentz and polarization effects and absorption using Blessing's method as incorporated into the program SADABS^{3,4} with 1211 unique. The SHELXTL⁵ program package was implemented to determine the probable space group and set up the initial files. System symmetry, systematic absences and intensity statistics indicated the centrosymmetric rhombohedral space group R-3 (no. 148). The structure was determined by direct methods with the successful location of a majority of the atoms of the molecules unique portions using the program XS6. The structure was refined with XL6. The data collected were merged based upon identical indices yielding 6918 data [$R(\text{int})=0.0167$] that were truncated to $2\theta_{\text{max}}=55.00^\circ$ resulting in 5349 data that were further merged during least-squares refinement to 919 unique data [$R(\text{int})=0.0282$]. One least-squares difference-Fourier cycle was required to locate the remaining non-hydrogen atoms. All full occupancy non-hydrogen atoms

*-X-ray crystal structure was solved by Dr. James C. Fettinger

were refined anisotropically. Hydrogen atoms were placed in calculated positions throughout the convergence process. The structure did not converge so Rotax7 was implemented and a 180 degree rotation about 1 0 0 (1 0 0 -1 -1 0 0 0 -1) was among the many twin laws suggested and found to allow convergence. There was a single disorder optimized in the molecule of interest and found to be 80:20. All attempts to have a similar convergence in R-3m failed so the final structure was refined to convergence with $R(F)=2.29\%$, $wR(F2)=5.52\%$, $GOF=1.115$ for all 919 unique reflections [$R(F)=2.09\%$, $wR(F2)=5.40\%$ for those 839 data with $F_o > 4\sigma(F_o)$]. The final difference-Fourier map was featureless indicating that the structure is both correct and complete. Full data on this determination are given in tables 1.1-1.5.

Table 1.1 - Crystal data and structure refinement for **41** SbF₆⁻

Empirical formula - C₉H₁₅F₆OSb

Formula weight - 374.96 g/mol

Temperature - 90(2) K

Wavelength - 0.71073 Å

Crystal system - rhombohedral

Space group - R-3

Unit cell dimensions a = 10.2858(7) Å α = 90°.

b = 10.2858(7) Å β = 90°.

c = 19.3715(14) Å γ = 120°.

Volume 1774.9(2) Å³

Z = 6

Density (calculated) - 2.105 Mg/m³

Absorption coefficient - 2.391 mm⁻¹

F(000) 1092

Crystal size - 0.50 x 0.11 x 0.10 mm³

Crystal color and habit – colorless rod

Diffractometer Bruker SMART APEXII CCD

Theta range for data collection 3.11 to 27.49°.

Index ranges -13 ≤ h ≤ 13, -13 ≤ k ≤ 13, -25 ≤ l ≤ 25

Reflections collected 5349

Independent reflections 919 [R(int) = 0.0282]

Observed reflections (I > 2σ(I)) 839

Completeness to theta = 27.49° 99.7 %

Absorption correction Semi-empirical from equivalents

Max. and min. transmission 0.7977 and 0.3822

Solution method SHELXS-97 (Sheldrick, 2008)

Refinement method SHELXL-97 (Sheldrick, 2008) Full-matrix least-squares on F₂

Data / restraints / parameters 919 / 3 / 67

Goodness-of-fit on F₂ - 1.115

Final R indices [$I > 2\sigma(I)$] R1 = 0.0209, wR2 = 0.0540

R indices (all data) R1 = 0.0229, wR2 = 0.0552

Largest diff. peak and hole 0.977 and -0.598 e. Å⁻³

Table 1.2 - Atomic coordinates ($\times 10^4$) and equivalent isotropic displacement parameters ($\text{\AA}^2 \times 10^3$) for **41** SbF_6^- . $U(\text{eq})$ is defined as one third of the trace of the orthogonalized U_{ij} tensor.

	x	y	z	$U(\text{eq})$
Sb(1)	0	10000	5000	16(1)
F(1)	944(2)	9224(2)	5557(1)	30(1)
Sb(2)	3333	6667	6667	18(1)
F(2)	3518(3)	8236(2)	6109(1)	42(1)
O(1)	0	0	6962(2)	16(1)
C(1)	960(4)	1620(3)	7223(2)	22(1)
C(2)	1964(4)	1479(4)	7747(2)	25(1)
C(3)	2186(6)	197(6)	7461(4)	28(1)
O(11)	0	0	8087(7)	16(1)
C(11)	1020(20)	1585(13)	7804(10)	67(6)
C(12)	1920(40)	1370(30)	7255(12)	92(9)
C(13)	2130(60)	170(50)	7650(20)	82(18)

Table 1.3 - Bond lengths [\AA] and angles [$^\circ$] for **41** SbF_6^- .

Sb(1)-F(1)#1	1.8761(13)
Sb(1)-F(1)#2	1.8761(13)
Sb(1)-F(1)	1.8761(13)
Sb(1)-F(1)#3	1.8761(13)
Sb(1)-F(1)#4	1.8761(14)
Sb(1)-F(1)#5	1.8761(13)
Sb(2)-F(2)#6	1.8715(17)
Sb(2)-F(2)	1.8715(17)
Sb(2)-F(2)#7	1.8715(17)
Sb(2)-F(2)#8	1.8715(17)
Sb(2)-F(2)#9	1.8715(17)
Sb(2)-F(2)#10	1.8715(17)
O(1)-C(1)	1.537(3)
O(1)-C(1)#11	1.537(3)
O(1)-C(1)#12	1.537(3)
C(1)-C(3)#11	1.492(7)
C(1)-C(2)	1.506(5)
C(1)-H(1)	1.0000
C(2)-C(3)	1.549(7)
C(2)-H(2A)	0.9900
C(2)-H(2B)	0.9900
C(3)-C(1)#12	1.492(7)

C(3)-H(3A) 0.9900
C(3)-H(3B) 0.9900
O(11)-C(11)#11 1.532(10)
O(11)-C(11) 1.532(10)
O(11)-C(11)#12 1.532(10)
C(11)-C(13)#11 1.48(5)
C(11)-C(12) 1.498(11)
C(11)-H(11) 1.0000
C(12)-C(13) 1.554(12)
C(12)-H(12A) 0.9900
C(12)-H(12B) 0.9900
C(13)-C(11)#12 1.48(5)
C(13)-H(13A) 0.9900
C(13)-H(13B) 0.9900
F(1)#1-Sb(1)-F(1)#2 180.000(1)
F(1)#1-Sb(1)-F(1) 89.77(6)
F(1)#2-Sb(1)-F(1) 90.23(6)
F(1)#1-Sb(1)-F(1)#3 90.23(6)
F(1)#2-Sb(1)-F(1)#3 89.77(6)
F(1)-Sb(1)-F(1)#3 180.000(1)
F(1)#1-Sb(1)-F(1)#4 90.23(6)
F(1)#2-Sb(1)-F(1)#4 89.77(6)
F(1)-Sb(1)-F(1)#4 89.77(6)
F(1)#3-Sb(1)-F(1)#4 90.23(6)

F(1)#1-Sb(1)-F(1)#5 89.77(6)
F(1)#2-Sb(1)-F(1)#5 90.23(6)
F(1)-Sb(1)-F(1)#5 90.23(6)
F(1)#3-Sb(1)-F(1)#5 89.77(6)
F(1)#4-Sb(1)-F(1)#5 180.0
F(2)#6-Sb(2)-F(2) 180.00(16)
F(2)#6-Sb(2)-F(2)#7 90.02(8)
F(2)-Sb(2)-F(2)#7 89.98(8)
F(2)#6-Sb(2)-F(2)#8 90.02(8)
F(2)-Sb(2)-F(2)#8 89.98(8)
F(2)#7-Sb(2)-F(2)#8 89.98(8)
F(2)#6-Sb(2)-F(2)#9 89.98(8)
F(2)-Sb(2)-F(2)#9 90.02(8)
F(2)#7-Sb(2)-F(2)#9 180.0
F(2)#8-Sb(2)-F(2)#9 90.02(8)
F(2)#6-Sb(2)-F(2)#10 89.98(8)
F(2)-Sb(2)-F(2)#10 90.02(8)
F(2)#7-Sb(2)-F(2)#10 90.02(8)
F(2)#8-Sb(2)-F(2)#10 179.999(1)
F(2)#9-Sb(2)-F(2)#10 89.98(8)
C(1)-O(1)-C(1)#11 109.76(16)
C(1)-O(1)-C(1)#12 109.76(16)
C(1)#11-O(1)-C(1)#12 109.76(16)
C(3)#11-C(1)-C(2) 119.2(4)

C(3)#11-C(1)-O(1) 102.4(3)
C(2)-C(1)-O(1) 102.5(3)
C(3)#11-C(1)-H(1) 110.6
C(2)-C(1)-H(1) 110.6
O(1)-C(1)-H(1) 110.6
C(1)-C(2)-C(3) 103.9(3)
C(1)-C(2)-H(2A) 111.0
C(3)-C(2)-H(2A) 111.0
C(1)-C(2)-H(2B) 111.0
C(3)-C(2)-H(2B) 111.0
H(2A)-C(2)-H(2B) 109.0
C(1)#12-C(3)-C(2) 104.2(3)
C(1)#12-C(3)-H(3A) 110.9
C(2)-C(3)-H(3A) 110.9
C(1)#12-C(3)-H(3B) 110.9
C(2)-C(3)-H(3B) 110.9
H(3A)-C(3)-H(3B) 108.9
C(11)#11-O(11)-C(11) 107.9(9)
C(11)#11-O(11)-C(11)#12 107.9(9)
C(11)-O(11)-C(11)#12 107.9(9)
C(13)#11-C(11)-C(12) 123(3)
C(13)#11-C(11)-O(11) 98(2)
C(12)-C(11)-O(11) 104.0(16)
C(13)#11-C(11)-H(11) 110.2

C(12)-C(11)-H(11) 110.2
 O(11)-C(11)-H(11) 110.2
 C(11)-C(12)-C(13) 97(3)
 C(11)-C(12)-H(12A) 112.5
 C(13)-C(12)-H(12A) 112.5
 C(11)-C(12)-H(12B) 112.5
 C(13)-C(12)-H(12B) 112.5
 H(12A)-C(12)-H(12B) 110.0
 C(11)#12-C(13)-C(12) 103(3)
 C(11)#12-C(13)-H(13A) 111.1
 C(12)-C(13)-H(13A) 111.1
 C(11)#12-C(13)-H(13B) 111.1
 C(12)-C(13)-H(13B) 111.1
 H(13A)-C(13)-H(13B) 109.0

Symmetry transformations used to generate equivalent atoms:

#1 $y-1, -x+y, -z+1$ #2 $-y+1, x-y+2, z$ #3 $-x, -y+2, -z+1$
 #4 $x-y+1, x+1, -z+1$ #5 $-x+y-1, -x+1, z$ #6 $-x+2/3, -y+4/3, -z+4/3$
 #7 $-y+1, x-y+1, z$ #8 $-x+y, -x+1, z$ #9 $y-1/3, -x+y+1/3, -z+4/3$
 #10 $x-y+2/3, x+1/3, -z+4/3$ #11 $-y, x-y, z$ #12 $-x+y, -x, z$

Table 1.4 - Anisotropic displacement parameters ($\text{\AA}^2 \times 10^3$) for **41** SbF_6^-

- The anisotropic displacement factor exponent takes the form: $-2\pi^2 [h^2 a^{*2} U_{11} + \dots + 2 h k a^* b^* U_{12}]$

	U11	U22	U33	U23	U13	U12
Sb(1)	17(1)	17(1)	15(1)	0 0	0 8(1)	
F(1)	33(1)	37(1)	30(1)	2(1)	-4(1)	23(1)
Sb(2)	19(1)	19(1)	18(1)	0 0	0 9(1)	
F(2)	59(1)	34(1)	40(1)	11(1)	1(1)	26(1)
O(1)	15(1)	15(1)	18(2)	0 0	0 8(1)	
C(1)	25(2)	14(1)	24(1)	0(1)	3(1)	8(1)
C(2)	20(2)	29(2)	28(2)	-8(2)	-8(1)	12(2)
C(3)	17(2)	36(3)	36(3)	2(2)	-1(2)	17(2)
O(11)	15(1)	15(1)	18(2)	0 0	0 8(1)	

Table 1.5 - Hydrogen coordinates ($\text{\AA}^2 \times 10^4$) and isotropic displacement parameters ($\text{\AA}^2 \times 10^3$) for **41** SbF_6^- .

	x	y	z	U(eq)
H(1)	1568	2301	6838	26
H(2A)	1480	1217	8207	30
H(2B)	2936	2427	7784	30
H(3A)	2909	556	7073	34
H(3B)	2556	-211	7826	34
H(11)	1694	2256	8176	80
H(12A)	2889	2299	7165	110
H(12B)	1357	985	6819	110
H(13A)	2639	-229	7352	98
H(13B)	2717	585	8074	98

Crystal Structure Determination and Refinement for Trimethyloxatriquinane

PF₆⁻(42)*.

A colorless cut block with approximate orthogonal dimensions 0.42 x 0.42 x 0.26mm³ was placed and optically centered on the Bruker SMART1000¹ CCD system at 90(2)K. The initial unit cell was indexed using a least-squares analysis of a random set of reflections collected from three series of 0.3° wide ω -scans, 10 seconds per frame, and 25 frames per series that were well distributed in reciprocal space. Four ω -scan data frame series were collected [MoK α] with 0.3° wide scans, 20 seconds per frame and 606 frames were collected, at varying phi angles ($\phi=0^\circ, 90^\circ, 180^\circ, 270^\circ$), for each series. The crystal to detector distance was 4.32cm, thus providing a complete sphere of data with processing to $2\theta_{\max}=54.91^\circ$.

Structural determination and Refinement:

All crystallographic calculations were performed on a Personal computer (PC) with a Pentium 3.20GHz processor and 4GB of extended memory. A total of 18803 reflections were collected and corrected for Lorentz and polarization effects and absorption using Blessing's method as incorporated into the program SADABS^{2,3} with 4546 unique. The SHELXTL⁴ program package was implemented to determine the probable space group and set up the initial files. System symmetry transformed to a cubic unit cell with $a=11.422$, Volume=1490, with no systematic absences and intensity statistics, $|E^2-1|=0.496$, indicative of a potentially twinned system and/or system of lower symmetry. Attempts were made to determine the structure in P32, lowest symmetry cubic system to no avail. Further analysis of the Xprep file

*- X-ray crystal structure was solved by Dr. James C. Fettingner.

indicated that the rhombohedral obverse system in a hexagonal setting produced slightly lower averaging statistics and was now pursued. Due to the low E^*E-1 value and lack of systematic absences, R3 (no 146), R-3 (no 148), R32 (no 155), R3m (no 160), and R-3m (no 166) were all possible. R3 was chosen since it possessed the least symmetry and if additional symmetry were present it would be noted. The structure was determined by direct methods with the successful location of a majority of the two unique molecules of interest using the program XS⁵. The structure was refined with XL⁵. A series of difference-Fourier maps were required to locate the remaining non-hydrogen atoms within the two molecules of interest and the two PF₆ counterions. Molecule one's oxygen atom, O(1), sits on a three fold position with only one-third that molecule unique while the second molecule of interest is in a general position and was disordered in a ratio 73:27. Convergence ceased and, due to the intensity statistics values listed previously, Platon's TwinRotMat⁶ function was now implemented to suggested the generation of 4 twin components. These four twin laws were $(1-2\ 0)[0-1\ 0]$, $(1\ 0\ 1)[2\ 1\ 1]$, $(0\ 1\ -1)[1\ 2\ -1]$, $(1-1\ -1)[1-1\ -1]$, i.e., 180° rotations about direct lattice directions $0\ 1\ 0$, $2\ 1\ 1$, $-1\ -2\ 1$, and $-1\ 1\ 1$, respectively and all with predicted BASF values of about 0.50. Convergence again proceeded smoothly with the latter twin law BASF value approaching zero. TwinRotMat was implemented a second time with usage of only the first three twin laws above and the final BASF parameters were 0.18, 0.18 and 0.20 indicating that major domain was present about 44% of the time. ISOR and EADP commands were implemented for several atoms that were either close to another atom in another part, due to the disorder, or would not refine anisotropically. DFIX commands were also implemented to restrain equal bond distances to be equal with the disordered

molecule. Attempts to increase the symmetry were fruitless and this is probably due to the nature of the disorder in molecule two, i.e., O11/O31. All full occupancy non-hydrogen atoms were refined anisotropically. Hydrogen atoms were placed in idealized positions throughout the remainder of the convergence process. The final structure was refined to convergence with BASF values of 0.182, 0.177 and 0.203 with $R(F)=6.96\%$, $wR(F^2)=17.86\%$, $GOF=1.075$ for all 3615 twin generated reflections [$R(F)=6.93\%$, $wR(F^2)=17.83\%$ for those 3608 twin generated data with $F_o > 4\sigma(F_o)$]. The final difference-Fourier map was featureless indicating that the structure is both correct and complete. An empirical correction for extinction was not attempted due to the twinning. Full data on this determination are given in tables 2.1-2.5.

Table 2.1 - Crystal data and structure refinement for **42 PF₆⁻**.

Empirical formula	C ₁₂ H ₂₁ F ₆ O P	
Formula weight	326.26	
Temperature	90(2) K	
Wavelength	0.71073 Å	
Crystal system	rhombohedral	
Space group	R 3	
Unit cell dimensions	a = 16.1531(9) Å	a = 90°.
	b = 16.1531(9) Å	b = 90°.
	c = 19.7817(11) Å	g = 120°.
Volume	4470.0(4) Å ³	
Z	12	
Density (calculated)	1.454 Mg/m ³	
Absorption coefficient	0.242 mm ⁻¹	
F(000)	2040	
Crystal size	0.42 x 0.42 x 0.26 mm ³	
Crystal color and habit	Colorless Block	
Diffractometer	Bruker SMART1000 CCD	
Theta range for data collection	1.78 to 25.18°.	
Index ranges	-19 ≤ h ≤ 19, -19 ≤ k ≤ 19, -23 ≤ l ≤ 23	
Reflections collected	3615	
Independent reflections	3615 [R(int) = 0.0000]	
Observed reflections (I > 2σ(I))	3608	

Completeness to theta = 25.18°	99.9 %
Absorption correction	Semi-empirical from equivalents
Max. and min. transmission	0.9388 and 0.9053
Solution method	SHELXS-97 (Sheldrick, 2008)
Refinement method	SHELXL-97 (Sheldrick, 2008) Full-matrix least-squares on F ²
Data / restraints / parameters	3615 / 224 / 297
Goodness-of-fit on F ²	1.075
Final R indices [I > 2sigma(I)]	R1 = 0.0693, wR2 = 0.1783
R indices (all data)	R1 = 0.0696, wR2 = 0.1786
Absolute structure parameter	0.6(4)
Largest diff. peak and hole	0.497 and -0.459 e.Å ⁻³

Table 2.2 - Atomic coordinates ($\times 10^4$) and equivalent isotropic displacement parameters ($\text{\AA}^2 \times 10^3$) for **42** PF_6^- . $U(\text{eq})$ is defined as one third of the trace of the orthogonalized U_{ij} tensor.

	x	y	z	U(eq)
O(1)	10000	10000	8946(5)	5(1)
C(1)	9550(6)	8957(5)	9219(4)	7(2)
C(2)	10420(6)	8923(6)	9495(5)	18(2)
C(3)	8852(6)	8902(6)	9749(4)	12(2)
C(4)	9110(6)	8324(6)	8612(4)	15(2)
O(11)	4930(6)	4807(6)	9051(4)	17(2)
C(11)	5332(9)	5504(9)	8452(6)	37(4)
C(12)	5004(8)	6209(8)	8603(7)	21(3)
C(13)	4047(10)	5627(11)	8961(8)	36(3)
C(14)	4186(9)	4983(10)	9435(7)	41(4)
C(15)	4767(10)	5424(10)	10066(7)	26(3)
C(16)	5375(12)	4984(12)	10246(7)	37(4)
C(17)	5701(8)	4892(8)	9542(6)	18(2)
C(18)	6523(11)	5824(11)	9281(7)	46(4)
C(19)	6387(9)	5836(11)	8530(7)	31(3)
C(20)	4900(12)	4864(13)	7836(8)	38(4)
C(21)	3302(10)	3995(10)	9562(8)	34(3)
C(22)	5790(9)	4020(8)	9460(7)	17(2)

O(31)	5231(12)	5257(14)	9090(9)	17(2)
C(31)	4434(12)	5169(13)	8624(9)	-8(4)
C(32)	3565(15)	4281(17)	8880(11)	18(7)
C(33)	3733(14)	4260(20)	9627(11)	16(7)
C(34)	4771(13)	4603(15)	9732(9)	4(5)
C(35)	5162(19)	3949(17)	9567(18)	37(10)
C(36)	6175(15)	4528(17)	9303(12)	5(5)
C(37)	6009(16)	5106(18)	8769(12)	39(10)
C(38)	5440(20)	4610(30)	8149(15)	39(10)
C(39)	4820(30)	5030(30)	7953(12)	38(4)
C(40)	4410(30)	6090(20)	8600(20)	36(3)
C(41)	5260(30)	5260(30)	10346(15)	37(4)
C(42)	6860(20)	6090(20)	8710(20)	52(12)
P(41)	6756(2)	8452(2)	7528(2)	26(1)
F(41)	5660(4)	8132(4)	7632(4)	30(1)
F(42)	7857(5)	8801(5)	7398(4)	36(2)
F(43)	6884(5)	8284(5)	8268(4)	33(2)
F(44)	6622(4)	8634(5)	6744(3)	26(1)
F(45)	6477(5)	7371(4)	7339(4)	30(1)
F(46)	7063(5)	9560(4)	7692(4)	33(2)
P(51)	6667	3333	7432(3)	41(1)
F(51)	6236(6)	3851(6)	6982(4)	48(2)
F(52)	7102(6)	2829(5)	7914(4)	42(2)

Table 2.3 - Bond lengths [\AA] and angles [$^\circ$] for **42** PF_6^-

(1)-C(1)	1.560(8)
O(1)-C(1)#1	1.560(9)
O(1)-C(1)#2	1.560(8)
C(1)-C(4)	1.506(11)
C(1)-C(3)	1.510(11)
C(1)-C(2)	1.534(11)
C(2)-C(3)#1	1.545(11)
C(2)-H(2A)	0.9900
C(2)-H(2B)	0.9900
C(3)-C(2)#2	1.545(11)
C(3)-H(3A)	0.9900
C(3)-H(3B)	0.9900
C(4)-H(4A)	0.9800
C(4)-H(4B)	0.9800
C(4)-H(4C)	0.9800
O(11)-C(17)	1.529(11)
O(11)-C(11)	1.538(13)
O(11)-C(14)	1.563(13)
C(11)-C(12)	1.507(13)
C(11)-C(19)	1.518(14)
C(11)-C(20)	1.523(15)
C(12)-C(13)	1.523(13)

C(12)-H(12A)	0.9900
C(12)-H(12B)	0.9900
C(13)-C(14)	1.499(13)
C(13)-H(13A)	0.9900
C(13)-H(13B)	0.9900
C(14)-C(15)	1.509(13)
C(14)-C(21)	1.539(14)
C(15)-C(16)	1.515(13)
C(15)-H(15A)	0.9900
C(15)-H(15B)	0.9900
C(16)-C(17)	1.523(13)
C(16)-H(16A)	0.9900
C(16)-H(16B)	0.9900
C(17)-C(22)	1.494(12)
C(17)-C(18)	1.515(13)
C(18)-C(19)	1.504(13)
C(18)-H(18A)	0.9900
C(18)-H(18B)	0.9900
C(19)-H(19A)	0.9900
C(19)-H(19B)	0.9900
C(20)-H(20A)	0.9800
C(20)-H(20B)	0.9800
C(20)-H(20C)	0.9800
C(21)-H(21A)	0.9800

C(21)-H(21B)	0.9800
C(21)-H(21C)	0.9800
C(22)-H(22A)	0.9800
C(22)-H(22B)	0.9800
C(22)-H(22C)	0.9800
O(31)-C(31)	1.530(18)
O(31)-C(37)	1.533(19)
O(31)-C(34)	1.580(19)
C(31)-C(40)	1.50(2)
C(31)-C(32)	1.507(14)
C(31)-C(39)	1.53(2)
C(32)-C(33)	1.505(15)
C(32)-H(32A)	0.9900
C(32)-H(32B)	0.9900
C(33)-C(34)	1.493(15)
C(33)-H(33A)	0.9900
C(33)-H(33B)	0.9900
C(34)-C(35)	1.513(15)
C(34)-C(41)	1.54(2)
C(35)-C(36)	1.515(15)
C(35)-H(35A)	0.9900
C(35)-H(35B)	0.9900
C(36)-C(37)	1.520(15)
C(36)-H(36A)	0.9900

C(36)-H(36B)	0.9900
C(37)-C(42)	1.50(2)
C(37)-C(38)	1.504(15)
C(38)-C(39)	1.508(15)
C(38)-H(38A)	0.9900
C(38)-H(38B)	0.9900
C(39)-H(39A)	0.9900
C(39)-H(39B)	0.9900
C(40)-H(40A)	0.9800
C(40)-H(40B)	0.9800
C(40)-H(40C)	0.9800
C(41)-H(41A)	0.9800
C(41)-H(41B)	0.9800
C(41)-H(41C)	0.9800
C(42)-H(42A)	0.9800
C(42)-H(42B)	0.9800
C(42)-H(42C)	0.9800
P(41)-F(43)	1.523(8)
P(41)-F(41)	1.590(7)
P(41)-F(42)	1.595(7)
P(41)-F(44)	1.612(7)
P(41)-F(45)	1.613(6)
P(41)-F(46)	1.634(6)
P(51)-F(51)	1.600(8)

P(51)-F(51)#3	1.600(8)
P(51)-F(51)#4	1.600(8)
P(51)-F(52)#3	1.625(8)
P(51)-F(52)#4	1.625(8)
P(51)-F(52)	1.625(8)
C(1)-O(1)-C(1)#1	108.7(4)
C(1)-O(1)-C(1)#2	108.7(4)
C(1)#1-O(1)-C(1)#2	108.7(4)
C(4)-C(1)-C(3)	115.4(7)
C(4)-C(1)-C(2)	112.9(7)
C(3)-C(1)-C(2)	114.9(7)
C(4)-C(1)-O(1)	105.3(7)
C(3)-C(1)-O(1)	103.6(6)
C(2)-C(1)-O(1)	102.8(6)
C(1)-C(2)-C(3)#1	104.3(7)
C(1)-C(2)-H(2A)	110.9
C(3)#1-C(2)-H(2A)	110.9
C(1)-C(2)-H(2B)	110.9
C(3)#1-C(2)-H(2B)	110.9
H(2A)-C(2)-H(2B)	108.9
C(1)-C(3)-C(2)#2	105.1(6)
C(1)-C(3)-H(3A)	110.7
C(2)#2-C(3)-H(3A)	110.7
C(1)-C(3)-H(3B)	110.7

C(2)#2-C(3)-H(3B)	110.7
H(3A)-C(3)-H(3B)	108.8
C(1)-C(4)-H(4A)	109.5
C(1)-C(4)-H(4B)	109.5
H(4A)-C(4)-H(4B)	109.5
C(1)-C(4)-H(4C)	109.5
H(4A)-C(4)-H(4C)	109.5
H(4B)-C(4)-H(4C)	109.5
C(17)-O(11)-C(11)	113.4(8)
C(17)-O(11)-C(14)	109.9(8)
C(11)-O(11)-C(14)	108.8(8)
C(12)-C(11)-C(19)	118.1(11)
C(12)-C(11)-C(20)	117.2(11)
C(19)-C(11)-C(20)	111.9(11)
C(12)-C(11)-O(11)	102.8(9)
C(19)-C(11)-O(11)	99.7(9)
C(20)-C(11)-O(11)	103.7(11)
C(11)-C(12)-C(13)	104.9(10)
C(11)-C(12)-H(12A)	110.8
C(13)-C(12)-H(12A)	110.8
C(11)-C(12)-H(12B)	110.8
C(13)-C(12)-H(12B)	110.8
H(12A)-C(12)-H(12B)	108.8
C(14)-C(13)-C(12)	105.1(10)

C(14)-C(13)-H(13A)	110.7
C(12)-C(13)-H(13A)	110.7
C(14)-C(13)-H(13B)	110.7
C(12)-C(13)-H(13B)	110.7
H(13A)-C(13)-H(13B)	108.8
C(13)-C(14)-C(15)	117.6(12)
C(13)-C(14)-C(21)	116.0(11)
C(15)-C(14)-C(21)	112.9(11)
C(13)-C(14)-O(11)	102.6(10)
C(15)-C(14)-O(11)	97.8(9)
C(21)-C(14)-O(11)	106.9(10)
C(14)-C(15)-C(16)	111.7(10)
C(14)-C(15)-H(15A)	109.3
C(16)-C(15)-H(15A)	109.3
C(14)-C(15)-H(15B)	109.3
C(16)-C(15)-H(15B)	109.3
H(15A)-C(15)-H(15B)	107.9
C(15)-C(16)-C(17)	99.6(10)
C(15)-C(16)-H(16A)	111.9
C(17)-C(16)-H(16A)	111.9
C(15)-C(16)-H(16B)	111.9
C(17)-C(16)-H(16B)	111.9
H(16A)-C(16)-H(16B)	109.6
C(22)-C(17)-C(18)	116.7(11)

C(22)-C(17)-C(16)	113.0(10)
C(18)-C(17)-C(16)	112.9(11)
C(22)-C(17)-O(11)	107.7(9)
C(18)-C(17)-O(11)	98.3(9)
C(16)-C(17)-O(11)	106.5(9)
C(19)-C(18)-C(17)	106.7(11)
C(19)-C(18)-H(18A)	110.4
C(17)-C(18)-H(18A)	110.4
C(19)-C(18)-H(18B)	110.4
C(17)-C(18)-H(18B)	110.4
H(18A)-C(18)-H(18B)	108.6
C(18)-C(19)-C(11)	104.0(11)
C(18)-C(19)-H(19A)	111.0
C(11)-C(19)-H(19A)	111.0
C(18)-C(19)-H(19B)	111.0
C(11)-C(19)-H(19B)	111.0
H(19A)-C(19)-H(19B)	109.0
C(31)-O(31)-C(37)	117.0(14)
C(31)-O(31)-C(34)	109.2(13)
C(37)-O(31)-C(34)	112.0(13)
C(40)-C(31)-C(32)	118.9(19)
C(40)-C(31)-O(31)	111.3(18)
C(32)-C(31)-O(31)	103.1(13)
C(40)-C(31)-C(39)	109.2(19)

C(32)-C(31)-C(39)	113.8(19)
O(31)-C(31)-C(39)	98.6(14)
C(33)-C(32)-C(31)	105.1(15)
C(33)-C(32)-H(32A)	110.7
C(31)-C(32)-H(32A)	110.7
C(33)-C(32)-H(32B)	110.7
C(31)-C(32)-H(32B)	110.7
H(32A)-C(32)-H(32B)	108.8
C(34)-C(33)-C(32)	108.1(16)
C(34)-C(33)-H(33A)	110.1
C(32)-C(33)-H(33A)	110.1
C(34)-C(33)-H(33B)	110.1
C(32)-C(33)-H(33B)	110.1
H(33A)-C(33)-H(33B)	108.4
C(33)-C(34)-C(35)	119.3(19)
C(33)-C(34)-C(41)	117.5(19)
C(35)-C(34)-C(41)	113(2)
C(33)-C(34)-O(31)	101.7(13)
C(35)-C(34)-O(31)	94.2(14)
C(41)-C(34)-O(31)	105.5(19)
C(34)-C(35)-C(36)	110.0(16)
C(34)-C(35)-H(35A)	109.7
C(36)-C(35)-H(35A)	109.7
C(34)-C(35)-H(35B)	109.7

C(36)-C(35)-H(35B)	109.7
H(35A)-C(35)-H(35B)	108.2
C(35)-C(36)-C(37)	98.6(16)
C(35)-C(36)-H(36A)	112.0
C(37)-C(36)-H(36A)	112.0
C(35)-C(36)-H(36B)	112.0
C(37)-C(36)-H(36B)	112.0
H(36A)-C(36)-H(36B)	109.7
C(42)-C(37)-C(38)	120(2)
C(42)-C(37)-C(36)	111(2)
C(38)-C(37)-C(36)	119(2)
C(42)-C(37)-O(31)	105(2)
C(38)-C(37)-O(31)	95.1(15)
C(36)-C(37)-O(31)	102.8(15)
C(37)-C(38)-C(39)	109.8(19)
C(37)-C(38)-H(38A)	109.7
C(39)-C(38)-H(38A)	109.7
C(37)-C(38)-H(38B)	109.7
C(39)-C(38)-H(38B)	109.7
H(38A)-C(38)-H(38B)	108.2
C(38)-C(39)-C(31)	104.7(18)
C(38)-C(39)-H(39A)	110.8
C(31)-C(39)-H(39A)	110.8
C(38)-C(39)-H(39B)	110.8

C(31)-C(39)-H(39B)	110.8
H(39A)-C(39)-H(39B)	108.9
C(31)-C(40)-H(40A)	109.5
C(31)-C(40)-H(40B)	109.5
H(40A)-C(40)-H(40B)	109.5
C(31)-C(40)-H(40C)	109.5
H(40A)-C(40)-H(40C)	109.5
H(40B)-C(40)-H(40C)	109.5
C(34)-C(41)-H(41A)	109.5
C(34)-C(41)-H(41B)	109.5
H(41A)-C(41)-H(41B)	109.5
C(34)-C(41)-H(41C)	109.5
H(41A)-C(41)-H(41C)	109.5
H(41B)-C(41)-H(41C)	109.5
C(37)-C(42)-H(42A)	109.5
C(37)-C(42)-H(42B)	109.5
H(42A)-C(42)-H(42B)	109.5
C(37)-C(42)-H(42C)	109.5
H(42A)-C(42)-H(42C)	109.5
H(42B)-C(42)-H(42C)	109.5
F(43)-P(41)-F(41)	92.6(4)
F(43)-P(41)-F(42)	89.5(4)
F(41)-P(41)-F(42)	177.7(5)
F(43)-P(41)-F(44)	179.8(4)

F(41)-P(41)-F(44)	87.4(4)
F(42)-P(41)-F(44)	90.5(4)
F(43)-P(41)-F(45)	91.1(4)
F(41)-P(41)-F(45)	90.8(3)
F(42)-P(41)-F(45)	90.3(4)
F(44)-P(41)-F(45)	89.1(3)
F(43)-P(41)-F(46)	90.6(4)
F(41)-P(41)-F(46)	90.5(4)
F(42)-P(41)-F(46)	88.4(4)
F(44)-P(41)-F(46)	89.2(4)
F(45)-P(41)-F(46)	177.8(4)
F(51)-P(51)-F(51)#3	92.1(4)
F(51)-P(51)-F(51)#4	92.1(4)
F(51)#3-P(51)-F(51)#4	92.1(4)
F(51)-P(51)-F(52)#3	89.1(4)
F(51)#3-P(51)-F(52)#3	177.8(5)
F(51)#4-P(51)-F(52)#3	89.8(4)
F(51)-P(51)-F(52)#4	89.8(4)
F(51)#3-P(51)-F(52)#4	89.1(4)
F(51)#4-P(51)-F(52)#4	177.8(5)
F(52)#3-P(51)-F(52)#4	89.0(5)
F(51)-P(51)-F(52)	177.8(5)
F(51)#3-P(51)-F(52)	89.8(4)
F(51)#4-P(51)-F(52)	89.1(4)

F(52)#3-P(51)-F(52) 89.0(5)

F(52)#4-P(51)-F(52) 89.0(5)

Symmetry transformations used to generate equivalent atoms:

#1 $-y+2, x-y+1, z$ #2 $-x+y+1, -x+2, z$ #3 $-y+1, x-y, z$

#4 $-x+y+1, -x+1, z$

Table 2.4 - Anisotropic displacement parameters ($\text{\AA}^2 \times 10^3$) for **42** PF_6^- . The anisotropic displacement factor exponent takes the form:

$$-2p^2[h^2 a^*2U^{11} + \dots + 2 h k a^* b^* U^{12}]$$

	U ¹¹	U ²²	U ³³	U ²³	U ¹³	U ¹²
O(1)	5(1)	5(1)	4(2)	0	0	3(1)
C(1)	6(2)	7(2)	7(2)	0(1)	-1(1)	4(1)
C(2)	18(2)	18(2)	19(2)	1(1)	-1(1)	10(1)
C(3)	12(2)	12(2)	12(2)	1(1)	1(1)	6(1)
C(4)	15(2)	15(2)	14(2)	-1(1)	0(1)	7(1)
O(11)	18(2)	17(3)	19(2)	3(2)	-1(2)	11(2)
C(11)	36(4)	38(4)	36(4)	-1(2)	1(2)	18(3)
C(12)	22(3)	19(3)	23(3)	2(2)	1(2)	10(2)
C(13)	35(4)	37(4)	37(4)	-1(2)	-1(2)	18(2)
C(14)	42(4)	41(4)	40(4)	3(2)	-2(2)	20(3)
C(15)	26(3)	25(3)	26(4)	0(2)	-2(2)	12(2)
C(16)	38(4)	36(4)	35(4)	2(2)	1(2)	18(2)
C(17)	18(3)	20(3)	18(3)	3(2)	-2(2)	11(2)
C(18)	45(5)	46(5)	45(5)	-1(2)	1(2)	22(3)
C(19)	30(4)	32(4)	31(4)	2(2)	1(2)	15(2)
C(20)	37(4)	39(4)	37(4)	0(2)	-1(2)	18(2)
C(21)	34(4)	34(4)	34(4)	0(2)	-1(2)	17(2)
C(22)	17(3)	17(3)	17(3)	0(2)	-1(2)	8(2)

O(31)	18(2)	17(3)	19(2)	3(2)	-1(2)	11(2)
C(39)	37(4)	39(4)	37(4)	0(2)	-1(2)	18(2)
C(40)	35(4)	37(4)	37(4)	-1(2)	-1(2)	18(2)
C(41)	38(4)	36(4)	35(4)	2(2)	1(2)	18(2)
P(41)	12(1)	22(1)	39(2)	-11(1)	-15(1)	4(1)
F(41)	26(3)	10(2)	49(4)	-12(2)	-4(3)	5(2)
F(42)	30(3)	31(3)	45(4)	-13(3)	-6(3)	14(3)
F(43)	33(3)	46(4)	30(4)	-11(3)	-11(3)	28(3)
F(44)	18(3)	30(3)	33(3)	-13(3)	-4(2)	15(3)
F(45)	28(3)	14(3)	45(4)	1(2)	-7(3)	7(2)
F(46)	36(3)	11(3)	53(4)	-13(3)	2(3)	14(3)
P(51)	55(2)	55(2)	12(2)	0	0	28(1)
F(51)	60(4)	65(5)	26(4)	5(3)	3(3)	37(4)
F(52)	55(4)	33(3)	24(3)	8(3)	2(3)	12(3)

Table 2.5 - Hydrogen coordinates ($\times 10^4$) and isotropic displacement parameters ($\text{\AA}^2 \times 10^3$) for **42** PF_6^- .

	x	y	z	U(eq)
H(2A)	10728	8744	9135	22
H(2B)	10232	8456	9870	22
H(3A)	9170	9114	10194	14
H(3B)	8310	8241	9792	14
H(4A)	8553	8364	8462	22
H(4B)	8911	7661	8732	22
H(4C)	9581	8534	8245	22
H(12A)	4927	6493	8181	25
H(12B)	5468	6729	8899	25
H(13A)	3877	6050	9213	44
H(13B)	3533	5248	8631	44
H(15A)	4330	5331	10446	31
H(15B)	5185	6119	9996	31
H(16A)	4995	4354	10468	44
H(16B)	5921	5411	10539	44
H(18A)	6518	6374	9498	55
H(18B)	7141	5861	9383	55
H(19A)	6553	5396	8297	37
H(19B)	6787	6488	8345	37

H(20A)	4242	4728	7771	57
H(20B)	4901	4264	7905	57
H(20C)	5280	5189	7434	57
H(21A)	2840	4070	9839	51
H(21B)	3496	3586	9800	51
H(21C)	3007	3701	9129	51
H(22A)	6166	3982	9835	26
H(22B)	6110	4057	9032	26
H(22C)	5152	3451	9461	26
H(32A)	2978	4314	8798	22
H(32B)	3500	3704	8654	22
H(33A)	3545	4671	9873	20
H(33B)	3345	3595	9800	20
H(35A)	4753	3477	9222	45
H(35B)	5154	3596	9978	45
H(36A)	6405	4117	9104	6
H(36B)	6626	4940	9658	6
H(38A)	5030	3917	8241	47
H(38B)	5874	4688	7773	47
H(39A)	4289	4581	7656	46
H(39B)	5199	5642	7715	46
H(40A)	4142	6168	9017	55
H(40B)	4019	6069	8213	55
H(40C)	5065	6624	8540	55

H(41A)	4922	5598	10464	55
H(41B)	5926	5718	10234	55
H(41C)	5244	4867	10732	55
H(42A)	6654	6538	8567	78
H(42B)	7311	6087	8384	78
H(42C)	7174	6290	9156	78
